POLITECNICO
MILANO 1863

SCHOOL OF INDUSTRIAL AND INFORMATION ENGINERING

MASTER OF SCIENCE IN MECHANICAL ENGINEERING

NUMERICAL AND EXPERIMENTAL APPROACH FOR THE DESIGN AND VALIDATION OF SOLUTION TO PROTECT WORKS OF ART FROM VIBRATION DURING TRANSPORT

Supervisor:

Prof. Emanuele ZAPPA

Co-supervisor:

Ing. Simone PAGANONI

Master thesis of:

Stefano VIGANO' Matr. 877464

Academic Year 2018 - 2019

Abstract

The protection of works of art even during transport is of primary importance, for this reason a continuous evolution of protection systems is necessary. Hence the need to create a procedure for the design and validation of solution to protect the works of art from the vibrations generated during transport. This procedure, developed in the ambit of the project Tech4MUBAS, funded by the Italian Ministry of Cultural Heritage and Activities, consists in the creation of a finite element model which is then validated through experimental tests. A polymeric matrix material, called Sorbothane, is considered to be used as an interface between the source of vibrations and the crate in which the works of art to be transported is placed. In this case of study, as artwork to be transported, an earthenware made vase is considered. It is chosen with shapes and dimensions that can be representative of most of the works of art of this type. A study of the material is therefore necessary in order to determine the information relating to its hyperelastic and viscoelastic properties, obtaining the parameters necessary for the material definition in Abaqus CAE software, used for the realization of the finite element model. Studies relating to the dynamics of the vase are conducted in order to determine its resonance frequencies, identifying the first vibration modes at a frequency equal to 950 Hz. This value is important since the protection system must be implemented to filter below this frequency. The determined material parameters are than used for the creation of finite element models for very simple configurations, composed of steel parallelepipeds supported by Sorbothane pads of various shapes and sizes. Experimental tests on these configurations are then conducted in order to validate the models, obtaining, with some approximations, good results. It is then considered a more complex configuration which consists of a wood crate, of dimensions suitable to contain the “typical” object represented by the vase, supported by four Sorbothane pads. Also for this configuration, a finite element model is created and then validated through experimental tests, obtaining a vertical proper frequency very close to that obtained experimentally. The considered procedure can therefore be repeated for other case studies and for other configurations.

Sommario

La salvaguardia delle opere d'arte anche durante il trasporto è di primaria importanza, per tale ragione è necessaria una continua evoluzione dei sistemi di protezione. Da qui nasce l'esigenza di realizzare una procedura per la progettazione e la validazione di soluzioni per proteggere le opere d'arte dalle vibrazioni che si vengono a generare durante il trasporto. Tale procedura, sviluppata nell'ambito del progetto Tech4MUBAS, fondato dal Ministero Italiano dei beni e delle attività culturali, consiste nella realizzazione di un modello ad elementi finiti che poi viene validato attraverso test sperimentali. È stato considerato un materiale a matrice polimerica, denominato Sorbothane, per essere utilizzato come interfaccia tra la sorgente delle vibrazioni e la cassa in cui è contenuta l'opera d'arte da trasportare. In questo caso di studio, come opera da trasportare, è stata considerata un'anfora di terracotta, scelta con forme e dimensioni tali da poter essere rappresentativa della maggior parte delle opere di questa tipologia. Si è reso quindi necessario uno studio del materiale con lo scopo di determinare le informazioni relative alle sue proprietà iperelastiche e viscoelastiche, ottenendo i parametri necessari per la definizione del materiale all'interno del software Abaqus CAE, utilizzato per la realizzazione del modello ad elementi finiti. Studi relativi alla dinamica del vaso sono stati condotti in modo da determinare le sue frequenze proprie, individuando il primo modo di vibrare alla frequenza di 950 Hz. Tale valore risulta essere importante in quanto il sistema di protezione dovrà essere realizzato per filtrare al di sotto di tale frequenza. I parametri del materiale determinati sono quindi stati utilizzati per la creazione di modelli ad elementi finiti per configurazioni molto semplici, composte da parallelepipedi di acciaio supportati da tappetini di Sorbothane di varie forme e dimensioni. Successivi test sperimentali su tali configurazioni sono stati condotti con lo scopo di validare il modello, ottenendo con alcune approssimazioni, dei buoni risultati. Si è passati quindi ad una configurazione più complessa che consiste in una cassa di legno, di dimensioni adatte a contenere l'oggetto "tipo" rappresentato dall'anfora, supportata da quattro tappetini di Sorbothane. Anche per tale configurazione è stato realizzato un modello ad elementi finiti che è stato validato attraverso test sperimentali ottenendo una frequenza propria verticale molto vicina a quella ottenuta sperimentalmente. La procedura considerata può essere quindi ripetuta per altri casi di studio e per altre configurazioni.

Table of contents

Introduction

The safety of travelling works of art, especially during the phases of handling and transport, is a top priority in implementing policies for cultural promotion in a period, like the one we are living in, where globalization constitutes a characterizing phenomenon with a consequent increase of relationships and exchanges in different contexts on a global scale, where often the concept of fruition of a good goes to conflict of with that of its conservation.

For this reason, a project named Technology For the MUseum of the BASilicata (Tech4MUBAS)[1] has the purpose of creating a procedure that allows to identify the most effective packaging and damping system's design starting from the knowledge of the information of the artwork that must be handled (e.g. material, weight, weaknesses, etc.).

The companies involved in the project are the following:

POLITECNICO MILANO 1863	**Politecnico di Milano, Dipartimento di Meccanica**	https://www.mecc.polimi.it/
	C.B.C. Conservazione Beni Culturali Soc. Coop.	http://cbccoop.it/
ARTERÌA	**Arterìa S.r.l.**	http://www.arteria.it/
3D RESEARCH	**3D Research S.r.l.**	http://www.3dresearch.it/

Each of these companies provides their own expertise in the various areas of the project.

Thanks to the experience acquired over the years in the area of restoration of works of art, the C.B.C. company follows the aspects related to the restoration, cataloguing and risks assessment. 3D Research company, instead, deals with 3D scans, FE modelling of works of art and for the design of customized support solutions. Arterìa, finally, is one of the major Italian companies in the field of logistics of works of art, and it takes care of the problematic tied to the transport and the packaging of such valuable objects, supplying indications regarding techniques and material mainly used in

[1] Project funded by the Ministero dei beni e delle attività culturali, Istituto Superiore per la Conservazione ed il Restauro, as a part of the project PON Cultura e Sviluppo ERDF 2014-2020 Asse I – ISCR Project "Capolavori in 100 Km, un viaggio reale e virtuale nella cultura della Basilicata, per conoscere, conservare, valorizzare". Partnership procedure for innovation according to art. 65 of Legislative Decree 18 April 2016, n. 50 for the development of services for the transport and exhibition of artistic artefacts of museums of Basilicata to be realized with innovative systems of management and movement of the elements in relation to the priority objective of vibration reduction.

this field to the Department of Mechanical Engineering of Politecnico di Milano, which then perform experimental tests and modelling through FEM technique to find the best solution for the vibration reduction during transport.

An important aspect of this project regards the crate protection. The idea is to design pads using material with damping capabilities and to attach them at the base of the crate in order to reduce the vibration transmission.

A preliminary research among the materials with damping behaviour available on the market and a study of their properties is needed in order to select those that have characteristics suitable for our purpose.

After this preliminary analysis the materials selected, and considered during the project, are:

- Sorbothane
- Plastazote
- Ethafom
- Polyester Urethane Polymer

The materials considered are all polymeric. The intrinsic characteristics of this kind of materials make them suitable for vibration absorption. The mechanical properties of this type of materials depend on preload and frequency and this make difficult to understand the behaviour in different situations. In particular, they usually show both viscoelastic and hyperelastic behaviour and so they cannot be treated as pure solid or pure fluids materials. For this reason, it is useful to present the static and dynamic characteristics and mechanical properties of this type of materials as well as the various models found in literature that make possible a correctly characterization.

A correct material characterization is necessary for the creation of finite element models to predict the damping capacity of the material under different load levels. The models must then be validated experimentally.

In this thesis only Sorbothane is considered. Some simple predictive models are realized in Abaqus CAE using the viscoelastic and hyperelastic properties determined through a characterization procedure. These models are then experimentally tested in laboratory in order to be validate.

A study case of this project is related to the protection of an earthenware vase, 3D scanned by the company 3D Research and faithfully reproduced by a ceramist. This vase is chosen because it has very common dimensions and shapes resulting representative of many works of art of this category usually transported. The characterization of this vase is important since in order to adequately protect it, it is necessary to know its mechanical properties. In particular, in this thesis work, its vibration modes are determined through experimental test, considering the deformed shapes obtained by the FE model realized by 3D Research.

The knowledge of the dimension of the typical vase is important in this work since the crate considered to be supported by Sorbothane pads, is chosen in order to be able to contains the characterised vase. A FE model is realized for this configuration and the Sorbothane properties,

object of validation for simple configuration, are then reported in this model. To verify the correctness of the model experimental tests also on this configuration are performed.

The Chapter 1 is divided in two main parts. In the first one the attention is focused on the problem related to the undesired vibrations generated during transport of valuable artworks, analysing the common adopted packaging techniques, the common transportation methods and the common insulation methods used to reduce this problem, considering their evolution over the years. In the second part of the chapter there is a detailed explanation of the polymer characteristics and mechanical properties in order to understand the reason to choose this kind of material as vibration absorber. Common methods find in literature to characterize viscoelastic and hyperelastic properties are also described.

The Chapter 2 presents the Sorbothane material and the fitting procedure used to characterize this polymeric material in terms of hyperelasticity and viscoelasticity obtaining the fundamental parameters needed for the material definition in Abaqus CAE software used to create the FE model and to perform the FE analysis.

The Chapter 3 describes the steps carried out to create the finite element models representative of five simple configurations and the implementation of the Sorbothane properties previously determined to model the pads. The results obtained after the FE simulations are then compared to the ones obtained through an experimental testing procedure performed in laboratory, detailed described in this chapter, on the same configurations modelled. The comparison of the results has the aim of validating the FE models.

The Chapter 4 contains a detailed description of the experimental evaluation procedure used in order to determine the vibration modes of a reproduction of an ancient ceramic vase. A comparison between the transfer function obtained experimentally and the deformation obtained for each mode from the FE simulation is performed in order to determine the frequency corresponding to each mode.

The Chapter 5 presents the finite element model creation for a complex configuration composed by a real crate supported by four Sorbothane pads modelled using the material parameters validated in the chapter 3. The results obtained by the FE model simulations are than compared to the ones obtained from experimental tests also described, in order to validate the material characterization also for this configuration.

1. Problem assessment and literature review

1.1Safety transportation of artworks

1.1.1 Introduction to transportation

The transport of unique priceless masterpieces is a delicate operation and there are several specialized companies that work specifically on this field. A European standard [1] tries to regulate all the aspects related to the collection mobility defining principles to be considered when transporting movable cultural heritage. It is a result of a collaboration with a lot of professionals from Europe regarding all the parties involved in the transport presenting the successive steps of moving objects using relevant means of transport and providing recommendations for the safe and secure transport of cultural heritage. In particular, it indicates the roles and the responsibilities of the various parties involved and provides a guideline for choosing the type of transport considering some factors as the dimensions and the weights of the objects and their conditions. In addition it is also specified the requirement that the means of transport should have to guarantee greater safety during transport.

Since the transport involves risks, the planning starts with the assessment of these risks in order to choose the transportation method appropriate to the particular situation, to take necessary measures to avoid damage to the objects.

In the previous reported standard there are no indications regarding the practices commonly used for packaging artworks, for this reason the collaboration with Arteria, that is one of the most important Italian companies that deals with the transport of artworks, is crucial since thanks to the experience gained over the years can help us to understand the usually adopted solutions.

1.1.2 General packaging operations

Once is verified that an artwork can be moved without a huge increase of risk of damage, the packaging phase can start. Each artefact is unique, it shows particularities and problems related to constitutive materials, shape, weight and dimensions and in some cases alterations due to previous impacts. For these reasons it is fundamental the collaboration between museum curators and packing technicians. Objects have to be packed in a way that is in solidarity with the case [2]. Each company use a different packaging strategy, but usually it is made up by three layers of protective materials.

The first one is the one in contact with the object and protects it from dust and scratches. For this important layer the material used must be chemically and physically neutral. It is also good to have a transparent material in order to enable to see the object under this first protection. Depending on

case and budget the material that can be used are for example tissue paper, glassine, Melinex, or polyester fiber based compound.

The second layer is an intermediate cushion material used to reduce vibrations, to absorb impacts and to attenuate temperature variation. The temperature control during transport is very important especially for paintings. The most used cushioning materials are polyethylene foam or polyurethane in all its form, thickness and densities.

The last layer is a rigid shell, realized to be impact resistant and to facilitate the handling. This one is practically the crate. The crates in which the artworks are transported are commonly made by wood, especially plywood. The type of case is chosen as function of the artefact to be transported and its fragility.

Not always are necessary all the three layers, it depends on the kind of work of art that has to be transported.

The earthenware, marble and metallic sculpture are always transported in crate, single or double [3]. The double crate is realized by inserting into the external crate another crate with a layer of damping material in between. The choice is made on the specific case.

The object placed in the crate has to be generally fixed with shaped and padded wooden spacers or partitions that have to be positioned in the points in which friction between the surface of the artwork and the crate can occur, to avoid the consequent generation of stress due to the pressure.

It may also be necessary to provide a padding or a filling with polyurethane foam in the point of weakness or fragility of the object; this represent the second layer of protection described above.

If the object to be transported is sensitive to humidity and temperature changes, it is necessary to seal the crates and size them in order to contain also a sufficient quantity of stabilizing material to maintain the relative humidity within the allowed range for the best conservation of the object. To obtain better efficiency the stabilizing material has to be uniformly distributed in the crate to have the largest exchange surface [2].

Particular attention must also be paid to the choice of material used to make the cases and those that come into contact with the artwork (fills material, spacers, etc.) which must not emit harmful substances.

When the artwork is correctly packed, the transport phase can start.

1.1.3 Types of transport

It is important to know all the phases of the operations to which the object is subjected during transport. The shipper must be informed of all the particularities and the weaknesses of the artwork.

The total size of the packed object and the need to travel in a vertical or horizontal position must also be specified. This information is relevant to choose the mode in which the transport can be carried out. Usually the transport is carried out on the road or by airway.

The transport on the road, carried out using trucks, is chosen for relative short distance or where the dimensions of the object does not permit the use of air carriers. To avoid transport "trauma", trucks used for this kind of transports are equipped with air suspension, temperature control and with hydraulic tailgate for loading and unloading operation in safety conditions.

When the size of the crate allows it, it is better to use air transport because it is faster and less expensive. Air shipment can be of two types:

Freight: In this case the artwork is placed in the hold of a passenger or cargo plane. This kind of shipment is correlated to the crate dimension and positioning (vertically or horizontally directed) in which it must travel. To ensure stability of the crates it is preferable to use flights that can accommodate containers or pallets, but on most flight for European destinations it is possible to load crates with a maximum height of 80 – 114 cm [3].

Hand-Carry: The artwork travel with the attendant in the cabin of the aircraft. For this kind of transport, the size of the crate must be similar to that of a hand luggage. The artwork must be placed under the front seat or on an extra seat next to the passenger seat [3].
Whichever types of transport is chosen, special attention must be given to the vibration transmitted to the crate containing the artwork.

1.1.4 Crate design and configurations – Literature review

Over the years, various solutions have been proposed for the realization of crates designed to transport valuable and fragile goods.

The first patent found in literature regards a crate capable of withstanding minimum force of 300G and frequency from 0 Hz to 50 Hz [4]. This light weight, reusable crate with also humidity control and breathing control have an internal crate suspended by means of cable-type isolators usually composed by stainless steel cable and aluminium retaining bars. This kind of isolators are corrosion resistant.

It can be considered as the first double crate configuration.

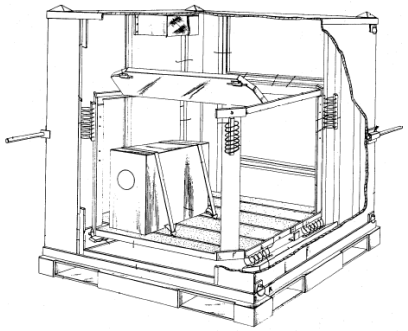

Figure 1.1: Schematic representation of the double crate configuration [4]

An evolution of the previous patent is presented many years later [5]. It consists in a double crate configuration, composed by an outer housing that contains an inner housing realized by means of a solid and ductile material. The outer housing is constituted by two parts which are a body and a lid defining a meeting plane to connect the two parts through bolts. Shock absorbing suspensions are realized in natural rubber and are placed between the two cases.

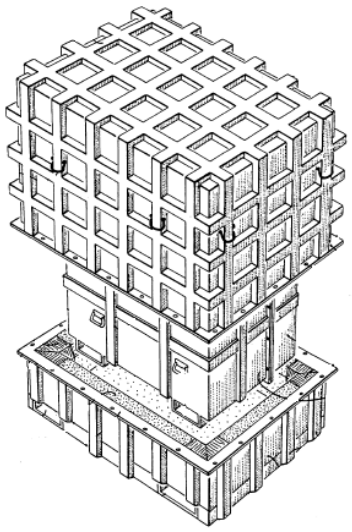

Figure 1.2: Schematic representation of the double crate configuration [5]

A patent registered in the last decade [6] can be considered as an alternative method for packing valuable articles to protect them against damage during transportation and storage, with an increased ease to construction and economy of materials. It maximises the effective protective packaging tailored specifically to the particular dimensions and configuration of a valued article, such as artwork, an antiquity or a collectible, with minimal expense.

It enables an increased ease of unpackaging valued articles with a minimize risk of damage during this phase and with a reduced waste of materials.

The container is composed by an inner crate having an interior for receiving the article to be transported with filler material interposed between the object and the outer wall of this box, and by an outer wall including an exterior surface that extends circumferentially around the inner case. The internal crate is separated by the outer one by means of suspenders dimensioned to ensure precise insertion. The suspenders establish an open gap along circumferential distances between adjacent suspenders in addition to suspending the inner crate from the outer crate. The suspender is constructed of a shock absorbent material for deterring the transmission of shocks from the outer crate to the inner crate; a material that can be considered for this purpose is the polyurethane foam in fluid form injected into each corner in the space between the two crates. Spacers, realized using a relative weak material, are used as dams to confine the fluid foam to the corner. To protect the artwork in the internal crate, filler blocks are interposed; the preferred mode to package vessel is to inject a fluid polyurethane foam into the inner case to establish the lower filler block, then the vessel, covered by a suitable lower parting sheet, is pressed into the poured volume. Then an upper part of parting sheet is placed over the vessel and a sufficient quantity of polyurethane foam is injected to cover the vessel to realize the upper filler block. Once the polyurethane foam is dried, the artwork results safety confined in the filler block. The successive removal of the artwork from the inner case is facilitated by the parting sheets. Once the inner case is correctly isolated an outer cover member is mounted in juxtaposition with the frame of the outer case.

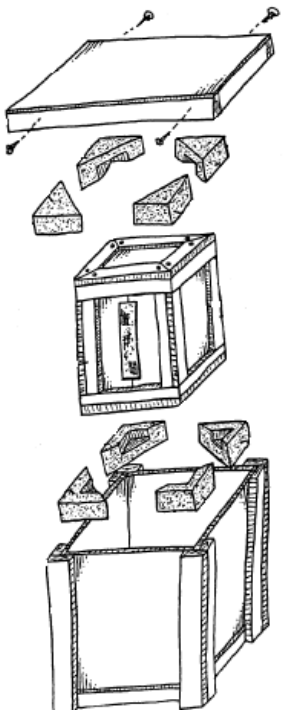

Figure 1.3: Schematic representation of the double crate configuration [6]

1.1.5 Vibration isolation and impact protection

One of the main problems to face during the transport of the artwork is the vibration transmitted from the source to the object. The range of vibration that can be considered during transport goes from about 0 Hz to 300 Hz depending on the transportation method used.

Vibrations produced during transportation are controllable, with known and programmable times and with the possibility of acting effectively by in reducing the produced stress, also through the use of packaging and suspension systems correctly designed.

Previous illustrated methods to package and transport fragile articles such as artwork are studied to reduce this problem. Lot of work is done in previous years in order to isolate internally the object with respect to the crate but only in the last years, important galleries and companies specialized in transport of works of art, start to consider the possibility to protect the crate (external crate in case of double crate configuration) from vibration and impacts produced during the transport and generally during the handling phase.

Recently, to improve the impact protection, devices called skid mates have been used. They consist in an air dampened cushioning device made of polyethylene, a chemically inert material, for extra shock absorption that can easily mounted on the base of the crate by bolted joint. Since they are designed to avoid damages due to impacts from falling, their behaviour related to vibration absorption has not been thoroughly analysed.

1.2 Polymeric materials

1.2.1 General description and classification

The commercial success of polymer based product has generated a demand that the total production of plastics, by volume, has exceeded the combined production of all metals for more than 20 years. [7] The Polymer Science evolved from the following five separated technologies:

- Plastics
- Rubbers or Elastomers
- Fibers
- Surface Finishes
- Protective Coatings.

In more recent years, polymers have become an engineering structural material of choice due to low cost, ease of processing, weight savings, corrosion resistance and other advantages.

The knowledge of the natural polymer's composition was generally unknown before the middle of nineteenth century. At that time, the chemical or molecular character of a material's composition

was defined in terms of its stoichiometric formula and its properties were defined in terms of colour, crystal habit, specific gravity and other characteristics.

Only at the beginning of the twentieth century the attentions are carried to the chemical structure of material, which together with advances in measurement techniques, led finally to understanding and later to acceptance of polymers as consisting of large covalently bonded molecules.

In the late nineteenth century, materials now defined as molecular high polymers were thought to be composed of large molecules or colloidal aggregates. These colloidal aggregates were said to form from smaller molecules through the action of intermolecular forces of "mysterious origin" which were responsible for the unusual properties such as high viscosity, long-range elasticity, and high strength [8].

The critical problem in evaluating the molecular nature of polymers in the early twentieth century was the lack of quantitative characterization methods. Perhaps the greatest limitation lies in the limited ways available to accurately measure the high molecular weights of macromolecular materials, since the vapor density method which was widely applied for low molecular weight material could not be employed. After a lot of studies, polymer scientists introduced the concepts of statistical thermodynamics to describe the characteristics of long chain polymers of high molecular density.

More than 30 individuals have been awarded the Nobel prize for Chemistry for their contributions either directly or indirectly to the development of polymer science and associated technology.

Nowadays it can be said that a polymer is composed of many simple molecules that are repeating structural units called monomers. Each single polymer molecule consists of hundreds or of a million of monomers and may have a linear branched, or network structure. The covalent bonds hold atoms in the polymer molecules together and the secondary bonds holds groups of polymer chains together to form the polymeric material. An example of molecular chain is present in the following figure in which can be seen the molecular structure of polyurethane

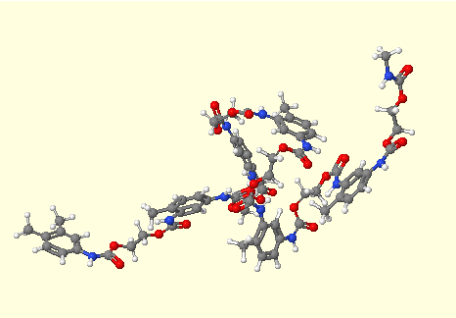

Figure 1.4: 3D representation of polyurethane molecular structure

Exist a variety of way to characterize polymers accordingly to their molecular structure, but generally most of the polymers can be divided in two important groups, thermoplastic and

thermosets. The fundamental physical difference is referred to the bonding between molecular chains.

In particular, thermoplastics have only secondary bonds between molecular chains, while thermosets also have primary bonds between chains. This difference can be seen by looking at the material properties.

Thermoplastic polymers may be either amorphous or crystalline (rarely over 50% crystalline). Crystalline polymers are often more dense than amorphous due to the closer packing of their long molecular chain molecules. In general, the following properties are enhanced:

- Hardness
- Friction and wear
- Less creep or time dependent behaviour
- Corrosion resistance and/or resistance to environmental stress cracking

An example of this kind of polymers is polyethylene.

In general, this kind of polymers are easier to produce and cost less than thermosets.

A special subgroup is Thermoplastic Elastomers (TPE) that exhibit properties of both thermoplastic and elastomers, which are typically thermosets. They consist of two different polymers in a block copolymer arrangement which phase segregate into hard and soft domains.

Thermosetting polymers are used when high thermal and dimensional stability are required. They show a glass transition temperature below the room temperature. This kind of polymers are irreversibly hardened by curing from a soft solid or viscous liquid prepolymer or resin.

An example of this kind of polymers is polyurethane.

A particular class of thermosetting polymers is represented by elastomers that exhibit high flexibility and are used in application such as seals, dampers, insulation and tires. This kind of polymers are amorphous and molecular chains are held together by relatively weak intermolecular bonds, which permit them to stretch in response to a macroscopic stresses.

Sometimes a pure synthetic polymer may not have desirable characteristic for a particular application. With the use of some additive or fillers, various properties such as toughness can be modified.

For the same reason two or more plastics are mixed (alloyed) to achieve special properties and are known as polyblends. An example of this kind of plastic is the ABS (acrylonitrile butadiene and styrene) often used in engineering applications with polycarbonate.

As result many structural plastics are composites, obtained by combination of several materials. In this way engineers can obtain a material with desired properties by combining the effect of various additives.

The additives alter the polymer, and this may cause a polymer to be both heterogeneous and anisotropic and since most of the test made to measure properties are performed by considering the

material homogeneous and isotropic, this can be not adequate to evaluate long-term structural performance of a polymer used in engineering design.

1.2.2 Fields of applications

Polymers are widely used in all the common industries thanks to their intrinsic characteristics. We have also to consider that the cost to produce polymers is sometime less than the cost to produce certain metals.

Polymer products are replacing other material for a lot of non-structural applications, because the modulus and strength of polymers are lower than the ones of the metal for example and cannot work very well in some structural fields. The exception is for fiber reinforced polymers but then the production cost is often much higher.

1.2.3 Mechanical properties of polymers

Polymers are materials that have unique response to mechanical loads and are treated so that in some instances behave as elastic solids and, in some instances, behave as viscous fluids.

Considering that their properties (mechanical, optical, electrical, etc.) are time dependent and cannot be treated mathematically by the laws of either solids or fluids, the study of such material began long before the macromolecular nature of polymers was understood.

As the knowledge of the physical nature of polymers increased and synthesis techniques was improved, many polymers of widespread usage were developed. Since these materials were employed in devices and structures become necessary to analyse and understand from an engineering point of view the response of polymers to load and other environmental variables, such temperature and moisture.

Today, high performance polymer composites are used for critical applications, and thus the study of the mechanics of polymers as a structural material is an important research area.

We are now able to say that the fundamental difference between polymers and other material resides in the inherent rheological or viscoelastic properties of polymers. This can be seen by looking that the mechanical properties of polymers such as Young Modulus, Poisson's ratio vary with time. This time dependent behaviour depends on their unique molecular structure. In particular, we can say that the long chain molecular structure of polymer give rise to the phenomena of "fading memory", and this create the need to determine engineering properties in a different way compared to those used for traditional structural materials.

Generally, studying the mechanics of materials, there are five fundamental assumptions normally made about the characteristics of the material for which analysis can be considered valid.

These are:

- **Linear:** Two types of linearity can be considered: Material linearity (Hookean stress-strain behaviour) or linear relation between stress-strain, Geometrical linearity or small strain deformation.
- **Homogeneous:** Material properties are the same at every point.
- **Isotropic:** Material which have same mechanical properties in in all directions.
- **Elastic:** Deformations due to external load are completely and instantaneously reversible upon the load removal.
- **Continuum:** Matter is continuously distributed for all size scales, no holes or void in the composition.

Under these assumptions the elementary analysis can be valid independently on the material considered. However, if these assumptions cannot be satisfied, serious errors occur if the analysis performed are not changed accordingly.

These elementary definitions are not always valid to determine the stress-strain characteristics of polymers, for example if polymers are loaded varying the strain rate, the behaviour varies significantly.

Sometimes the polymer manufacturer specifies elastic modulus, yield strength, strain to yield, etc. as determined by these elementary techniques. So, we must pay attention to this, considering that if we need more appropriate specifications, other consideration has to be made.

The mechanical properties of polymer are typically obtained by performing a uniaxial tensile test at constant rate of strain or head motion, similarly to those used for metals and other materials.

We can find some stress- strain diagrams that indicates the types of solid polymers, for example the following one [7].

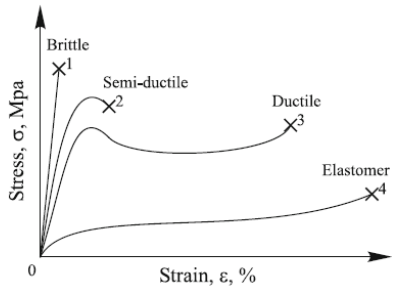

Figure 1.5: Stress-Strain diagrams for solid Polymers [7]

In the diagram we can see four curves, the curve 1 represent a linear elastic and brittle material (e.g. polystyrene), curve 2 is similar to the one of a semi-ductile material (e.g. PMMA), curve 3 is similar

to the one of a ductile material (e.g. PET), curve 4 is similar to the one of a typical elastomer (e.g. flexible urethane).

For an elastomer, the stress-strain curve is highly non-linear, and the deformation is mostly reversible up to elongation at break that can be several hundred percent. This behaviour is also known as hyperelasticity.

The determination of mechanical parameters is usually performed toward the elementary definitions as explained above except for the determination of yield stress for which the common method used is to consider it equal to the proportional limit stress or the first peak in the stress-strain diagram.

If some tests are performed at different constant strain rate or temperatures, resultant stress-strain diagram will be different and so the modulus and yield stress vary with both temperature and rate [7].

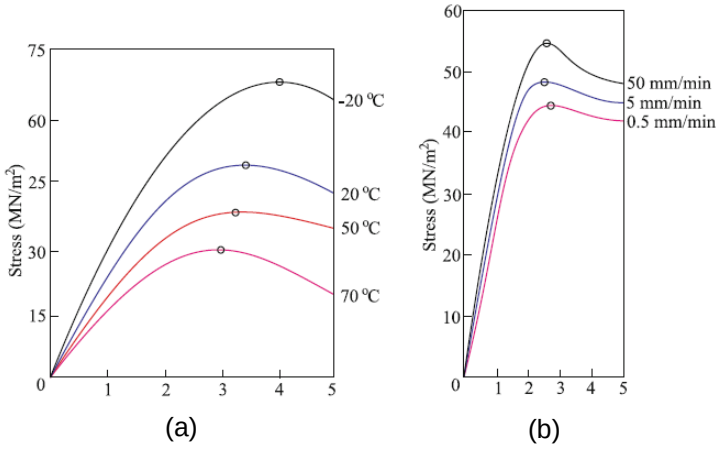

Figure 1.6: Stress- Strain variation, function of temperature (a) and rate (b)

We can also say that the stress-strain response appears nonlinear even for low stress levels. In all the cases we have to pay attention during the interpretation of the information obtained from elementary tests.

Most industry specifications for properties are determined using standards provided by American Standard of Testing Material (ASTM). By looking at the standard used, we can understand the kind of test performed to obtain the value found on the datasheet, and this can be a good way to understand the robustness of the data.

1.2.4 Viscoelasticity

Since the mechanical properties of polymers varies as function of the load application rate and consequently the response of polymer-based materials, due to their unique molecular structure, depends on time, it's clear the difference from time dependence induced in other materials such as

metals by fatigue, corrosion or other environmental factors. The same environmental factors affect polymers with different results compared to other materials due to the intrinsic viscoelastic nature of the molecular structure [7].

To understand the viscoelastic behaviour of a polymer a constant strain can be applied to a specimen in a quasi-statically way. If the specimen is maintained fixed, so that the strain remains constant, the stress needed to maintain this deformation decreases with time. This is also the aim of the so called relaxation test.

The stress can go to zero for an ideal thermoplastic polymer. The following figure shows the typical thermoset and thermoplastic material behaviour under relaxation test.

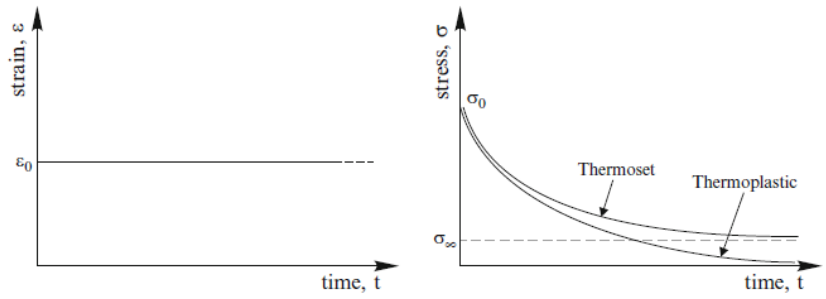

Figure 1.7: Behaviour of Thermoplastic and Thermosetting polymers under Relaxation Test

It can now be said that since the stress is function of time and the strain is constant, the modulus will also vary on time. The modulus obtained is defined as relaxation modulus of the polymer and is given by the following relation:

$$E(t) = \frac{\sigma(t)}{\varepsilon_0} \tag{1.1}$$

or

$$\sigma(t) = \varepsilon_0 \, E(t) \tag{1.2}$$

Values of limiting moduli at time t=0 and time t=∞ are defined as,

$$E(t=0) = \frac{\sigma(t=0)}{\varepsilon_0} = Initial\ Modulus \tag{1.3}$$

$$E(t=\infty) = \frac{\sigma(t=\infty)}{\varepsilon_0} = Equilibrium\ Modulus \tag{1.4}$$

Another example that can be used to explain the viscoelastic behaviour of polymers may be to take a specimen and subject it to a constant stress. Maintaining the load constant it can be seen that the strain increases with time.

This is also the procedure used to perform the so called creep test and as result a quantity called creep compliance can be defined as,

$$D(t) = \frac{\varepsilon(t)}{\sigma_0} \tag{1.5}$$

so that,

$$\varepsilon(t) = \sigma_0 D(t) \tag{1.6}$$

In a creep test the strain will reach a constant value after long time for thermoset polymers and increase without bound for thermoplastic polymers.

Values of initial and for equilibrium compliance can be defined similarly to initial and equilibrium modulus

Performing a constant stress test can be important to analyse what happens to the strain if the stress is removed, this is called creep recovery test. We can see in the following figure [7] that for an ideal thermoset polymer the strain goes to zero after an enough time interval, long compared to loading time. For an ideal thermoplastic polymer, a residual deformation will remain even after a very long (or infinite) time.

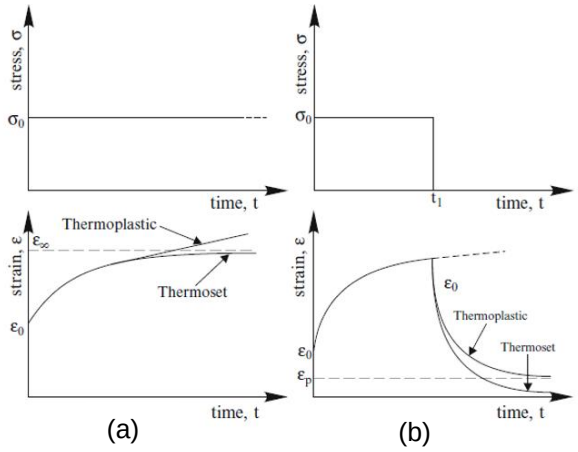

Figure 1.8: Behaviour of Thermoplastic and Thermosetting Polymers under creep test (a) and under creep and recovery tests (b)

Deformation mechanisms associated to relaxation and creep are related to the long molecular chain structure of polymers. Continuous loading induces gradually strain accumulation in creep as the polymer molecules rotate and unwind to accommodate the load. In a relaxation test in which there is a constant strain, the initial sudden strain occurs more rapidly than can be accommodated by the molecular structure, but with time the molecules will again rotate and unwind so that low stress is needed to maintain the constant strain level.

It is now clearer that polymers have some characteristic of solid and some characteristics of a fluid.

In a relaxation test, the ratio of initial stress strain is:

$$E(t=0)=\frac{\sigma_0}{\varepsilon_0} \tag{1.7}$$

and from creep test we obtain,

$$D(t=0)=\frac{\varepsilon_0}{\sigma_0} \tag{1.8}$$

analogous to the behaviour of elastic solid.

On the other hand, in a creep test the rate of change of the strain (slope) for a thermoplastic material is,

$$\frac{d\varepsilon(t=\infty)}{dt}=constant \tag{1.9}$$

after a sufficiently long time, which is a characteristic of fluid.

This flow characteristics of thermoplastic polymer are due to the lack of primary bonds between molecular chains and the solid characteristics of thermoset polymers are due to the presence of primary bonds between individual chains.

In both thermoset and thermoplastic polymer, creep is related to the motion of molecules between entanglements, while the mechanism for creep are limited to motion between crosslinking sites for thermosets.

We must pay attention that if a very soft material is tested in creep, the cross sectional area may change as the material creeps, in that case the test may not be significant. In that case the load must be changed in time such that the amount of load divided by the changing area remains constant.

1.2.5 Phenomenological models for viscoelastic materials

Elementary mechanical models can be used to describe the viscoelastic polymeric behaviour. These simple models are very helpful in order to obtain physical understanding of the phenomena of creep, relaxation and other procedures used to understand the stress-strain behaviour for this kind of materials.

The simplest one consists of two elements: a spring to simulate the elastic behaviour and a damper to simulate the viscous behaviour.

First it is introduced a model of a linear spring to represent an Hookean bar under axial tension where the spring constant is the modulus of elasticity.

Now considering a semi-infinite fluid. If a flat plate at the top of fluid is moved with a certain velocity V, with the hypothesis of Newtonian fluid, that means that the viscosity is constant and independent form the velocity at which is measured, or alternatively the shear deformation varies linearly from top to bottom assuming a no slip boundary condition between fluid and plate and between fluid and container [7].

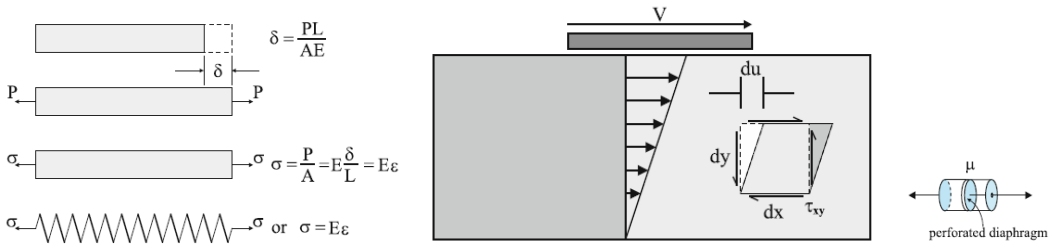

Figure 1.9: Physical description of simple phenomenological model for viscoelastic materials

The Newtonian law of viscosity for the shear process may be expressed as,

$$\tau = \mu \frac{d}{dt}\left(\frac{du}{dy}\right) = \mu \frac{d\gamma}{dt} = \mu\dot{\gamma} \tag{1.10}$$

where μ is the viscosity and $\frac{du}{dy}$ represents the strain in an infinitesimal element of the fluid.

A linear viscous damper can be used to model a Newtonian fluid such that it can form a uniaxial fluid analogue to a tensile bar. The housing of the damper contains a fluid with viscosity μ. The diaphragm is perforated and when it is pulled through the fluid by a force, motion occurs following the Newtonian Laws of viscosity.

Spring and damper element can be combined in order to simulate the viscoelastic response.

Maxwell model combine a linear spring in series with a Newtonian damper [7].

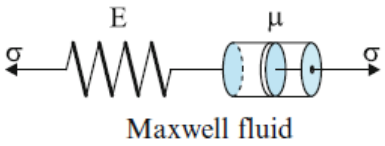

Figure 1.10: Maxwell fluid model

As said before, this model is useful to describe mathematical relations between stress and strain in viscoelastic polymers and in giving insight to their response to creep, relaxation and other types of loading.

For Maxwell model the equation between stress and strain can be obtained using equilibrium and kinematic equations for the system and constitutive equations for the elements.

In this case the equilibrium gives,

$$\sigma = \sigma_s = \sigma_d \tag{1.11}$$

with σ is the applied stress, σ_s is the stress in the spring and σ_d is the stress in the damper

Kinematic condition is,

$$\varepsilon = \varepsilon_s + \varepsilon_d \tag{1.12}$$

with ε is the total strain in Maxwell element, ε_s is the strain in the spring and ε_d is the strain in the damper.

Constitutive equations are,

$$\sigma_s = E\varepsilon_s = \sigma \tag{1.13}$$

and

$$\sigma_d = \mu\frac{d\varepsilon_d}{dt} = \mu\dot{\varepsilon_d} = \sigma \tag{1.14}$$

Differentiating the kinematic condition and replacing the strain rate of the spring and of the damper, the relation between stress and strain is obtained,

$$\dot{\sigma} + \frac{E}{\mu}\sigma = E\dot{\varepsilon} \tag{1.15}$$

This differential equation can be solved for particular cases of stresses and strains. Usually the equation is written in standard form with the ascending derivatives from right to left on both sides of the equation obtaining,

$$\sigma + \frac{\mu}{E}\dot{\sigma} = \mu\dot{\varepsilon} \tag{1.16}$$

In this form the inverse of the coefficient of the stress rate is defined as the relaxation time $\tau = \frac{\mu}{E}$.

To obtain the solution in case of creep test, in which the applied stress is constant and can be written as,

$$\sigma(t) = \sigma_0 H(t) \tag{1.17}$$

with H(t) called Heavyside function and defined as,

$$\begin{aligned} H(t) &= 1 \; for \; t > 0 \\ H(t) &= 0 \; for \; t < 0 \end{aligned} \tag{1.18}$$

That means stress constant for time greater than zero. Having this input, the solution will be

$$\varepsilon(t) = \sigma_0\left(\frac{1}{E} + t\frac{1}{\mu}\right) \tag{1.19}$$

or

$$\varepsilon(t) = \sigma_0 D(t) \tag{1.20}$$

where

$$D(t) = \left(\frac{1}{E} + \frac{1}{\mu}\right) \tag{1.21}$$

represent the creep compliance.

The solution of equation (1.15) in case of relaxation test is obtained using a step input in strain,

$$\varepsilon(t) = \varepsilon_0 H(t) \tag{1.22}$$

with a resulting stress output,

$$\sigma(t) = \varepsilon_0 E e^{-t/\tau} \tag{1.23}$$

where

$$E(t) = E e^{-t/\tau} \tag{1.24}$$

represent the relaxation modulus.

The stress at time equal to the relaxation time is defined as,

$$\sigma(t = \tau) = \frac{\sigma_0}{e} \tag{1.25}$$

This represent the definition of the relaxation time for a polymer, allowing to find the relaxation time easily from experimental data without the use of a mathematical model.

Relaxation time can be used as material property to give an information of the time scale associated with viscoelastic response of polymers.

We can say that Maxwell model provide a defining relationship for the viscosity of a material.

In order to understand better, we can consider the response to a Maxwell fluid under a constant strain rate loading.

In case of constant strain rate, we have that,

$$\varepsilon = Rt \tag{1.26}$$

$$\frac{d\varepsilon}{dt} = R = constant \tag{1.27}$$

The differential equation becomes

$$\sigma + \frac{\mu}{E}\dot{\sigma} = \mu R \tag{1.28}$$

with solution that has the form,

$$\sigma(t) = \tau E R \left(1 - e^{-\frac{t}{\tau}}\right) \tag{1.29}$$

or knowing that $t = \varepsilon/R$

$$\sigma(\varepsilon) = \tau ER\left(1 - e^{-\frac{\varepsilon}{\tau R}}\right) \tag{1.30}$$

Hence for various constant strain rate, several results are obtained. This can be seen looking at the figure below [7]

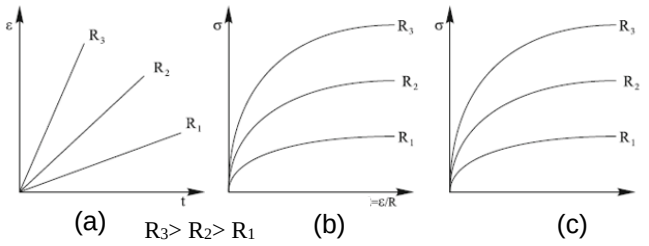

R3> R2> R1

Figure 1.11: Constant strain rate - Strain VS time (a) - Stress VS time (b) - Apparent stress-strain response (c)

While the stress versus time curves would be linear for a single spring (pure elastic material), the result for the Maxwell element appears nonlinear since the damper continuously relaxes some of the stress as time increases. The stress strain behaviour is shown in figure (c).

The stress strain response might be mistakenly interpreted as nonlinear, even though the model is composed only by linear element; the reason for this is due to the relationship among strain and time.

We can say that is not possible to determine if the material is linear only by looking at the shape of an experimentally determined response to a constant strain rate test as generally conducted in laboratory. Linearity can only be assessed by determining if the material response is independent of stress regardless of loading type.

Now considering a viscoelastic material subjected to a constant stress imposed at the initial time t_0, defined σ_0, as in case of the above described creep test, the elastic element of the Maxwell model is suddenly deformed, and the viscous element deforms with a constant strain rate.

$$\varepsilon(t) = \frac{\sigma_0}{E} + t\frac{\sigma_0}{\mu} \tag{1.31}$$

If at time $t_1 > t_0$ the stress is released, the deformation of the elastic element is completely recovered ($\varepsilon_{reversible}$), instead the deformation of the viscous element is not recovered ($\varepsilon_{irreversible}$).

$$\varepsilon_{reversible} = \frac{\sigma_0}{E} \tag{1.32}$$

$$\varepsilon_{irreversible} = t_1\frac{\sigma_0}{\mu} \tag{1.33}$$

Since no transient response is shown in a creep test, i.e. creep response is linear with time, for this reason we can say that the Maxwell model is typically not able to describe real polymer behaviour.

This model can be used as building blocks of more general models. By coupling different models, we can describe the more complicated time behaviour to mechanical load that can be different in various parts of polymer chain. The result is a wide spectrum of relaxation times.

The differential equation governing the response for any mechanical model may be obtained considering constitutive equations for each element as well as the overall equilibrium and kinematic constraints of the network. The differential equation obtained can be solved for particular loading, the solution for simple creep or relaxation loading provides the creep compliance or the relaxation modulus.

1.2.6 Generalized Maxwell and Weichert models

To represent the behaviour of a polymer under the condition of relaxation as many as 5-15 or more elements are necessary. A model with many elements is called Generalized Maxwell model.

The differential equation for this model can be expressed as,

$$\sigma + p_1\dot{\sigma} + p_2\ddot{\sigma} + \cdots\ p_n\dot{\sigma}^n = q_1\dot{\varepsilon} + q_2\ddot{\varepsilon} + \cdots q_n\dot{\varepsilon}^n \tag{1.34}$$

In which $\dot{\sigma}^n = D^n\sigma$, p_0 is taken equal to one and n represent the number of parallel Maxwell elements in the considered model.

Remembering that a mechanical model constructed by Maxwell element can in general represented through a differential equation of the standard form

$$\sum_{k=0}^{n} p_k \frac{d^k\sigma}{dt^k} = \sum_{k=0}^{m} q_k \frac{d^k\varepsilon}{dt^k} \tag{1.35}$$

With n=m and $q_0 = 0$ for the generalized Maxwell model.

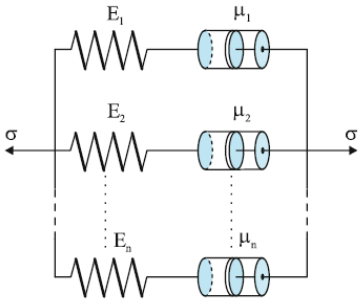

Figure 1.12: Generalized Maxwell Model representation [7]

The solution of the Generalized Maxwell model for a given strain input $\varepsilon(t)$, can be found by superposition of n first order differential equation or equivalently by solution of the single n^{th} order differential equation.

The first order differential equations are all expressed in the form

$$\sigma_j + \tau_j D\sigma_j = \mu_j D\varepsilon_j(t) \tag{1.36}$$

where j ranges from 1 to n.

The kinematic constraint provides that strain in each element is the same as the global strain ($\varepsilon_j(t) = \varepsilon(t)$).

The equilibrium constraint provides that the solution for the global stress is the sum of the individual stresses

$$\sigma(t) = \sigma_1(t) + \sigma_2(t) + \cdots \sigma_n(t) \tag{1.37}$$

For the condition of stress relaxation $\varepsilon(t) = \varepsilon_0 H(t)$, the solutions of these linear differential equations can be found by superposition

$$\sigma(t) = \varepsilon_0 \sum_{j=1}^{n} E_j \, e^{-t/\tau_j} \tag{1.38}$$

Therefore, the relaxation modulus of a Generalized Maxwell Model is given by

$$E(t) = \sum_{j=1}^{n} E_j \, e^{-t/\tau_j} \tag{1.39}$$

This representation can be called a **Prony series expansion** and it is often used to describe the relaxation modulus of a viscoelastic material.

The generalized model described above can only be used to describe a thermoplastic polymer if all the μ_j values are different from zero.

In order to represent thermoset polymer and also elastomers in which we are mainly interested in, a free spring is often included obtaining as result the so called Wiechert model [7], reported in the following figure

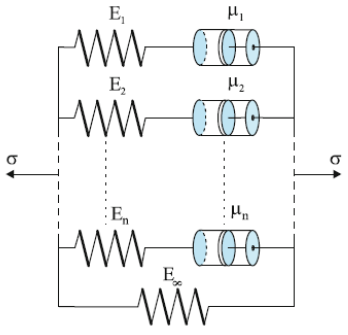

Figure 1.13: Wiechert model representation

For this model the solution for stress relaxation con be expressed as,

$$\sigma(t) = \varepsilon_0 \left(\sum_{j=1}^{n} E_j \, e^{-\frac{t}{\tau_j}} + E_\infty \right) \tag{1.40}$$

where E_∞ represent the equilibrium modulus.

The exponential Prony series, already previously mentioned, and defined as,

$$E(t) = E_\infty + \sum_{j=1}^{N} E_j e^{-t/\tau_j} \tag{1.41}$$

or,

$$D(t) = \frac{1}{E_0} + \sum_{j=1}^{n} \frac{1}{E_j} \left(1 - e^{-\frac{t}{\tau_j}} \right) \tag{1.42}$$

is an exact representation for this Weichert model and it usually implemented in the FEM software.

First of all, the coefficient can be related to simple spring and damper coefficients in a mathematical model, and so easy to be interpreted. Second, the Prony series are simple exponential functions so easy to manipulate and to store, since derivatives and integration of the terms are trivial. Third, if we need to find a numerical solution for a particular boundary value problem, using Prony series form for the material modulus makes possible the use of recursive algorithm for fast solution of convolution integral law [9]. That consideration is important to calculate viscoelastic response at long time, as integrating over time history sufficiently long, requires only to hold terms at the previous time step.

Experimental data for a particular material produce modulus or compliance functions for a polymer as a function of time (Relaxation or Creep data) or frequency (DMA test). Given also the time scale of polymeric response, sometimes is needed to perform separate tests at different temperatures in order to obtain a full spectrum needed to generate the master curve of the data in frequency or in time domain.

The defiance is to find the parameters τ_J and E_J to obtain a good fit over all time of the data. To solve this problem were presented a lot of method in literature including Procedure X [10], collocation method [11], windowing method [12] and the sign control method [13] based on multidata method.

This last method work selecting as first step the time scale of the data. The selection of the relaxation times is done by mathematical convenience.

Since real polymers have a continuous distribution of relaxation times, a subset of these are chosen to provide a function that will fit the material data.

Once relaxation times are selected, the problem is to find coefficients E_J so that the Prony series function matches the provided time domain data. The Least Squares approach [14] is commonly used. The values provided for E_J are both positive and negative. The solution was given by iterative Levemberg- Marquadt method based on the first derivatives relative to each unknown coefficient.

By this procedure at the end we have optimal values of E_J such that Prony series fits the entire data range.

The sign control method [13] can also be used for fitting frequency domain data. That can be useful since the most used method to measure storage and loss moduli for polymer, as said before, is the DMA following presented. In this case storage and loss moduli function of frequency are used as data to be fit.

1.2.7 Dynamic properties evaluation

In previous sections we analysed the Creep test and the Relaxation test performed to determine the time behaviour of the viscoelastic materials. A different approach that can be used to determine the viscoelastic properties, already mentioned in the last section, is called dynamic mechanic analysis (DMA) test. In this procedure the viscoelastic properties are determined with steady state oscillation or vibration tests using small compressive bars or thin cylinders.

The differential equations obtained from the generalized mechanical models can be valid also to describe the dynamical properties.

Considering a small uniaxial sample that is load with a strain input of the form

$$\varepsilon(t) = \varepsilon_0 e^{i\omega t} \tag{1.43}$$

Only the real (or imaginary) part, sine or cosine wave, will be input, but the algebra associated to exponential function is easy to manipulate and will be used for general derivation.

A simplification consists in neglecting the transient terms that in this moment are considered as inertial terms, in other words we analyse the steady-state dynamic response.

Given the differential equation expressed by the formula,

$$\sum_{k=0}^{n} p_k \frac{d^k \sigma}{dt^k} = \sum_{k=0}^{m} q_k \frac{d^k \varepsilon}{dt^k} \tag{1.44}$$

valid for a general mechanical model of a viscoelastic material and considering the exponential input above we obtain a stress output that is also of exponential form

$$\sigma(t) = \sigma^* e^{i\omega t} \tag{1.45}$$

In which ω represent the natural frequency and σ^* is a complex quantity that can be defined as,

$$\sigma^* = \varepsilon_0 E^*(i\omega) \tag{1.46}$$

Where E^* is called complex modulus and can be decomposed into imaginary and real parts as follows

$$E^*(i\omega) = E'(\omega) + iE''(\omega) \tag{1.47}$$

In this formula the real part is represented by $E'(\omega)$ also called storage modulus and the imaginary part is represented by $E''(\omega)$ also called loss modulus.

These two quantities can be associated to the energy stored and dissipated in a loading cycle.

We can also define a new quantity that express the phase lag since stress clearly lags the strain input by a parameter in literature known as "loss angle", "tan delta" or "damping ratio" and defined as

$$tan\delta(\omega) = \frac{E''(\omega)}{E'(\omega)} \tag{1.48}$$

Through DMA test it is possible to evaluate rapidly complex modulus, storage and loss modulus and phase angle or damping.

Using this test, steady state viscoelastic response can be found over a wide range of frequencies by sweeping (maintaining constant the temperature).

1.2.8 Hyperelasticity

Materials that tends to respond elastically when subjected to large strains are called hyperelastic. They show both nonlinear material behaviour and large shape changes. This is a typical characteristic of elastomers or rubber like materials. More important characteristics are:

- Large elastic deformations in order of around 100% to 700% which is fully recoverable, so the initial shape can be recovered once load is removed.
- Incompressibility, so if they are subjected to huge loads, they change its shape, but the total volume remains almost constant
- Show a highly nonlinear stress-strain relation

The relation between stress and strain can be generally expressed as

$$\sigma = f(\varepsilon) \tag{1.49}$$

For linear elastic materials f is a linear function and the stress-strain relation is simply $\sigma = E\varepsilon$, with E constant elastic modulus of materials, also named Young modulus.

For hyperelastic material, function f is nonlinear and there are different models that can be used to define this function.

This family of material is described in terms of a strain potential energy, $W(\varepsilon)$, defining the strain energy stored in a material per unit of reference volume (volume at the initial configuration) as function of strain at that point in the material. The stress-strain relation is function of strain energy potential and can be written as,

$$\overline{\sigma} = f\left(B_s, \frac{\partial W}{\partial I_1}, \frac{\partial W}{\partial I_2}\right) \tag{1.50}$$

In which B_s express the stretch tensor and I_1 and I_2 are respectively the first and the second invariant, defined as:

$$B_s = \begin{bmatrix} {\lambda_1}^2 & 0 & 0 \\ 0 & {\lambda_2}^2 & 0 \\ 0 & 0 & {\lambda_3}^2 \end{bmatrix}$$

$$\lambda_i = \text{principal stretch in i direction} = \frac{L}{L_0} = 1 + \varepsilon_i$$

$$I_1 = {\lambda_1}^2 + {\lambda_2}^2 + {\lambda_3}^2$$

$$I_2 = \frac{1}{{\lambda_1}^2} + \frac{1}{{\lambda_2}^2} + \frac{1}{{\lambda_3}^2}$$

And under the hypothesis of incompressible material, there is no dependence on the third invariant I_3 that results equal to one.

Considering the principle of virtual works, it is possible to write $\partial W = \sigma\, \partial\lambda$ and so the stress can be expressed as

$$\sigma = \frac{\partial W}{\partial \lambda} = \frac{\partial W}{\partial I_1}\frac{\partial I_1}{\partial \lambda} + \frac{\partial W}{\partial I_2}\frac{\partial I_2}{\partial \lambda} \tag{1.51}$$

There are a lot of forms of strain energy potentials to model incompressible isotropic elastomers. A possibility is to use the Polynomial model expressed as,

$$W = \sum_{i+j=1}^{N} C_{ij}(I_1 - 3)^i (I_2 - 3)^j \tag{1.52}$$

Where C_{ij} represent material coefficient to be experimentally determined.

Other models that are commonly used to express strain potential energy are the Neo-Hooke and Money-Rivlin models, that represent particular cases of the polynomial one.

- Neo-Hooke $W = C_{10}(I_1 - 3)$
- Money-Rivlin $W = C_{10}(I_1 - 3) + C_{01}(I_2 - 3)$

Since the material coefficient have to be determined experimentally, a uniaxial tensile or compression test can be performed. Stress-strain curve can be obtained and model parameter that best fit the experimental data can also find.

For uniaxial tension or compression, considering the incompressibility assumption, we can write:

$$\lambda_1 = \lambda \tag{1.53}$$

$$\lambda_2 = \lambda_3 = \frac{1}{\sqrt{\lambda}} \tag{1.54}$$

The first and the second invariant then becomes,

$$I_1 = {\lambda_1}^2 + {\lambda_2}^2 + {\lambda_3}^2 = \lambda^2 + \frac{2}{\lambda} \tag{1.55}$$

$$I_2 = {\lambda_1}^2{\lambda_2}^2 + {\lambda_2}^2{\lambda_3}^2 + {\lambda_3}^2{\lambda_1}^2 = 2\lambda + \frac{1}{\lambda^2} \tag{1.56}$$

and the stress can be expressed as,

$$\sigma = \frac{\partial W}{\partial I_1}\frac{\partial I_1}{\partial \lambda} + \frac{\partial W}{\partial I_2}\frac{\partial I_2}{\partial \lambda} = 2\left(\lambda - \frac{1}{\lambda^2}\right)\left(\frac{\partial \mathrm{W}}{\partial \mathrm{I}_1} + \frac{1}{\lambda}\frac{\partial \mathrm{W}}{\partial \mathrm{I}_2}\right) \tag{1.57}$$

Since the term $\lambda - \frac{1}{\lambda^2}$ is independent on the chosen polynomial model, a modified stress can be considered to fit experimental data

$$\sigma_m = \frac{\sigma}{\lambda - \frac{1}{\lambda^2}} = \frac{\partial W}{\partial I_1} + \frac{1}{\lambda}\frac{\partial W}{\partial I_2} \tag{1.58}$$

Depending on chosen model, best material parameters can be obtained by fitting modified stress σ_m and λ values. Considering for example Money-Rivlin model, we can have the expression,

$$\sigma_m = \frac{\partial W}{\partial I_1} + \frac{1}{\lambda}\frac{\partial W}{\partial I_2} = \mathrm{C}_{10} + \frac{1}{\lambda}\mathrm{C}_{01} \tag{1.59}$$

used for the fitting of experimental data to obtain material parameters C_{10} and C_{01}.

2. Sorbothane characterization

2.1 Material properties

Viscoelastic dampers are among the earliest types of passive control devices that are effectively used to solve dynamic problem in many fields. Thanks to their advantages of simple construction, easy manufacturing process, low cost, and excellent energy dissipation ability, viscoelastic dampers have been developed to attenuate vibrations.

Our attention is now focused on Sorbothane, a viscoelastic polymer (polyether based polyurethane), with a high damping coefficient over a wide range of temperatures compared to other polymers (from -20°C to +72°C). High damping coefficient means that this material can absorb a lot of vibrational energy and makes it suitable in difficult application in which is needed to operate near to the natural frequencies [15].

Sorbothane is a non-Newtonian material, this means that the stress is not proportional to strain, and mechanical energy is lost by conversion into heat. The response of this material depends on the rate of force application, so that the response varies with respect to frequency.

It is not easy to find a material able to combine all the above characteristics, but Sorbothane can do that guaranteeing a long fatigue life.

An important parameter is the durometer Shore 00, that indicates the measurement of relative stiffness (hardness scale for rubbers) and it is used to compare different polymers. Sorbothane results softer than rubber and most of other polymers.

On the company website it is possible to find an interesting comparison, in terms of damping effectiveness, between Sorbothane and various types of common vibration isolators used such as natural rubber and neoprene.

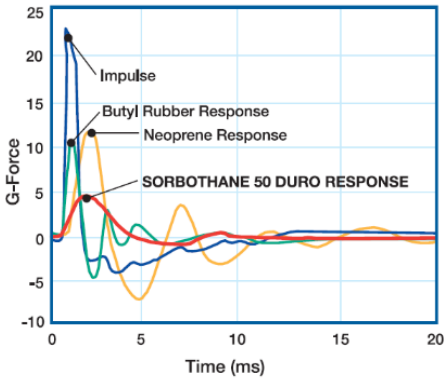

Figure 2.1: Response of tested material to impulse [15]

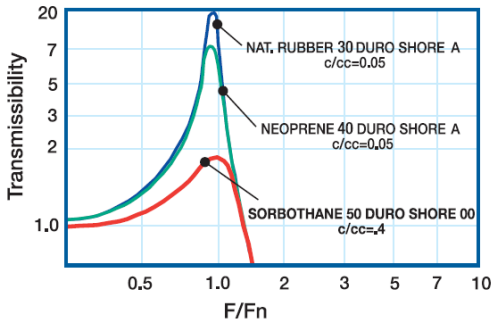

Figure 2.2: Relation between Transmissibility and ratio of excitation frequency and natural frequency [15]

By looking at the Figure 2.1, it can be seen that Sorbothane damp vibrations with a faster response by having smaller oscillations at a given impact forces (G-force).

Now considering the Figure 2.2, it can be observed that Sorbothane shows low transmissibility[2], compared to other isolators, maintaining a similar frequency ratio to neoprene and natural rubber. In practice low transmissibility means less damage to sensitive components.

Another interesting graph is the following one, realized and presented by the Sorbothane company, that shows the Hysteresis cycle comparison between the natural rubber and Sorbothane 50.

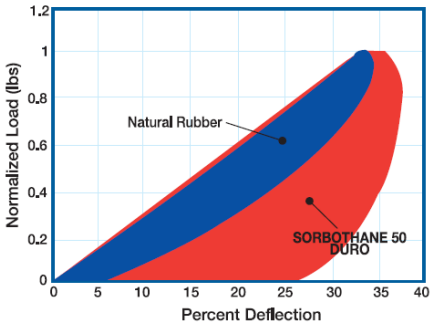

Figure 2.3: Hysteresis comparison Sorbothane 50 versus Natural Rubber [15]

It is known that the Hysteresis cycle can be obtained, for example, as response of a forcing sinusoidal input. It presents an elliptical shape if the considered material is linear viscoelastic. In case of nonlinear viscoelastic material, the shape results sharper. The area enclosed by the hysteresis cycle is a measure of the energy dissipated in a cycle. As can be seen, the dissipation guaranteed by the Sorbothane is much higher than the one of the natural rubbers.

Thanks to the above characteristic, it is now clear why the choice to use Sorbothane for our purpose.

[2] The transmissibility represents the forces ratio between output and input, T=output/input. T > 1 means amplification, and the maximum value of amplification occurs when the forcing frequency equals the natural frequency of the considered system.

2.1 Material characterization

As for other polymer, also the behaviour of Sorbothane is not easy to predict. The property variation function of frequency cannot be neglected and so it become necessary to use models present in literature for both Hyperelastic and Viscoelastic characterization.

The mechanical properties of Sorbothane material change significantly with the production batch and with the year of production. On the market it is possible to find Sorbothane produced in different years and so with different characteristics.

In order to show this difference, mechanical characteristics of our interest contained in the official datasheet [15] are here reported for both Sorbothane 2015 and 2018,

PROPERTY	DUROMETER (Shore 00)			UNITS	NOTES
	30	50	70		
Tensile Strength at 100% Strain	0.090	0.138	0.324	MPa	ASTM D 412-06a
Tensile Strength at 200% Strain	0.179	0.262	0.558	MPa	ASTM D 412-06a
Tensile Strength at 300% Strain	0.255	0.365	0.814	MPa	ASTM D 412-06a
Compressive Stress at 10% Strain	0.012	0.026	0.074	MPa	ASTM D 575-91, Method A
Compressive Stress at 20% Strain	0.032	0.061	0.165	MPa	ASTM D 575-91, Method A

Table 2.1: Mechanical Properties from Datasheet - Sorbothane 2015

PROPERTY	DUROMETER (Shore 00)			UNITS	NOTES
	30	50	70		
Tensile Strength at 100% Strain	0.041	0.090	0.400	MPa	ASTM D 412-06a
Tensile Strength at 200% Strain	0.083	0.165	0.779	MPa	ASTM D 412-06a
Tensile Strength at 300% Strain	0.145	0.276	1.076	MPa	ASTM D 412-06a
Compressive Stress at 10% Strain	0.006	0.019	0.081	MPa	ASTM D 575-91, Method A
Compressive Stress at 20% Strain	0.014	0.044	0.207	MPa	ASTM D 575-91, Method A

Table 2.2: Mechanical Properties from Datasheet - Sorbothane 2018

In the tables are reported three values for tensile stress corresponding to three different levels of deformations (i.e. 100%, 200% e 300%) and two values for compression stress corresponding to two compression levels (i.e. 10% e 20%). Both are obtained following standards provided by ASTM. Following the ASTM standard, the tensile test is performed at a rate of 500 mm/min and the compression test at a rate equal to 12 mm/min.

The variability of the mechanical properties has to be taken into account during both hyperelastic and viscoelastic characterization, since the obtained results have to be used to define the material properties of Sorbothane in Abaqus CAE software.

2.2.1 Hyperelastic Characterization

Considering this variability of the mechanical properties arise the need to perform a test directly on our material.

The idea is to perform a compression test following the standard ISO 7743:2017 Method A. The lubricate test piece is loaded at constant speed between the plates of the machine until a predetermined level of compression is reached (25% of the total thickness), then the load is removed at the same constant speed.

This cycle was repeated four times and the last load curve is considered for the material properties determination.

Figure 2.4: Sorbothane Pad under Compression test

The results in term of stresses and strains are then analysed in a Matlab script in which are also implemented the common models, described before, to define the strain energy potentials for Hyperelastic materials (i.e. Neo Hooke, Mooney-Rivlin, Polynomial, Reduced polynomial). The aim is to perform a fitting procedure between the data experimentally obtained and the model's

implementation in order to find the model that best describe the behaviour of the tested material. Once the best model is found, it is possible to extract the material coefficients previously indicated as C_{ij}. These coefficients are necessary to define the properties of the material in the CAE environment.

The result of the fitting procedure can be summed up in the following graph representing stress vs strain. It is possible to see that the better hyperelastic model to approximate the tested material behaviour is the Neo-Hooke one. It shows a curve most similar to the ones described by the experimental values and predict a coherent behaviour also out of this range. Mooney-Rivlin, reduced Polynomial and especially Polynomial models are not equally good since the curves shape show a very different behaviour before and after the experimental data range.

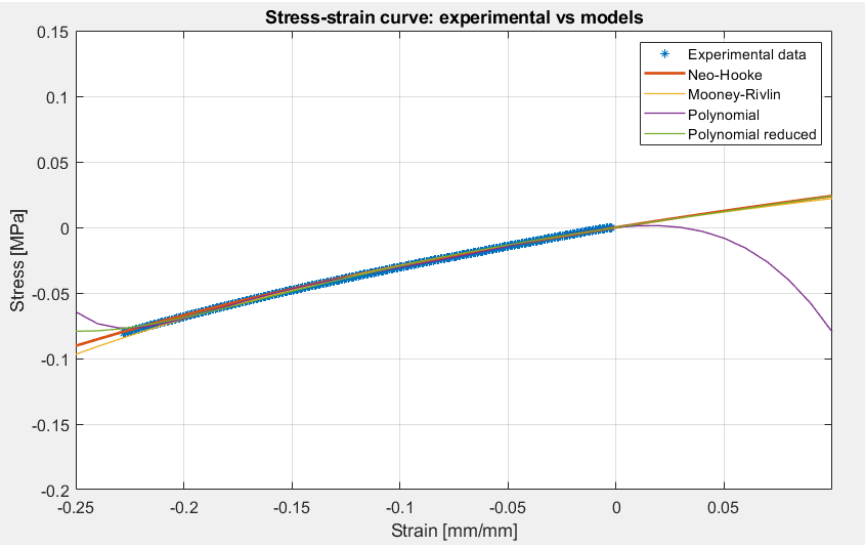

Figure 2.5: Stress strain representation of hyperelastic behaviour - Models and Experimental data

For the Neo-Hooke model the modified stress is defined as:

$$\sigma_m = C_{10} \tag{2.1}$$

The coefficient in which we are interested in is C_{10}, it can be determined by fitting modified stress σ_m and λ values obtained by the model with the ones experimentally obtained.

The following graph represents the $\frac{1}{\lambda} vs\ \sigma_m$ plot in which it can be seen the curve representing the experimental data and the curves obtained by the hyperelasticity models.

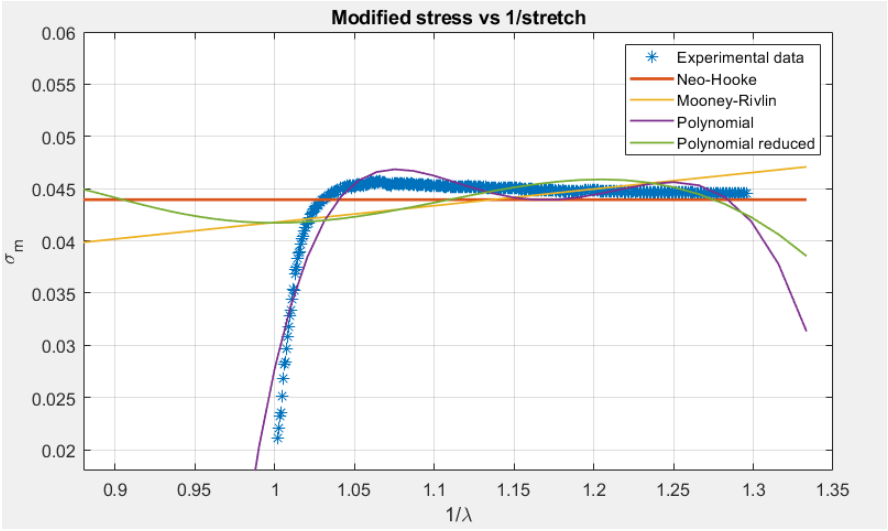

Figure 2.6: Modified Stress vs 1/Stretch - Models and Experimental data

As can be seen in the left part of the graph, the experimental data are not very good, and the Neo-Hooke model is not able to correctly describe the material behaviour, but after this initial trend the Neo-Hooke gives a good approximation of the experimental data.

The determined value for the Neo-Hooke coefficient is:

$$C_{10} = 0.0439 \tag{2.2}$$

2.2.2 Viscoelastic Characterization

To analyse the viscoelastic behaviour of Sorbothane, the knowledge of dynamical properties is needed. The manufacturer provided us some results regarding tests performed by imposing an averaging displacement in compression and then applying cyclic oscillation, with amplitude control. This kind of dynamical test is called DMA (Dynamic Mechanical Analysis) and its procedure is detailed described in the first chapter.

These tests are conducted varying the frequency in a range between 1Hz and 300Hz for three different values of averaged compression (i.e. 10%, 15% and 20% of the total thickness of the specimen).

Results are reported in the tables below with measurements units converted into the international system (IS). The results are representative of Sorbothane 50 produced in 2018.

Specified Frequency	Mean Level	Dynamic Amplitude	Axial force Mean Level	Phase	Tr	Tan Delta	E*/G*	E'/G'	E''/ G''
Hz	mm	mm	N	deg	--	--	N/mm^2	N/mm^2	N/mm^2
1	-1.27	0.3175	-16.35	24.71	1.00	0.46	0.32	0.29	0.13
5	-1.27	0.3175	-16.24	29.74	1.03	0.57	0.53	0.46	0.26
15	-1.27	0.3175	-16.12	31.95	1.22	0.62	0.78	0.66	0.41
30	-1.27	0.3175	-16.07	32.73	1.79	0.64	1.00	0.84	0.54
50	-1.27	0.3175	-15.69	33.19	1.10	0.65	1.21	1.01	0.66
75	-1.27	0.3175	-15.92	32.79	0.43	0.64	1.39	1.17	0.75
100	-1.27	0.3175	-15.68	32.84	0.25	0.65	1.54	1.30	0.84
125	-1.27	0.3175	-16.40	33.09	0.15	0.65	1.67	1.40	0.91
150	-1.27	0.3175	-16.15	32.94	0.11	0.65	1.77	1.49	0.96
175	-1.27	0.3175	-16.76	32.21	0.08	0.63	1.86	1.57	0.99
200	-1.27	0.3175	-15.81	32.57	0.07	0.64	1.95	1.64	1.05
225	-1.27	0.3175	-15.33	32.28	0.06	0.63	2.01	1.70	1.07
250	-1.27	0.3175	-15.94	32.14	0.05	0.63	2.07	1.75	1.10
275	-1.27	0.3175	-16.21	32.36	0.04	0.63	2.12	1.79	1.14
300	-1.27	0.3175	-15.93	32.03	0.03	0.63	2.18	1.85	1.16

Table 2.3: Sorbothane 50 2018- Properties Function of Frequency – AVG Compression 10%

Specified Frequency	Mean Level	Dynamic Amplitude	Axial force Mean Level	Phase	Tr	Tan Delta	E*/G*	E'/G'	E''/ G''
Hz	mm	mm	N	deg	--	--	N/mm^2	N/mm^2	N/mm^2
1	-1.905	0.47498	-23.43	24.17	1.00	0.45	0.37	0.34	0.15
5	-1.905	0.47498	-23.50	29.42	1.04	0.56	0.61	0.53	0.30
15	-1.905	0.47498	-23.55	31.76	1.30	0.62	0.89	0.76	0.47
30	-1.905	0.47498	-23.55	32.68	1.84	0.64	1.14	0.96	0.62
50	-1.905	0.47498	-23.29	33.04	0.76	0.65	1.37	1.15	0.75
75	-1.905	0.47498	-23.97	33.01	0.30	0.65	1.58	1.32	0.86
100	-1.905	0.47498	-23.51	33.05	0.18	0.65	1.74	1.46	0.95
125	-1.905	0.47498	-24.28	33.05	0.11	0.65	1.86	1.56	1.02
150	-1.905	0.47498	-24.43	32.68	0.08	0.64	1.98	1.67	1.07
175	-1.905	0.47498	-24.04	32.93	0.06	0.65	2.08	1.74	1.13
200	-1.905	0.47498	-23.43	32.73	0.05	0.64	2.10	1.77	1.14
225	-1.905	0.47498	-23.73	32.81	0.04	0.64	2.15	1.81	1.17
250	-1.905	0.47498	-23.28	32.79	0.03	0.64	2.21	1.86	1.20
275	-1.905	0.47498	-22.18	33.01	0.03	0.65	2.26	1.89	1.23
300	-1.905	0.47498	-22.31	32.91	0.02	0.65	2.28	1.91	1.24

Table 2.4: Sorbothane 50 2018 - Properties Function of Frequency – AVG Compression 15%

Specified Frequency	Mean Level	Dynamic Amplitude	Axial force Mean Level	Phase	Tr	Tan Delta	E*/G*	E'/G'	E''/ G''
Hz	mm	mm	N	deg	--	--	N/mm ^2	N/mm^2	N/mm^2
1	-2.54	0.635	-31.77	23.99	1.00	0.45	0.45	0.41	0.18
5	-2.54	0.635	-31.65	29.29	1.05	0.56	0.73	0.64	0.36
15	-2.54	0.635	-31.63	31.62	1.35	0.62	1.06	0.90	0.55
30	-2.54	0.635	-31.69	32.67	1.76	0.64	1.34	1.13	0.73
50	-2.54	0.635	-30.93	33.13	0.63	0.65	1.60	1.34	0.87
75	-2.54	0.635	-31.22	33.23	0.25	0.66	1.79	1.50	0.98
100	-2.54	0.635	-31.54	33.53	0.14	0.66	1.93	1.61	1.07
125	-2.54	0.635	-31.75	33.39	0.09	0.66	2.05	1.71	1.13
150	-2.54	0.635	-31.39	33.53	0.07	0.66	2.13	1.77	1.17
175	-2.54	0.635	-30.49	33.58	0.05	0.66	2.21	1.84	1.22
200	-2.54	0.635	-31.95	33.33	0.04	0.66	2.27	1.90	1.25
225	-2.54	0.635	-31.99	33.16	0.03	0.65	2.33	1.95	1.27
250	-2.54	0.635	-29.68	33.69	0.03	0.67	2.35	1.95	1.30
275	-2.54	0.635	-30.83	33.32	0.02	0.66	2.40	2.01	1.32
300	-2.54	0.635	-31.16	33.68	0.02	0.67	2.44	2.03	1.36

Table 2.5: Sorbothane 50 2018 - Properties Function of Frequency – AVG Compression 20%

Considering the elastic modulus values function of the frequency for the three preload levels, as show in the following graph, the generated curves are not coincident, and they show higher stiffness as the load increase. This behaviour confirms that it is correct to consider Sorbothane as Hyperelastic material. Stress-strain curve is not linear since depends on the deformation value applied.

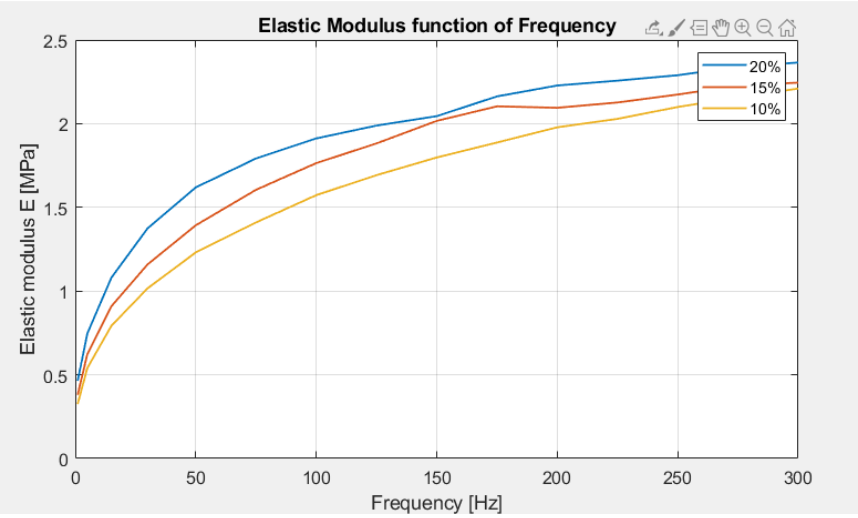

Figure 2.7: Elastic Modulus function of the frequency for different preloads - 10% - 15% - 20% - Sorbothane 50 – 2018

Considering now the elastic modulus normalized with respect to the instantaneous modulus (since we don't have other data we consider as instantaneous modulus the values at a frequency equal to 300 Hz) function of the frequency, as plotted below, it can be seen that curves corresponding to different preload levels not overlap very well, especially for higher deformation. That means that the hypothesis of linear viscoelasticity used for our following analysis may introduce some errors. For this reason, the fitting operations to obtain Prony parameters have to be performed considering the preload curve that is nearest to the one that is expected in a specific application.

For a linear viscoelastic material, the normalized elastic modulus has to be independent on the averaged applied load.

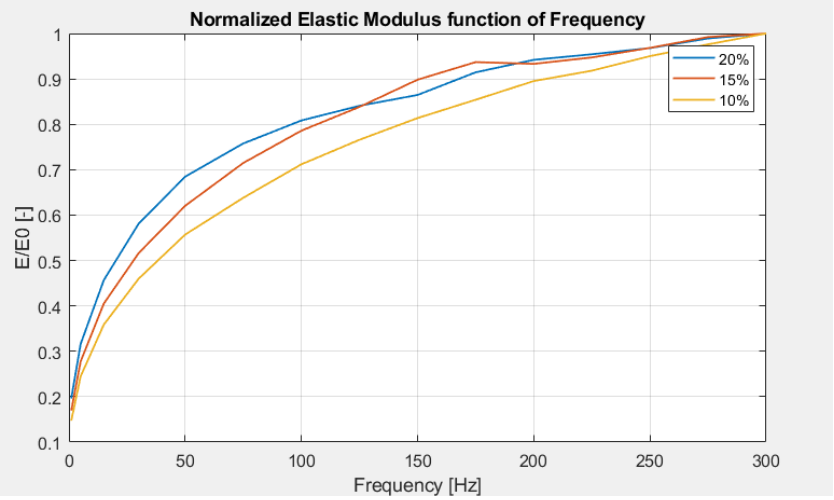

Figure 2.8: Normalized Elastic Modulus function of frequency for different preloads 10% - 15% - 20% - Sorbothane 50 – 2018

Since the Sorbothane at our disposal was produced in 2016, we ask to the manufacturer for the result of the dynamic test carried out on a product of that year since we need to consider the variability between the production batch. The data that producer give us are obtained through dynamic tests described above also for Sorbothane 2018.

The results are reported in the tables below converted in metric units (IS) for Sorbothane durometer 52. Since Sorbothane present also a variability in terms of durometer between various production batches the comparison between Sorbothane durometer 50 and Sorbothane durometer 52 is considered acceptable.

Specified Frequency	Mean Level	Dynamic Amplitude	Axial force Mean Level	Phase	Tr	Tan Delta	E*/G*	E'/G'	E''/ G''
Hz	mm	mm	N	deg	--	--	N/mm^2	N/mm^2	N/mm^2
1	-1.27	0.3175	-30.69	20.91	1.00	0.38	0.56	0.52	0.20
5	-1.27	0.3175	-30.06	25.98	1.04	0.49	0.86	0.77	0.38
15	-1.27	0.3175	-29.85	28.01	1.30	0.53	1.20	1.06	0.56
30	-1.27	0.3175	-29.71	28.74	2.04	0.55	1.49	1.31	0.72
50	-1.27	0.3175	-28.94	29.10	0.84	0.56	1.76	1.53	0.85
75	-1.27	0.3175	-28.25	29.05	0.34	0.56	2.00	1.74	0.97
100	-1.27	0.3175	-29.46	28.91	0.18	0.55	2.18	1.91	1.05
125	-1.27	0.3175	-29.03	28.90	0.12	0.55	2.33	2.04	1.13
150	-1.27	0.3175	-29.24	28.25	0.09	0.54	2.48	2.19	1.18
175	-1.27	0.3175	-29.54	28.27	0.06	0.54	2.60	2.29	1.23
200	-1.27	0.3175	-29.16	28.12	0.05	0.53	2.68	2.37	1.26
225	-1.27	0.3175	-28.94	28.08	0.04	0.53	2.78	2.45	1.31
250	-1.27	0.3175	-28.91	27.63	0.03	0.52	2.88	2.55	1.34
275	-1.27	0.3175	-28.95	27.83	0.03	0.53	2.95	2.61	1.38
300	-1.27	0.3175	-29.46	27.53	0.02	0.52	3.02	2.68	1.40

Table 2.6: Sorbothane 52 2016- Properties Function of Frequency – AVG Compression 10%

Specified Frequency	Mean Level	Dynamic Amplitude	Axial force Mean Level	Phase	Tr	Tan Delta	E*/G*	E'/G'	E''/ G''
Hz	mm	mm	N	deg	--	--	N/mm^2	N/mm^2	N/mm^2
1	-1.905	0.47498	-44.66	20.69	1.00	0.38	0.64	0.60	0.23
5	-1.905	0.47498	-44.21	25.76	1.05	0.48	0.97	0.88	0.42
15	-1.905	0.47498	-44.15	27.84	1.41	0.53	1.36	1.20	0.64
30	-1.905	0.47498	-43.95	28.68	1.83	0.55	1.69	1.48	0.81
50	-1.905	0.47498	-43.32	29.02	0.55	0.55	1.98	1.74	0.96
75	-1.905	0.47498	-42.83	29.07	0.23	0.56	2.21	1.93	1.08
100	-1.905	0.47498	-40.37	29.06	0.14	0.56	2.42	2.12	1.18
125	-1.905	0.47498	-41.16	28.73	0.09	0.55	2.48	2.17	1.19
150	-1.905	0.47498	-39.69	28.54	0.07	0.54	2.63	2.31	1.26
175	-1.905	0.47498	-41.51	28.48	0.05	0.54	2.73	2.40	1.30
200	-1.905	0.47498	-39.84	27.85	0.04	0.53	2.82	2.49	1.32
225	-1.905	0.47498	-40.64	28.06	0.03	0.53	2.89	2.55	1.36
250	-1.905	0.47498	-39.98	27.60	0.03	0.52	2.96	2.62	1.37
275	-1.905	0.47498	-39.82	27.81	0.02	0.53	3.04	2.68	1.42
300	-1.905	0.47498	-40.65	28.27	0.02	0.54	3.14	2.77	1.49

Table 2.7: Sorbothane 52 2016 - Properties Function of Frequency – AVG Compression 15%

Specified Frequency	Mean Level	Dynamic Amplitude	Axial force Mean Level	Phase	Tr	Tan Delta	E*/G*	E'/G'	E''/ G''
Hz	mm	mm	N	deg	--	--	N/mm ^2	N/mm^2	N/mm^2
1	-2.54	0.635	-58.35	20.65	1.00	0.38	0.76	0.71	0.27
5	-2.54	0.635	-57.89	25.63	1.06	0.48	1.15	1.03	0.50
15	-2.54	0.635	-57.89	27.91	1.48	0.53	1.59	1.41	0.75
30	-2.54	0.635	-57.78	28.98	1.60	0.55	1.98	1.73	0.96
50	-2.54	0.635	-56.75	29.20	0.47	0.56	2.29	2.00	1.12
75	-2.54	0.635	-54.54	29.25	0.19	0.56	2.37	2.06	1.16
100	-2.54	0.635	-55.66	29.75	0.10	0.57	2.49	2.16	1.24
125	-2.54	0.635	-53.85	29.32	0.07	0.56	2.72	2.37	1.33
150	-2.54	0.635	-54.49	29.42	0.05	0.56	2.94	2.56	1.44
175	-2.54	0.635	-58.22	28.88	0.04	0.55	3.12	2.74	1.51
200	-2.54	0.635	-56.48	28.70	0.03	0.55	3.26	2.86	1.56
225	-2.54	0.635	-55.68	28.61	0.03	0.55	3.33	2.92	1.59
250	-2.54	0.635	-55.31	28.41	0.02	0.54	3.39	2.98	1.61
275	-2.54	0.635	-53.73	28.68	0.02	0.55	3.42	3.00	1.64
300	-2.54	0.635	-56.53	28.11	0.01	0.53	3.53	3.12	1.66

Table 2.8: Sorbothane 52 2016 - Properties Function of Frequency – AVG Compression 20%

The same analysis performed for Sorbothane 2018 data are repeated for Sorbothane 2016. Considering the same three preload levels, as show in the following graph, as we expect, also in that case, the generated curves are not coincident, and they show the same behaviour of the ones regard Sorbothane 2018 with higher stiffness as the load increase.

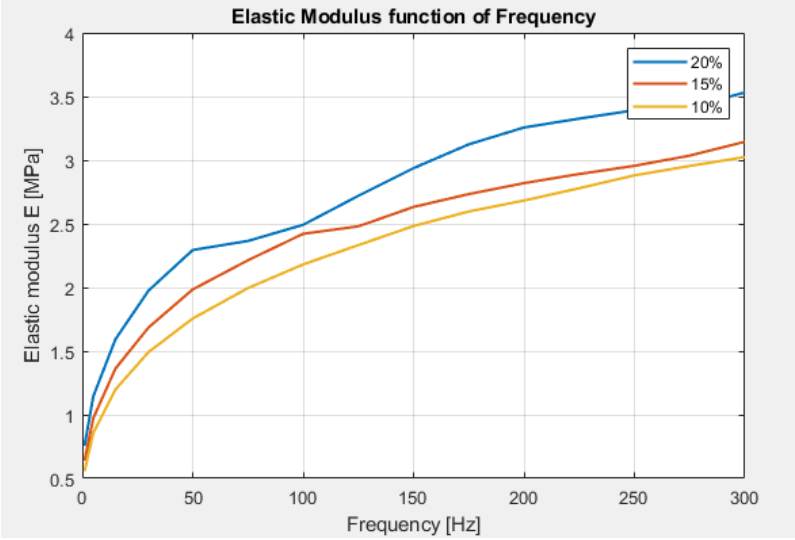

Figure 2.9: Elastic Modulus function of the frequency for different preloads 10% -15% -20% - Sorbothane 52 -2016

Also, the elastic modulus normalized with respect to the instantaneous modulus (modulus at 300 Hz as done before) function of frequency is plotted below for Sorbothane 2016. The curves corresponding to different preload levels overlaps better than the ones of Sorbothane 2018 so it is reasonable to assume that the hypothesis of linear viscoelasticity for this material may introduce less errors in the model.

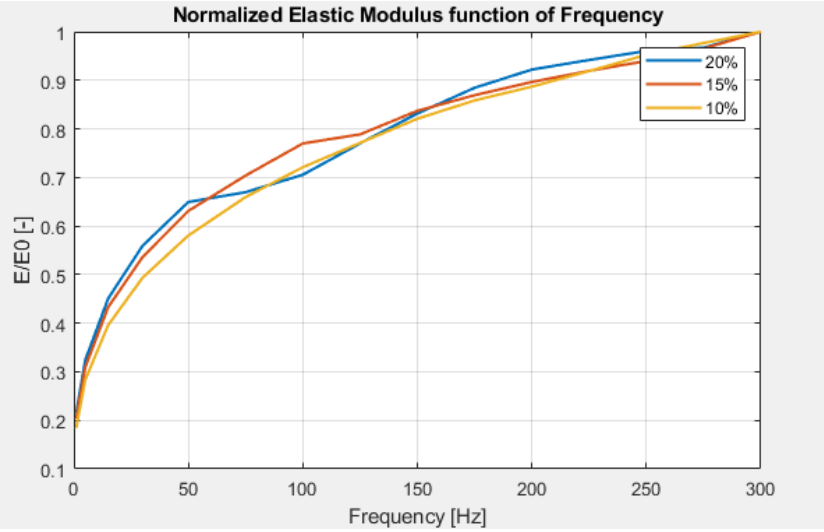

Figure 2.10: Normalized Elastic Modulus function of frequency for different preloads 10% - 15% - 20% - Sorbothane 52 – 2016

We want now to compare the data presented above for Sorbothane 2018 and Sorbothane 2016 with the data contained in the datasheet related to Sorbothane 2015 [15]. The table below presents the dynamic properties for Sorbothane 2015.

PROPERTY	DUROMETER (Shore 00)			UNITS	NOTES
	30	50	70		
Dynamic Young's Modulus at 5 Hz	0.30,0.34,0.40	0.61,0.70,0.81	1.24,1.41,1.64	MPa	10%, 15%, 20%
Dynamic Young's Modulus at 15 Hz	0.45,0.51,0.59	0.83,0.93,1.07	1.54,1.74,2.03	MPa	10%, 15%, 20%
Dynamic Young's Modulus at 30 Hz	0.59,0.65,0.76	1.01,1.14,1.31	1.78,2.01,2.33	MPa	10%, 15%, 20%
Dynamic Young's Modulus at 50 Hz	0.71,0.80,0.92	1.19,1.32,1.52	1.99,2.24,2.60	MPa	10%, 15%, 20%
Tangent Delta at 5 Hz excitation	0.58	0.40	0.20	--	
Tangent Delta at 15 Hz excitation	0.64	0.46	0.28	--	
Tangent Delta at 30 Hz excitation	0.68	0.50	0.33	--	
Tangent Delta at 50 Hz excitation	0.69	0.52	0.36	--	

Table 2.9: Dynamic Sorbothane 2015 Properties from Datasheet

Analysing the three sets of data (Sorbothane 2018, Sorbothane 2016 and Sorbothane 2015) in terms of dynamic modulus and correspondent phase, following graphs are presented:

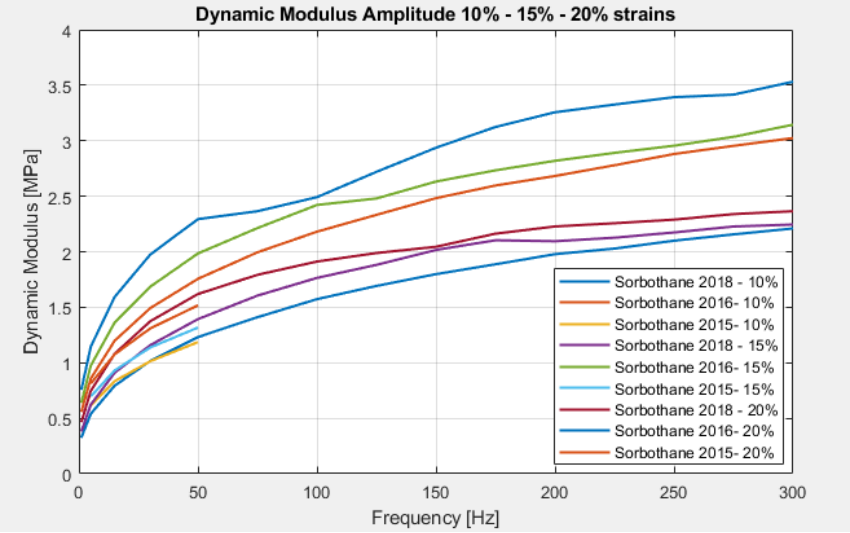

Figure 2.11: Dynamic Modulus Amplitude Comparison Sorbothane 2015 - Sorbothane 2016 - Sorbothane 2018

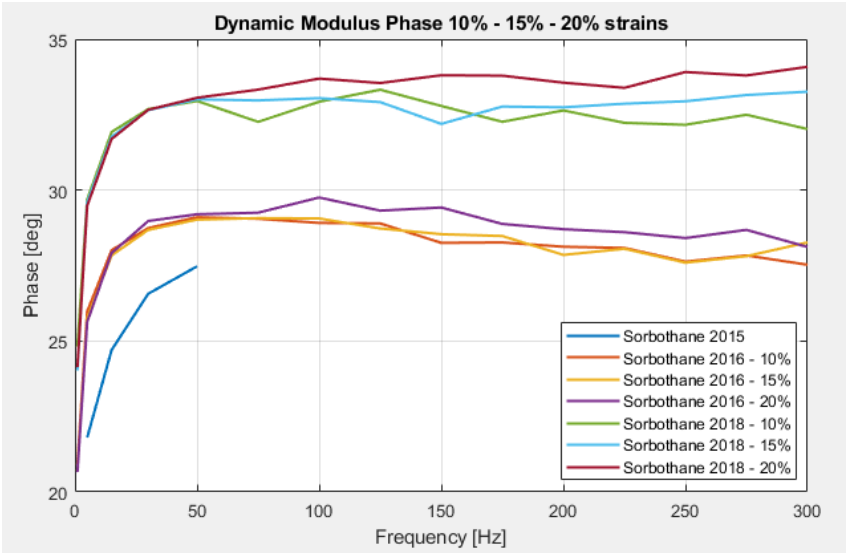

Figure 2.12: Dynamic Modulus Phase Comparison - Sorbothane 2015 - Sorbothane 2016 - Sorbothane 2018

We can see that there is a difference in both dynamic modulus amplitude and dynamic modulus Phase between the Sorbothane produced in different years. The dynamic modulus amplitude and the phase are lower for the Sorbothane 2015 and Sorbothane 2018 with respect to the ones of Sorbothane 2016, this can be due to the fact that Sorbothane 2015 and Sorbothane 2018 has shore durometer equal to 50 and Sorbothane 2016 has shore durometer a little bit higher and equal to 52.

The phase is obtained from $tan\delta(\omega)$, representative of the internal friction of the material. Looking at the above phase graph we can say that Sorbothane 2015 results more elastic than the ones of 2018 and 2016 or equivalently less viscous.

We can see also a big difference in phase between Sorbothane 2016 and Sorbothane 2018, this means that the last one is more viscous compared to the others.

Now it's clearer the variability of the material characteristics function of the year and the production batch. The comparison is needed since we have to choose the material to consider for the description of the viscoelastic behaviour.

For this reason, to describe the viscoelastic behaviour of Sorbothane through Prony series, it would have been better to perform dynamic tests directly on the material at our disposal. Unfortunately, it is not possible, and therefore the data supplied by the manufacturer are used. The choice to use in particular Sorbothane 2016 data is done since this one is more similar to the one at our disposal in terms of mean force level.

The Prony series parameters to be determined are E_0, e_k, τ_k , of generalized Weichert model. The fitting procedure adopted is based on the one detailed described in the article [16]. The number of Prony parameters requested are equal to five. The first operation consists into setting the upper and the lower boundary for the relaxation time τ, so that the number of the unknowns to be determinate are equal to $2\,k+1$ with k representing the number of damper and spring elements in the generalized Weichert model. These can be determinate by a least square optimization procedure. The function to be minimized is,

$$f(e_k, \dots, e_K, E_0) = \sum_{j=1}^{m} \left[\left(\log E'(\omega_j) - \log \overline{E'}(\omega_j) \right)^2 + 10 \left(\log E''(\omega_j) - \log \overline{E''}(\omega_j) \right)^2 \right] \quad (2.3)$$

where $E'(\omega_j)$ and $E''(\omega_j)$ are the storage modulus and the loss modulus calculated respectively with the real and the imaginary part of the equation,

$$E^*(\omega) = E_0 \left(1 - \sum_{k=1}^{K} e_k + \sum_{k=1}^{K} e_k \frac{\omega^2 {\tau_k}^2}{1 + \omega^2 {\tau_k}^2} + i \sum_{k=1}^{K} e_k \frac{\omega \tau_k}{1 + \omega^2 {\tau_k}^2} \right) \quad (2.4)$$

in which $E^*(\omega)$ is called complex modulus.

$\overline{E'}(\omega_j)$ and $\overline{E''}(\omega_j)$ are the storage and loss moduli that comes from experimental evaluation.

Following basic thermodynamic principles are considered during the parameter identification procedure:

$0 \leq e_k \leq 1$

$\sum_{k=1}^{K} e_k \leq 1$

$E_0 > 0 \; and \; E_\infty = E_0 \left(1 - \sum e_k \right)$

The value of E_∞ imposed is obtained from hyperelasticity model (Neo-Hooke) by deriving the stress-strain curve: the following elastic modulus versus strain curve is obtained.

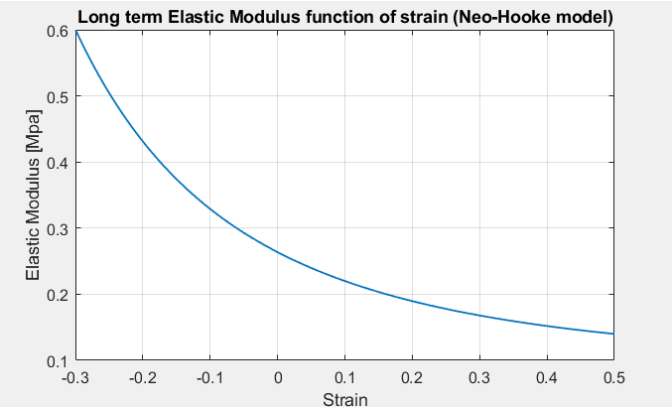

Figure 2.13: Long term Elastic Modulus from hyperelasticity Neo-Hooke model

From this graph, considering a compression equal to 10% (-0.1), we obtain $E_\infty = 0.328Mpa$. This value is the one considered in the fitting procedure.

The optimization problem was implemented in Matlab as a two-step procedure. In the first step a Genetic algorithm is used to generate suitable start parameters which are then used as input in a global gradient based optimization tool [16].

The following graphs show the comparison between the experimental data extract from Sorbothane 2016 data, and the two steps of the performed fitting procedure.

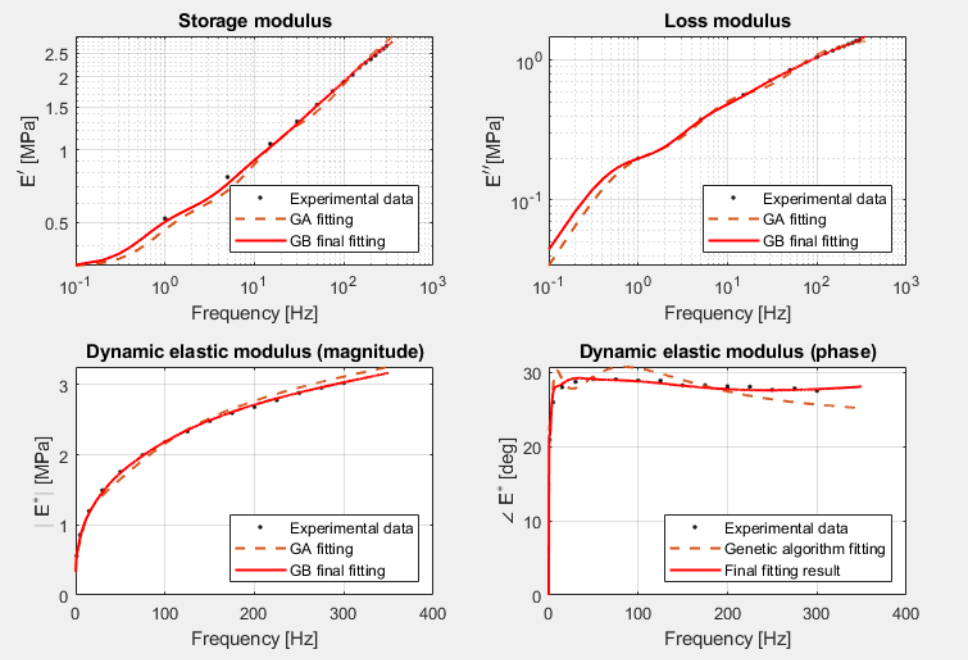

Figure 2.14: Comparison between experimental points from Sorbothane 2016 data and two step fitting curves

Since the considered function is nonlinear, a genetic algorithm is used in order to find the global minimum of this function, which, being nonlinear, can have a lot of local minima. The result obtained by the first fitting is used as starting point by the gradient base optimization in order to obtain the convergence in the global minimum more quickly. The shape of the curves obtained at the end of the last step, performed through this second algorithm, as can be seen in the above plot, fit precisely the experimental points. That fact is important because means that the Prony parameters that obtained as output of this procedure give us a more valid description of the Sorbothane viscoelastic behaviour.

The obtained Prony series parameters are reported in the table below.

$E_0[MPa]$	e_1	e_2	e_3	e_4	e_5	τ_1	τ_2	τ_3	τ_4	τ_5
7.5635	0.1514	0.0561	0.0313	0.0820	0.6375	0.0011	0.0232	0.2406	0.0046	0.0001

Table 2.10: The evaluated parameters of Prony series for Sorbothane 2016 (Durometer 52)

These data are needed to perform viscoelastic definition in Abaqus CAE software, used for the FEM simulation described in the details in the following chapter.

3. FEM of simple configurations and experimental validation

3.1 Overview

The parameters determined in the previous chapter for hyperelasticity and viscoelasticity are, as anticipated, at the base for the correct definition of Sorbothane behaviour into CAE environment. The finite element model has to be realized to best approximate the real behaviour of the material.

The aim of these tests is to evaluate the correctness of the characterization procedure of the chapter 2. In case of positive validation of the simple Finite element models through the experimental test, the values are reported in a Crate model in order to evaluate the Sorbothane damping capability in real conditions.

The use of small and simple geometries allows us to reduce the time needed to create the model and the time taken by the simulation process.

Another reason to choose small parts is to simplify the experimental tests on that objects, necessary to validate the FE model. The tests are performed by using a small shaker directly in laboratory, reducing the setup time and also making easy to test different configurations using different steel parts, with different shape and mass, and then different Sorbothane pads, in terms of dimension, number and position.

The tested parts are five, represented in the figure below, with a weight that goes from less than 0.4 kg to more than 2.1 kg.

Figure 3.1: Configuration 1 for experimental tests

Figure 3.2: Configuration 2 for experimental tests

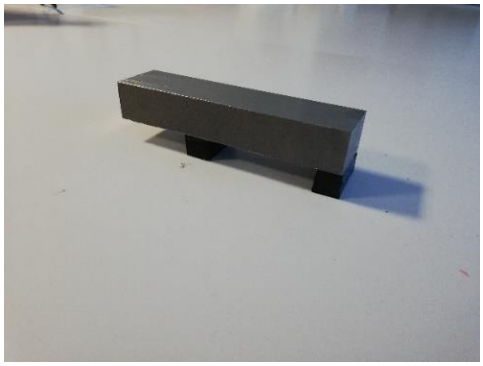

Figure 3.3: Configuration 3 for experimental tests

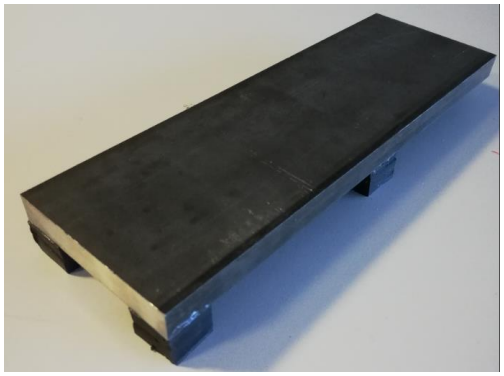

Figure 3.4: Configuration 4 for experimental tests

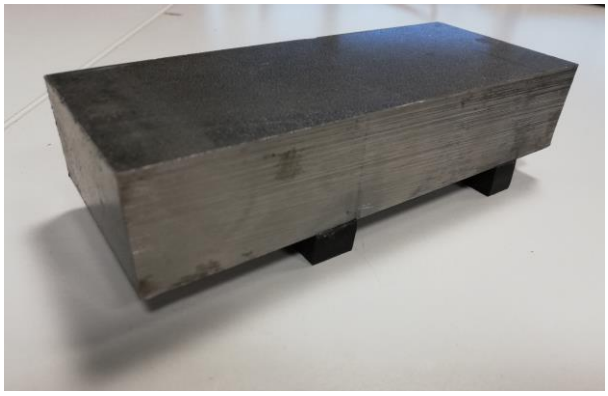

Figure 3.5: Configuration 5 for experimental tests

The pads are realized using Sorbothane durometer 50: this material is difficult to be cut by conventional technologies, so the producer recommends the use of waterjet technology. In this case, since the geometries needed are very simples the Sorbothane is cut using a simple manual cutter. The only dimension that remains constant in all the configurations is the height, this in order to avoid cut imperfection that can cause uneven support during the positioning on the shaker and a different mass distribution with respect to the FE model.

Since the pads height is constant and equal to 1.27 cm (0.5”), and since all the part considered have lower mass, the pad compression obtained in all the tests is a few percentage points and generally lower than the minimum value present on the Sorbothane datasheet that is equal to 10%.

The finite element models and analysis are realized by using Abaqus CAE, produced by Simulia. This is one of the few software able to model viscoelastic behaviour of materials. A general description of Abaqus CAE software is given in the next section together with an explanation of the steps necessary for the model creation and for the performed analyses.

The steps and the analysis are repeated for all the 5 parts considered in this chapter.

3.2 Finite Element Modelling with Abaqus CAE

The study of a component or a system of different part (or assembly) requires in any finite element based software three main steps which consist in pre-processing, solving and post-processing.

The pre-processing step is related to the preparation of the geometry and mesh. The geometry can be realized directly in the FE program or can be imported from another CAD. In both the cases a simplest representation of the part, avoiding small details that do not affect the general response of the system, is preferred in order to simplify the meshing process. Meshing consists in dividing the geometry into elements that are connected to one another at the nodal points. The dimension of the mesh is chosen by the user; using a coarser mesh can be useful to reduce the time required to perform the desired analysis but limits the accuracy of the analysis. The choice of the right mesh has to be performed case by case and depending on the analysis that has to be performed. In this step also the specification of the material properties is requested. So before starting the model creation is needed a well understood of the material that is needed to simulate.

The solution phase is related to the specification of the boundary conditions and loads imposed to component of the system and the solving of the problem. As can be seen in detail in the following sections, the boundary conditions can be expressed in form of restriction of degrees of freedom in the three directions (X, Y, Z), or in form of contact region between different areas of the same parts. The load type varies with the type of analysis that has to be performed but in general forces, displacements, pressures, velocities or accelerations are applied.

The post-processing phase regards the visualization of the results in graphical form. Deformed shapes, stresses, strains, reaction results and graph can be plotted, and the output can be compared with the desired parameters. The post-process should evaluate critically the validity of the obtained result in order to understand if some design modification or optimization work is needed.

The commercial finite element software most used is Abaqus CAE and it is also the one used to perform the following analysis.

Abaqus CAE is divided into modules, where each module defines a logical aspect of the modelling process, defining the geometry, the material properties and generating a mesh. Moving from modules, the model is built. From this model Abaqus/CAE generates an input file that is submitted to Abaqus/Standard or Abaqus/Explicit analysis products. The analysis product makes the analysis and send information to Abaqus/CAE to allow the monitoring progress of the job. An output database containing the result of the simulation is generated. This output file is used in the visualization module to view the results of the performed analysis [17].

An important thing to consider in working with Abaqus/CAE regards the measuring units, since this software doesn't have single system of predefined units of measurement but allows the use of different systems of units called consistent [18].

The following image provides example of consistent units.

MASS	LENGTH	TIME	FORCE	STRESS	ENERGY	DENSITY	YOUNG's	35MPH 56.33KMPH	GRAVITY
kg	m	s	N	Pa	J	7.83e+03	2.07e+11	15.65	9.806
kg	cm	s	1.0e-02 N			7.83e-03	2.07e+09	1.56e+03	9.806e+02
kg	cm	ms	1.0e+04 N			7.83e-03	2.07e+03	1.56	9.806e-04
kg	cm	us	1.0e+10 N			7.83e-03	2.07e-03	1.56e-03	9.806e-10
kg	mm	ms	kN	GPa	kN-mm	7.83e-06	2.07e+02	15.65	9.806e-03
g	cm	s	dyne	dyne/cm²	erg	7.83e+00	2.07e+12	1.56e+03	9.806e+02
g	cm	us	1.0e+07 N	Mbar	1.0e+07 Ncm	7.83e+00	2.07e+00	1.56e-03	9.806e-10
g	mm	s	1.0e-06 N	Pa		7.83e-03	2.07e+11	1.56e+04	9.806e+03
g	mm	ms	N	MPa	N-mm	7.83e-03	2.07e+05	15.65	9.806e-03
ton	mm	s	N	MPa	N-mm	7.83e-09	2.07e+05	1.56e+04	9.806e+03
lbf-s²/in	in	s	lbf	psi	lbf-in	7.33e-04	3.00e+07	6.16e+02	386
slug	ft	s	lbf	psf	lbf-ft	1.52e+01	4.32e+09	51.33	32.17
kgf-s²/mm	mm	s	kgf	kgf/mm²	kgf-mm	7.98e-10	2.11e+04	1.56e+04	9.806e+03
kg	mm	s	mN	1.0e+03 Pa		7.83e-06	2.07e+08		9.806e+03
g	cm	ms	1.0e+1 N	1.0e+05 Pa		7.83e+00	2.07e+06		9.806e-04

Figure 3.6: Example of consistent systems of units [18]

3.2.1 Models creation procedure

The model creation procedure following presented is valid for all the rectangular steel parts under which are attached Sorbothane made pads.

As said before, Abaqus CAE is divided into modules [17], the first one is called **Part** module and is the one used to create the geometry of the various pieces composing our system. In the presented case is needed the realization of five different systems, so for each one is needed a different part creation. Each model is composed by at least two parts that represent building blocks of an Abaqus CAE. The first one is the rectangular mass steel made and the second one is the Sorbothane pad. In the following table are presented the dimensions of each part composing the system for all the five systems.

Configuration N°	Steel part dimensions [mm]	Sorbothane Pad dimensions [mm]
1	40 x 40 x h 31	12x12x h 12.7
2	111.5 x 30 x h 27.3	30 x 12 x h 12.7
3	121.2 x 30 x h 19.2	30 x 12 x h 12.7
4	185 x 60 x h 9.9	15 x 15 x h 12.7
5	149 x 61 x h 30	11 x 11 x h 12.7

Table 3.1: Dimensions of different configurations

The first thing to do in this module is to define if the part that we want to create has to behave as rigid or deformable body. In our case, since the steel is more rigid than Sorbothane, we can consider the steel parts as rigid to save computational time, but since they are very simple we decide to consider all the parts deformable, not increasing so much the total time needed to perform the analysis.

Once a part is created, we can repeat the procedure for the second part. Following are reported as example the parts composing the configuration 4.

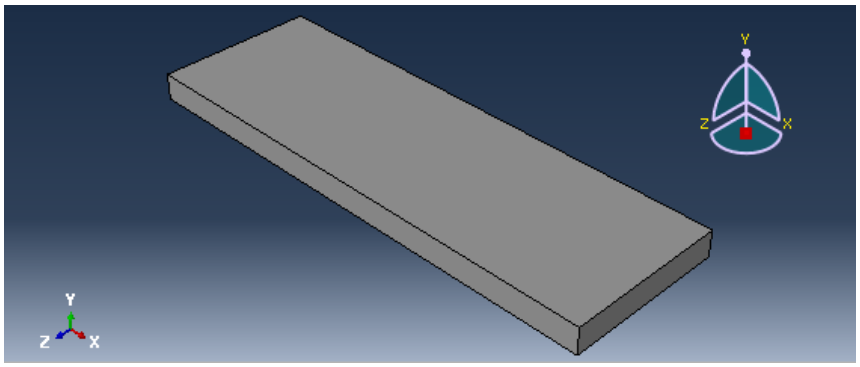

Figure 3.7: Steel part - Configuration 4

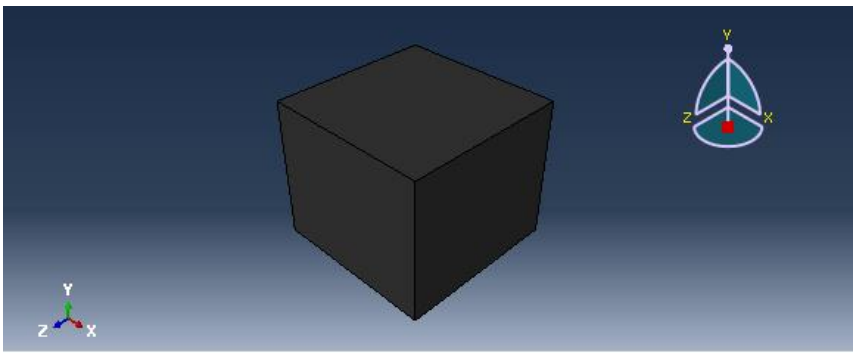

Figure 3.8: Sorbothane Pad configuration 4

Once the parts needed to compose the model are created, we have to pass to the **Property** module, in which it is possible to assign a material to each part create in previous module.

In this case we want to assign two materials, Steel and Sorbothane. In order to do that the first passage is to create the materials through apposite tool. After the material is named it is necessary to define its characteristics, for example in terms of density and its mechanical behaviour. For steel, this procedure is quite simple since it is an elastic material. As density we set a value equal to $7.82e^{-9}$ ton/mm^2 and as material property we choose elastic. The parameters needed to define the elastic behaviour are the Young modulus, imposed equal to 210'000 MPa, and the Poisson coefficient that for steel is equal to 0.3.

To define the Sorbothane behaviour in Abaqus CAE environment, we can also in this case set the value of density, found on the datasheet and equal to 1.345 e^{-9} ton/mm^2, and as mechanical properties we need to remind the observation made in the Chapter 2. Sorbothane is both a hyperelastic and a viscoelastic material, and these two are the mechanical properties that we have to consider also in the model, and for which the parameters are determined by the characterization procedures explained in the previous chapter. For the hyperelastic behaviour is used the Neo – Hooke strain potential energy form with the coefficient value obtained by fitting procedure. Below is reported the Abaqus CAE window in which hyperelastic parameters are present.

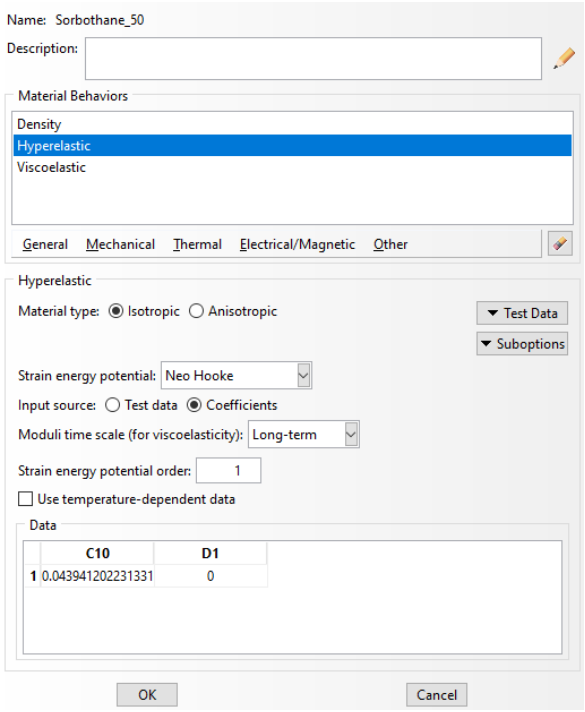

Figure 3.9: Sorbothane Hyperelastic Definition in Abaqus CAE model

Now we have to describe the viscoelastic properties of Sorbothane. This can be do in Abaqus CAE by directly using Prony series representation. We choose to set the Prony parameters in frequency domain, the reason of that choice regards the analysis that we need to perform, detailed described later. The Prony parameters that are needed for the material viscoelastic behaviour definition are the ones determined in the Chapter 2 through the two-step fitting procedure. In addition to that, the parameters related to the bulk relaxation modulus, indicated as k_i_Prony are put equal to zero in according to the incompressibility hypothesis.

Below is reported, as for the hyperelastic behaviour, the Abaqus CAE windows to show the parameters setting performed.

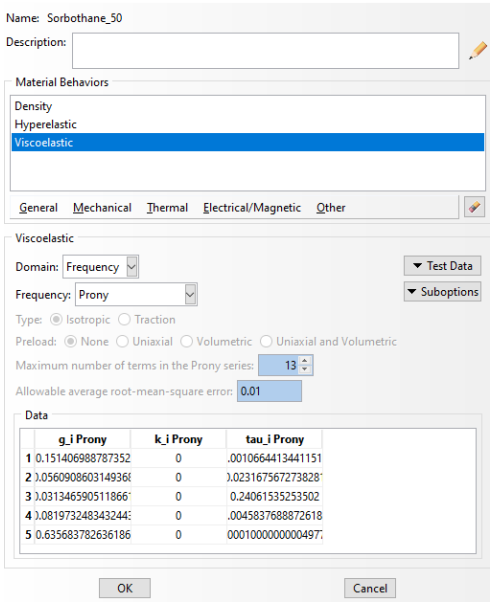

Figure 3.10: Sorbothane Viscoelastic definition in Abaqus CAE model

The materials are now created, and we need to assign them to the part previously created. In order to do that we create two solid homogeneous section, one for each material defined and we assign these sections to their respective parts; these two passages can be done in the property module by using the special tools.

Terminate the property definition procedure it is now necessary to create our configurations. This is possible through the **Assembly** module. In this module the instances can be create starting from the previous realized part, in order to move them relative to each other to compose the desired assembly. The positioning of the instance is realized by sequentially applying positioning constraints that align selected faces, edges or vertex or by applying simple translations or rotations.

In our case the assembly phase is different for all the configurations that we want to model, this because the positioning constraints and also the number of part instance differs in each configuration; some configuration is realized with a number of pads equals to four and some other with only two rectangular pads. In the following table is reported the number of part instance for each configuration.

Configuration N°	N° of steel part instance	N° of Sorbothane pad instance
1	1	4
2	1	2
3	1	2
4	1	4
5	1	4

Table 3.2: Part instances for each configuration

The part instances are constrained in a way to obtain the desired configurations. Once the procedure is finished, looking the Abaqus CAE interface, it is possible to see the final shape of the realized configuration. Here is reported the result of the assembly procedure for the configuration 4.

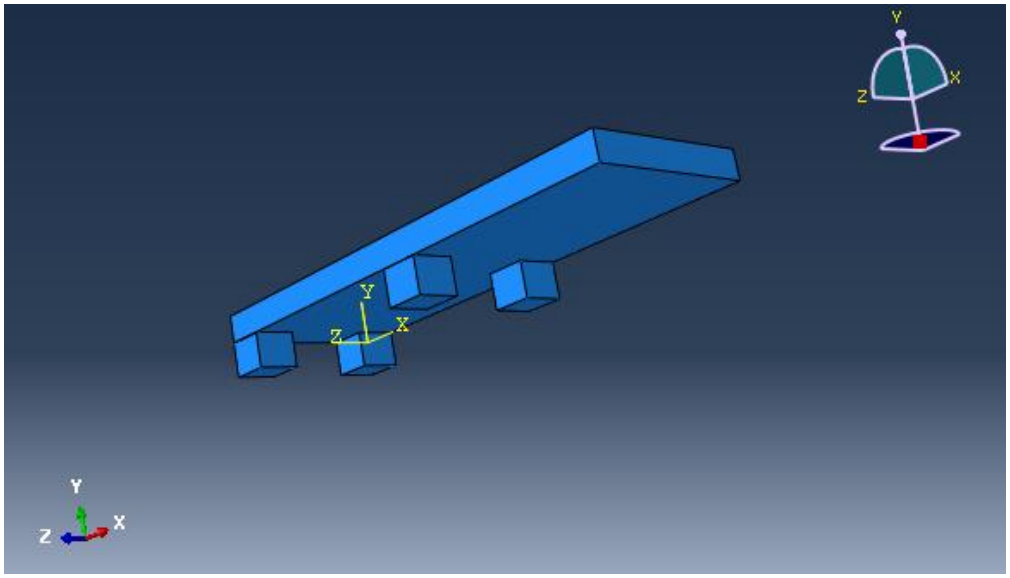

Figure 3.11: Final shape of configuration 4 after Assembly module

For all the configuration we choose to use dependent instance, that means that the create instance is only a pointer to the original part, so shares the geometry and the mesh of the original part. That means that when the original part is meshed, Abaqus automatically applies the same mesh to all the dependent instance of that part.

In this way by entering in the **Mesh** module, it is necessary to assign a mesh only at the original parts. In our case the number of parts for each configuration is equal to two, one that represents the steel part and the other representing the Sorbothane pad. Since most of the deformation is associated to Sorbothane pad, the mesh for this part is chosen to be finer with respect to the one of the steel mass that behave as quasi rigid body. This is due to the intrinsic characteristic of the materials. The approximate global size for the Sorbothane pad is 2 mm, that value is maintained for all the configurations. The mesh of the steel parts is maintained coarse enough to reduce time needed to perform the simulation. The structured mesh for both the parts are chosen with hexahedral elements of quadratic geometrical order. This kind of mesh is generated by using simple predefined mesh topology. Abaqus CAE transform the mesh of a regularly shaped region, such as a square or a cube, onto the geometry of the region that has to be meshed.

The following figure represent the meshed Sorbothane part of the configuration four.

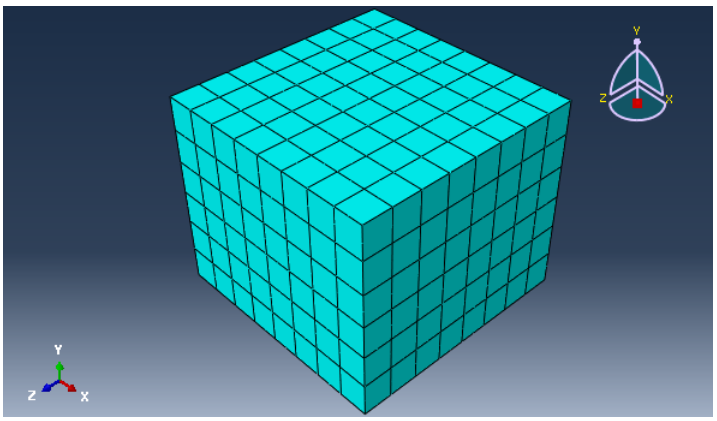

Figure 3.12: Meshed Sorbothane pad of configuration 4 – Hex element

To mesh the Sorbothane pad is necessary to select also the hybrid formulation during the specification of the element type. This kind of elements are used when the material behaviour is incompressible (Poisson's ratio equal to 0.5) or very close to incompressible (Poisson's ratio greater than 0.475) as for Sorbothane and other rubbers like materials.

The **Interaction** module is used to set constraints on the analysis degrees of freedom, whereas constraints defined in assembly module define constraint only on the initial positions of instance. In this module there is the possibility to constrain the degrees of freedom between the regions of a model, and these constraints can be suppressed or resumed to vary the analysis model. In our model we use the tie constraint in order to maintain the pads attached to the rectangular steel mass above. This geometrical constraint type allows to fuse together two surfaces, in our case the top face of all the pads and the bottom face of the steel part. In this way relative motion between them is avoided so the nodes of the two tied surfaces has the same motion.

Once the pre-processing phase is over, geometry and mesh of the various part composing our configuration are defined.

The first thing to do in the following phase, named solution phase, is to consider the problem that we have to solve through the model and understand the kind of analysis that is needed to perform. Within a model it is possible to define a sequence of one more analysis step by using the **Step** module. The step sequence provides a convenient way to capture changes in the loading and boundary conditions of the model, change in the way parts of the model interact with each other and any other changes that may occurs in the model during the analysis procedure. Steps allow to change the analysis procedure, the data output and various controls [17]. The step manager distinguishes between general nonlinear steps and linear perturbation steps. General nonlinear analysis steps define sequential events: the state of the model at the end of one general step provides the initial state for the start of the next general step. Linear perturbation analysis step provides the linear response of the model about the state reached at the end of the last general nonlinear step.

For each step in the analysis can be specified if Abaqus considers nonlinear effects from large displacements and deformations. Only if displacements in a model due to loading are relatively small during a step, the effect may be small enough to be neglected. In our analysis the non-linearities due to loads are considered and so the flag Nlgeom is set to ON.

After the initial step created by default by Abaqus, the first step that is considered is the static one. In this step inertia effects and the time-dependent material effects are neglected. The time period set for the analysis is equal to one second. This analysis can be useful in order to understand the effect of the rectangular steel part supported by the Sorbothane pad and to evaluate the compression effect induced on the pads due to the steel mass.

The second step that is tried to implement is a linear perturbation procedure named frequency. This procedure can be generally used to perform eigenvalue extraction to calculate the natural frequencies and the corresponding mode shapes of a system. To perform eigenvalue extraction the Lanczos method is used. It is necessary to set the maximum frequency of interest that in this case is equal to 300 Hz and the number of eigenvalues required. The problem with this step is that it is not able to consider the frequency dependence of the material properties, concept that is at the base of Sorbothane analysis. It is possible only to set a frequency values in which the material properties are evaluate and used for all this step. For this reason, the results obtained through this step can be considered only an approximation of the natural frequencies and of the mode shapes of the considered configuration.

Since the goal of these simulations is mainly to understand if Sorbothane properties are correctly considered, the idea is to perform a direct solution steady-state Dynamic Analysis that is a procedure that enables to calculate the response of the system directly in terms of the physical degrees of freedom of the model. This analysis is more accurate than the other steady-state dynamic procedures implemented in the Abaqus CAE software; the drawback is that takes more computational time. The steady-state dynamic analysis provides the steady-state amplitude and phase of the response of a system due to harmonic excitation at a given frequency. It is important to consider that this analysis linearize the behaviour of the considered system around the position reached in the previous general step. For this reason, the accuracy of the obtained results also depends on the amplitude of the vibration considered, in particular, good results are obtained when vibration amplitudes are sufficiently lower, as in our case.

When defining a direct solution steady state dynamic step is needed to specify the frequency range of interest, that in our case is considered from 0 Hz to 300 Hz, and the number of frequencies at which results are required in each range; in our case we decide to consider a point for each frequency, so 300 frequencies are requested. It is used a linear frequency spacing to have the frequency point equally spaced along the frequency axis. The choice of this type of analysis is due to consider the viscoelastic material properties.

Below is reported the Abaqus menu in which the analysis parameters are specified.

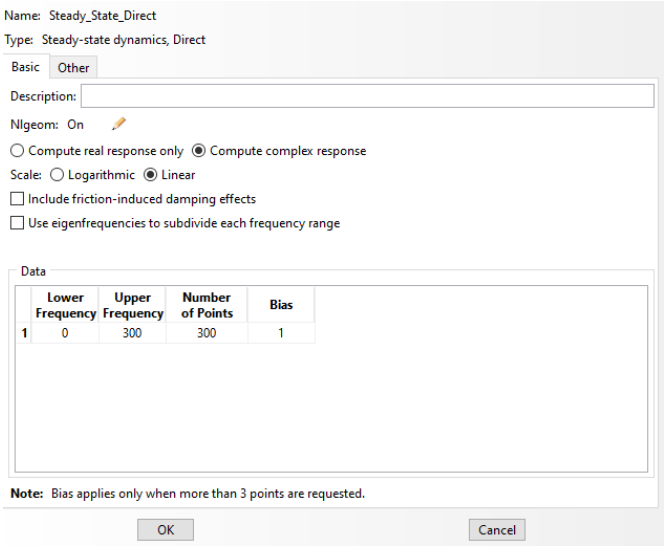

Figure 3.13: Parameters specification for Steady-state dynamics Direct analysis

The bias parameter can be used to provide a closer spacing of the results point either toward the middle or toward the end of each frequency interval. In the above figure it can be seen that this parameter is chosen equal to one, that means that the desired result points are equally spaced toward the frequency range.

It is now necessary to specify the loads and the boundary condition of the model, needed for the analysis steps. It is necessary to use the **Load** module that enables with specific toolboxes to specify for example the load types acting on a system. In this specific case it is needed to define a uniform acceleration acting in a fixed direction to simulate the gravity acceleration. Abaqus CAE software is able to calculate the loading using the acceleration magnitude entered in the gravity load definition and the density specified in the material definition. Below is reported the menu in which it can be seen the value of gravity load in Component 2 that represent the Y direction in Abaqus CAE reference system.

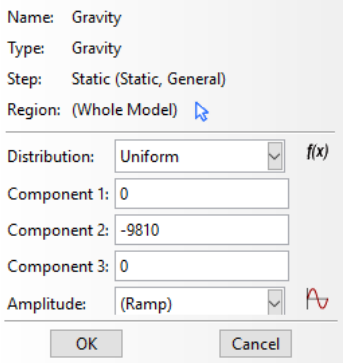

Figure 3.14: Gravity load specification in Y- direction

The minus sign indicates that, in accordance with the reference system used, the gravity acceleration must act downwards. The modulus equal to 9810 is expressed in mm/s^2 to be coherent with consistent units of Abaqus CAE. As can be seen the region selected is “whole model”, that means that the gravity acceleration equally acts on all the parts of the model. The specification of this load is done in the static step and is maintained in all the following steps composing the analysis procedure. No other loads are necessary in the performed analysis.

In this module it is also possible to define the boundary conditions needed for all the analysis steps. In static step, as shown in figure below, the bottom part of the Sorbothane pad is defined to have no displacement in all the directions: the model is fixed.

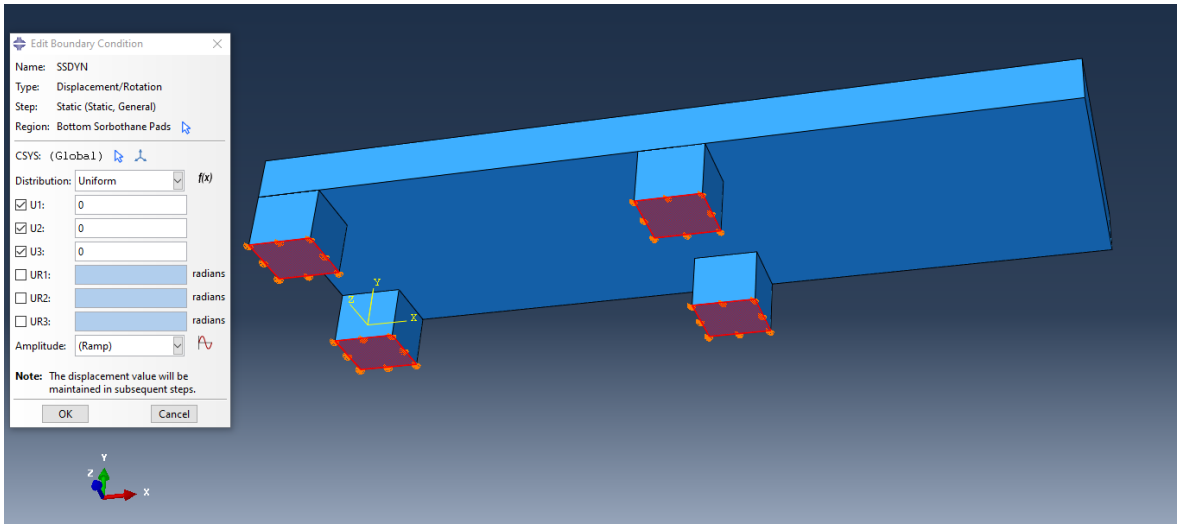

Figure 3.15: Boundary condition menu for Static step of Configuration 4

The type of boundary condition used is called Displacement/Rotation to constrain the movement of the selected degrees of freedom to zero or to prescribe the displacement or rotation for each selected degrees of freedom. In this case, as anticipated before, the values for the three direction U1, U2, U3, that corresponds to X, Y, Z directions are defined equal to zero to avoid any movement. This boundary condition is maintained for the static step and then modified in the following direct solution steady-state Dynamic step. In this last step generation of harmonic oscillation is needed to analyse the response of the system.

Boundary conditions can be applied to any of the displacement or rotation degrees of freedom. These boundary condition vary sinusoidally with time and it is possible to specify the real (in-phase) part of a boundary condition and the imaginary (out-of-phase) part of a boundary condition separately. In the realized models we consider the harmonic oscillation, in terms of displacement, only in vertical direction, U2 for Abaqus CAE, and by setting the amplitude only for the real part equal to 0.1.

Below it is reported the boundary condition menu for this step.

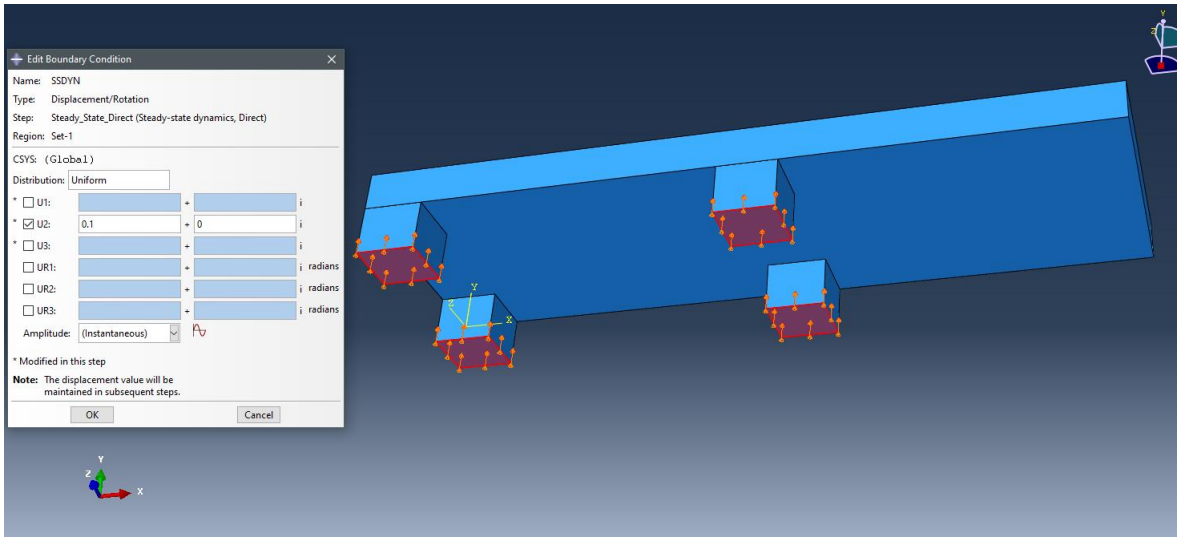

Figure 3.16:Boundary condition menu for the direct Steady-State Dynamics step of Configuration 4

Looking at the figure it can be seen that some arrows in correspondence of the Sorbothane pads are appeared. This because the harmonic excitation is exerted on that surfaces.

To understand the reason of that choice is necessary to remember the aim of this thesis work; we want study a material placed under the Crate that is able to absorb vibration coming from the source, represented by the means of transport, and transferred to the artwork contained in the Crate that is transported.

In these simple configurations, realized first of all to test the material parameters determined in Chapter 2, the parallelism with the Crate during transport becomes evident. The base concept of a mass, that is represented by the Crate containing the artwork in the real system, and here considered as a rectangular steel part, suspended through some Sorbothane pads that have the aim to absorb the vibration, is the same.

In these models the source excitation is represented through the above defined harmonic excitation in the last considered step.

Since all the task involved in the creation of the model are finished, it is necessary to enter in the **Job** module to perform the finite element analysis. It is necessary to create a job that has to be submitted for the analysis. In the job creation, the number of processors that are used to carry out the analysis can be selected. In this case to perform the simulations an Intel(R) Core (TM) i7-8750H CPU @2.20GHz is used. After the job submission it is possible to monitor the progress through apposite window.

When the analysis is finished, or equivalently the job is completed, passing into the **Visualization** module it is possible to have a graphical representation of the finite element model and results. It obtains model information from the current module database and result information from an

output database. In this module it is also possible to plot the desired quantities. In the simulation performed on the small parts the visualization module is used to visualize the displacement in vertical direction obtained from the static step; the mass of the rectangular specimen deforms the Sorbothane pads on which is supported. An example of these resultant deformation in vertical direction is represented in the following figure.

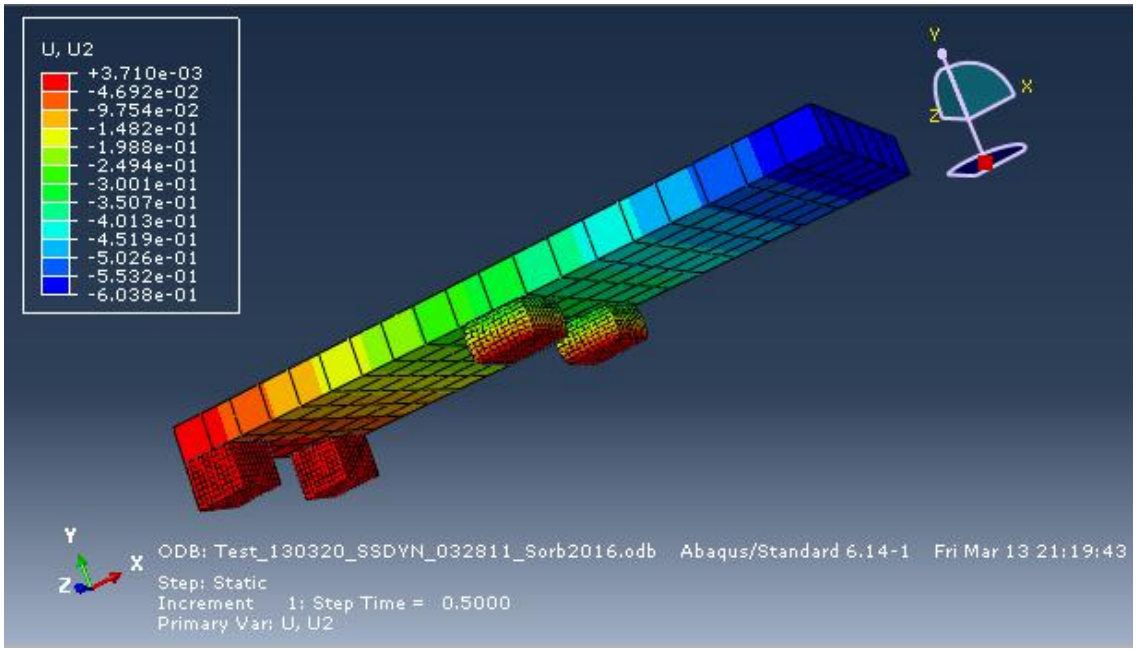

Figure 3.17:Example of Sorbothane Pad vertical displacement - Direction U2 - Configuration 4 - Static Step

Regarding the result of the direct steady-state dynamic step, the interest is mainly in the magnitude and phase of the vertical accelerations measured in correspondence of a node onto the base of the Sorbothane Pad on which the harmonic excitation is applied in order to have reference value of the acceleration transmitted to the model, and the accelerations measured in two nodes on the top surface of the steel made part. These three accelerations can be visualized as a X-Y plot directly in the visualization module of Abaqus CAE. Using the X-Y tool present in the visualization module toolbox it is possible to select the desired variable to plot, in this case the vertical component of acceleration represented in Abaqus as A2. Once the variable is selected it is possible to pick the node in which the quantity has to be measured. After the nodes are selected the desired plot is generated.

An example of magnitude and phase angle plots are reported in the following two figures, also in this case for Configuration 4.

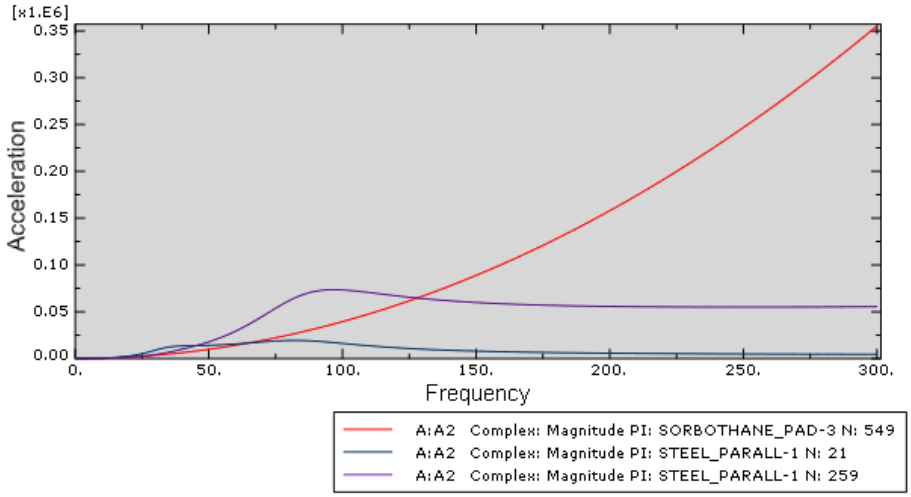

Figure 3.18: Magnitude plot Direct Steady-State Dynamics - Vertical Acceleration A2 - Configuration 4

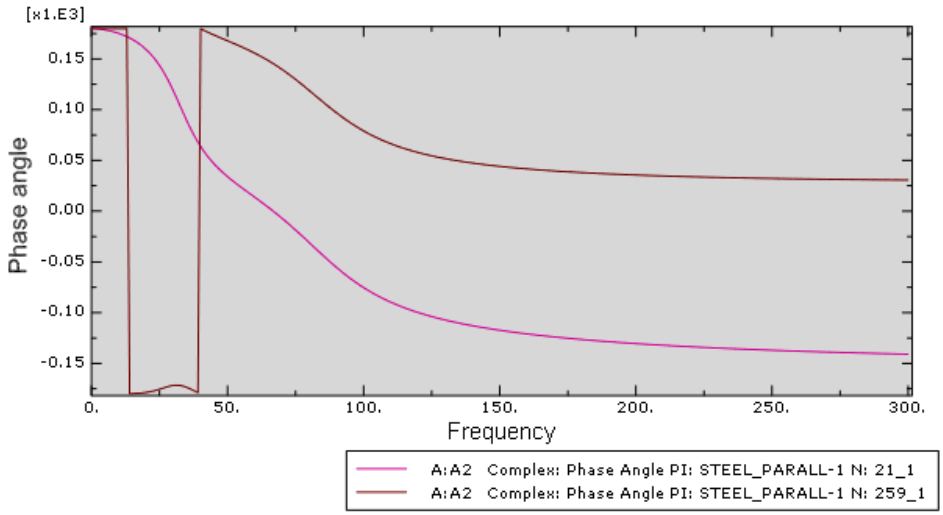

Figure 3.19: Phase angle plot Direct Steady-State Dynamics - Vertical Acceleration A2 - Configuration 4

Looking at the Figure 3.12 it can be noticed that the acceleration is expressed in mm/s^2 to be coherent with the consistent units of Abaqus CAE. The X-axis representing the frequencies goes from 0 Hz to 300 Hz considering all the points of the direct steady-state dynamics analysis.

The legend of both the plots indicates the correspondence between the curve in the graph and the part containing the nodes in which the quantity is measured.

The curves contained in the previous two plots are generated also for the other configuration treated in this chapter. The nodes for which the curves are generated are not randomly selected. The reason for the choice will be clear at the end of this chapter.

The data corresponding to the curves are finally exported from Abaqus and then analysed in Matlab.

3.3 Experimental tests procedure description

3.3.1 Creation of the testing configurations

To validate the finite element models realized by Abaqus CAE software, the idea is to set up an experimental procedure. Before starting with the test, the configurations considered and analysed through finite element analysis needs to be implemented in practice. The steel part is coupled with correspondent Sorbothane pads cut out from the original Sorbothane sheet by a manual cutter. The Sorbothane pads are then glued to the bottom surface of the steel specimens.

3.3.2 Performed test description and needed equipment

To determine the dynamic response under 300Hz, the idea is to use a shaker to force the realized simple systems. One configuration at time is glued over an aluminium plate mounted on the moving element of the shaker to prevent any movement of the testing element caused by oscillations, particularly for lower frequencies. The response to the generated excitation is measured through accelerometers placed on the top of the steel element. Another accelerometer is placed on the aluminium plate in order to measure the produced input. The input is generated using a function generator connected to the amplifier of the shaker. Accelerometers data are acquired by using an acquisition device connected to a PC in order to visualize and to save the test results for the following data analyses operations. The figure below shows the complete measurement chain.

Figure 3.20: Equipment used for testing operation and data acquisition

In the following table is presented a detailed description of the equipment employed to perform the tests

Type of instrument	Model	Additional notes
Accelerometer	PCB 333B30	Sensitivity 100mV/g
Accelerometer	PCB 333B30	Sensitivity 100mV/g
Accelerometer	PCB 333B30	Sensitivity 100mV/g
Function Generator	KEYSIGHT 33500 B	
Shaker	LDS V406	Usable freq. range 5 Hz-9 kHz
Power Amplifier	LDS PA 100 E	
Acquisition Device	NI 9234	4 channels, IEPE

Table 3.3: Instrumentations employed for measures

The total number of accelerometers used is equal to three: two accelerometers placed on the top surface of the steel element at the extremities and one used as reference on the aluminium plate on which the tested system is attached. This is true except for the first configuration, for which the symmetrical position of the Sorbothane pads allows to place only one accelerometer on the upper surface of the steel element.

Accelerometer positioning can be clearer by looking at the following figures that show the exact position and the correspondence between the accelerometer and the channel of the acquisition device. This information is useful for the following analysis of the acquired data.

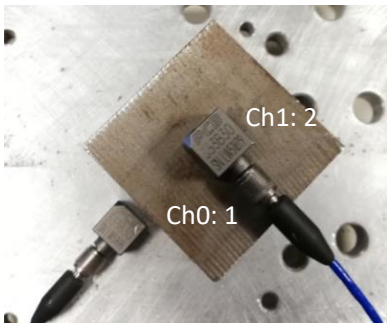

Figure 3.21: Accelerometers position - Configuration 1

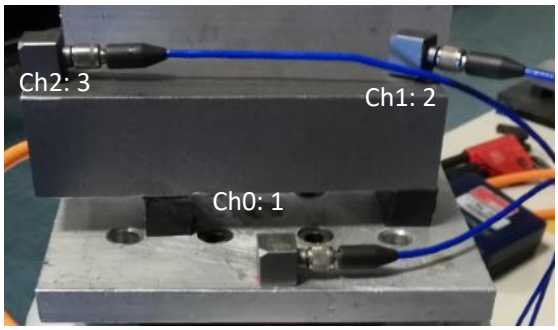

Figure 3.22: Accelerometers position - Configuration 2

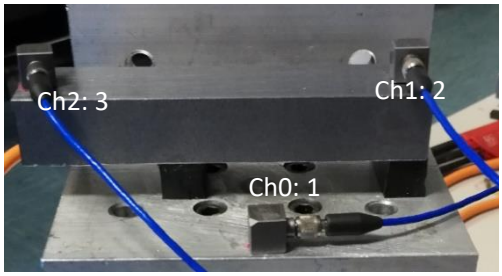

Figure 3.23: Accelerometers position - Configuration 3

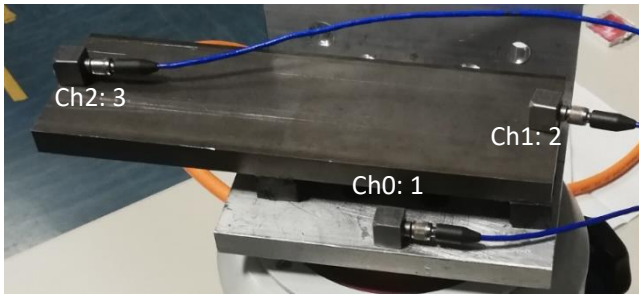

Figure 3.24: Accelerometers position - Configuration 4

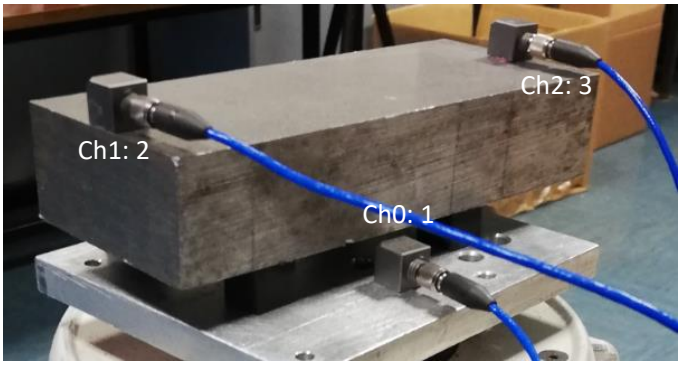

Figure 3.25: Accelerometers position – Configuration 5

As can be seen by looking at the above figure, accelerometer number 1 is always used as a reference point to read the produced input.

Two different input signals are used as input to force the systems: Random Noise and Sweep Sine. In the table reported below are specified all the characteristics of the tests performed for each of the five configurations.

Test N°	Configuration N°	Input Type	Frequency [Hz]	Sampling Frequency [Hz]	Acquisition Time [min]	Master Gain Value [V]
1	2	Random Noise	300	5120	6	8
2	2	Random Noise	300	5120	6	2
3	2	Random Noise	300	5120	6	4
4	2	Sweep	0.5 - 500	5120	5	2
5	2	Sweep	0.5 - 500	5120	5	4
6	3	Sweep	0.5 - 500	5120	5	2
7	3	Sweep	0.5 - 500	5120	5	4
8	3	Random Noise	300	5120	6	2
9	3	Random Noise	300	5120	6	4
10	4	Sweep	0.5 - 500	5120	5	2
11	4	Sweep	0.5 - 500	5120	5	4
12	4	Random Noise	300	5120	6	2
13	4	Random Noise	300	5120	6	4
14	1	Sweep	0.5 - 500	5120	5	2
15	1	Sweep	0.5 - 500	5120	5	4
16	1	Random Noise	300	5120	6	2
17	1	Random Noise	300	5120	6	4
18	5	Random Noise	300	5120	6	2
19	5	Random Noise	300	5120	6	4
20	5	Sweep	0.5 - 500	5120	5	2

Table 3.4: List of tests performed on the 5 configurations with detailed descriptions

The data obtained from the tests are then collected and analysed in Matlab. Detailed description of the adopted analysis procedure is described in the next section.

3.4 Validation procedure and results

As anticipated before in this chapter, it is needed to evaluate if the parameters chosen to define the material properties of Sorbothane in terms of Viscoelasticity and Hyperelasticity are correct, and also if the linearization around the final static position, performed on the models, in the steady-state dynamic analysis enables to obtain good results.

The idea is to identify the natural frequencies and vibration modes obtained from the experimental procedure and the ones obtained from the Abaqus CAE model. If the same or at least similar values are obtained the material characterization can be considered for the following analysis, if not, it is necessary to review the characterization procedure.

The experimental collected data are then separately analysed in Matlab for the five configurations; transfer functions, in terms of modulus and phase, between each accelerometer placed on the top surface of the steel part (Channel 1 and 2 or accelerometer n°2 and n°3) and the reference accelerometer (Channel 0 or equivalently accelerometer n°1) are plotted separately. In particular the transfer function between accelerometer two and accelerometer one is indicated as "TF 12" and the ones between accelerometer three and accelerometer one as "TF 13". To reduce the number of total plots, and to show the robustness of the experimental test, it is chosen to realize two plots for each configuration. The first one represents the modulus and phase of TF12 calculated for each test, and the second one the same for TF 13. The considered range is between 10 Hz and 300 Hz. Lower limit is given by the working field of the shaker (see Table 3.4) and the upper one represents the maximum frequency involved in the field of interest.

The data obtained by the finite element simulation in magnitude and phase for each of the five configurations has to be imported in Matlab in order to perform the desired analyses. As said before, the nodes for which the curves are generated are not randomly chosen, but they are selected to be representative of the mounting position of the accelerometers of the experimental configurations. This except for the reference one that in the model is chosen in the bottom surface of the pad since is one of the points in which the harmonic excitation is applied.

Due to consistent units the acceleration values in Abaqus is given in mm/s^2 and so to be comparable to the ones obtained experimentally they have to be converted in m/s^2. Also, the phase given by Abaqus needs to be converted from degrees into radiants.

Once the data are converted, transfer functions are calculated with the same criterion used for the experimental ones. These obtained curves are then ready to be superimposed to the experimental ones. At the end of this procedure the Matlab script is ready to directly plot the superimposition of the transfer function obtained from the experimental tests and the ones obtained by the finite element analysis. This script needs as inputs the experimental data and the data extracted from the Abaqus simulation so it can be adapted to each configuration by changing the input files.

In the next sections are presented the obtained plots for the five configurations and relative considerations.

3.4.1 Configuration 1 – Results and Considerations

The following plots present the superimposition of transfer functions, in both magnitude and phase, obtained by the model information with the ones obtained through the experimental procedure applied to the Configuration 1.

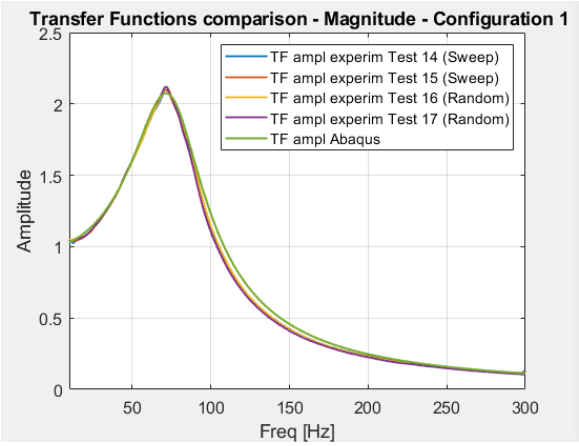

Figure 3.26: Transfer Functions Comparison - Magnitude - Configuration 1

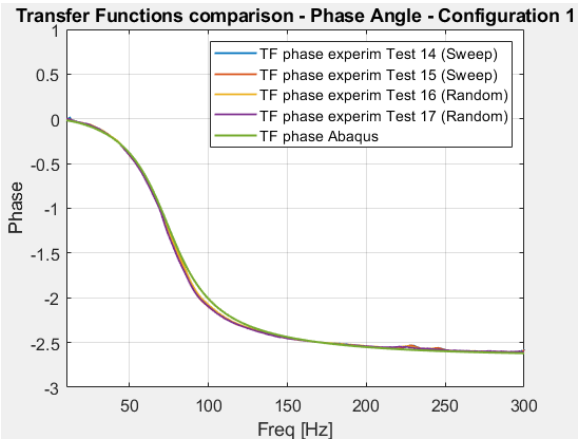

Figure 3.27: Transfer Functions Comparison - Phase Angle - Configuration 1

Looking at the above graph seems that in this first simple configuration, the Abaqus model shows the same behaviour of the real configuration experimentally tested. Also, the transfer functions obtained from sweep and random tests seems to give the same results. The amplitude peak is found at 71 Hz looking at the experimental curves and at 72 Hz looking at the Abaqus curve. This result can be considered satisfactory. The phase change is coherent with the peak in the amplitude plot.

3.4.2 Configuration 2 – Results and Considerations

For the second configuration the transfer function between the reference (or bottom pad point in the model) and the two accelerometers on the top surface of the rectangular steel mass are separately plotted.

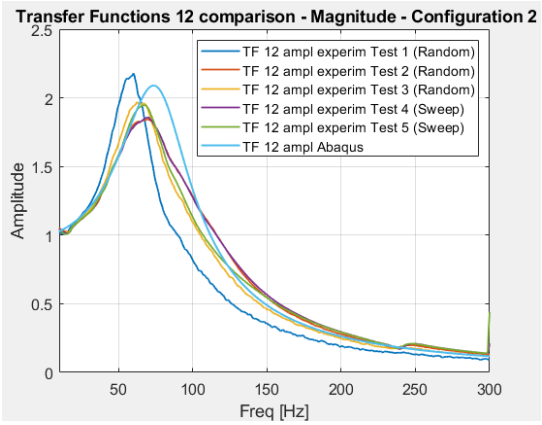

Figure 3.28: Transfer Functions 12 comparison - Magnitude - Configuration 2

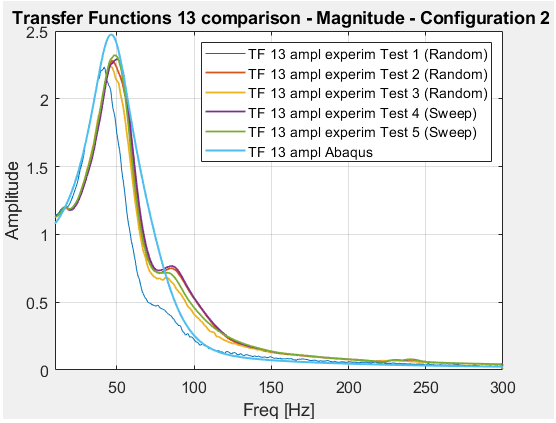

Figure 3.29: Transfer Functions 13 comparison - Magnitude - Configuration 2

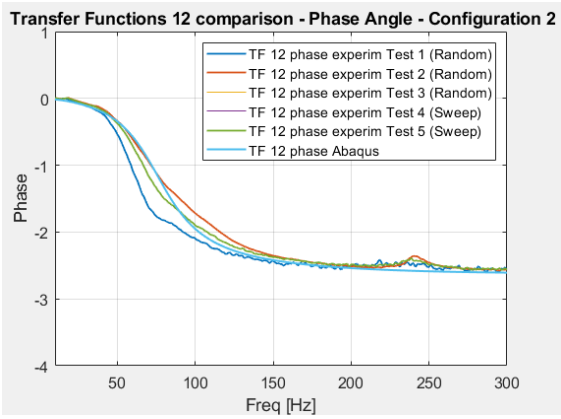

Figure 3.30: Transfer Functions 12 comparison - Phase Angle - Configuration 2

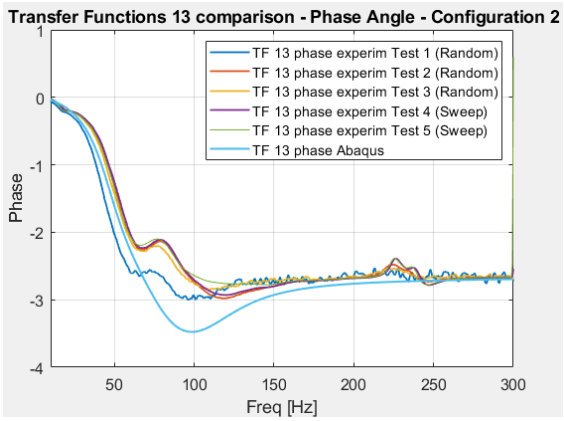

Figure 3.31: Transfer Functions 13 comparison - Phase Angle - Configuration 2

In this considered configuration some differences between the results are visible both for TF 12 and TF13.

Test 1 is performed without gluing the Sorbothane pads on the aluminium plate attached to the shaker. That result is maintained only to show that, without glue the pads, the measurement can be affected by some errors than can be produced by relative movement of the configuration with respect to the shaker produced oscillation.

Considering the TF12 plots it can be seen that the Abaqus transfer function is slightly shifted to the right compared to the experimental ones. But this difference can be considered acceptable. The phases seem to be coherent between them.

Looking now at the TF 13 plots, and considering the experimental curves, a sort of double peak is present.

The first hypothesis that can be done in order to explain the presence of this second small peak is that a mode, near to the vertical one, that is not perfectly vertical can be partially excited during the experimental testing procedure and then detected by the accelerometers. Considering the results given by frequency analysis, and remembering all its limitations above described, it can be seen that at a frequency near to the ones attributed to the vertical mode, appears another vibration mode. This vibration mode, reported in the figure below, can be associated to the second peak present in the experimental curves.

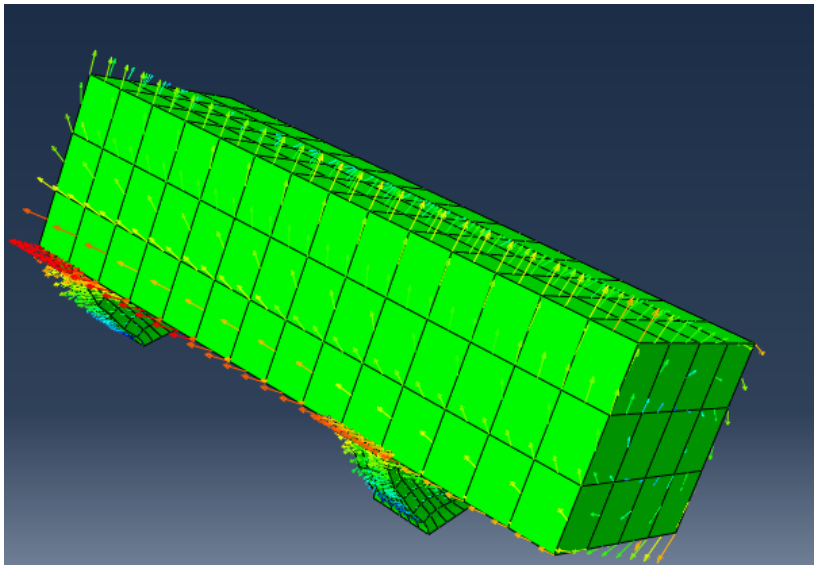

Figure 3.32: Frequency step - Representation of the vibration mode attributed to the experimental double peak

Comparing the experimental curves with the one of Abaqus it can be seen that the double peak here is not present. This can effort the theory of a mode that is not perfectly vertical directed, in particular it seems to be a torsional mode that in the analysis performed by Abaqus CAE on the ideal model cannot be seen, since the excitation is considered only in vertical direction.

The second hypothesis that can explain the presence of this double peak is that in Abaqus is modelled a material that is more damped than the real one. This because higher damping means lower peak and so in that case the peak in the Abaqus analysis can be covered.

This last concept can be explained considering a simple configuration, reported in the figure below, consisting of the same steel part used in configuration 2 under which, instead of the Sorbothane pads, is placed a linear spring-dashpot only to demonstrate how the damping can affect the presence of the double peak.

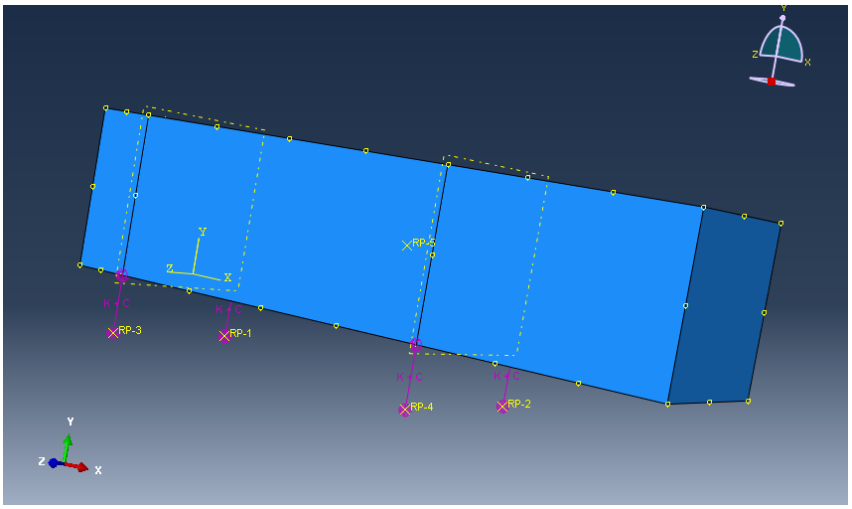

Figure 3.33: Simple configuration in which Sorbothane pads are replaced with spring-dashpot

In the figures below are reported the stiffness and damping parameters specified and the corresponding transfer functions (only magnitude), calculated considering the same node used to calculate the TF13 in the original configuration. The performed analysis is the same used for all the configurations described in this chapter. The difference between these two tests can be found in the damping value imposed, named Dashpot coefficient in Abaqus CAE menu. In the first test the damping value is half than in the second one.

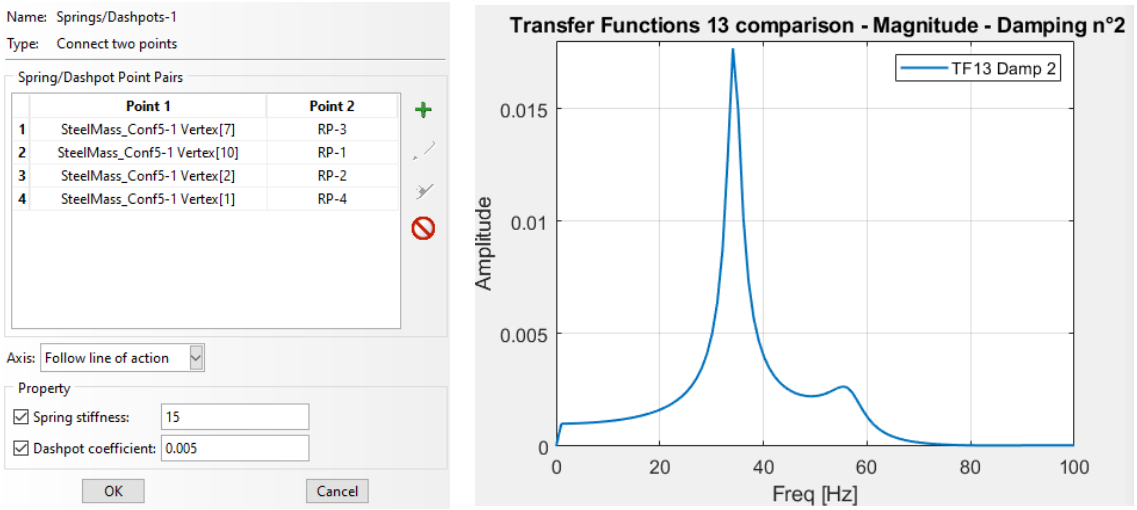

Figure 3.34: Transfer function 13 – Linear spring and dashpot configuration - Magnitude - Lower value of damping

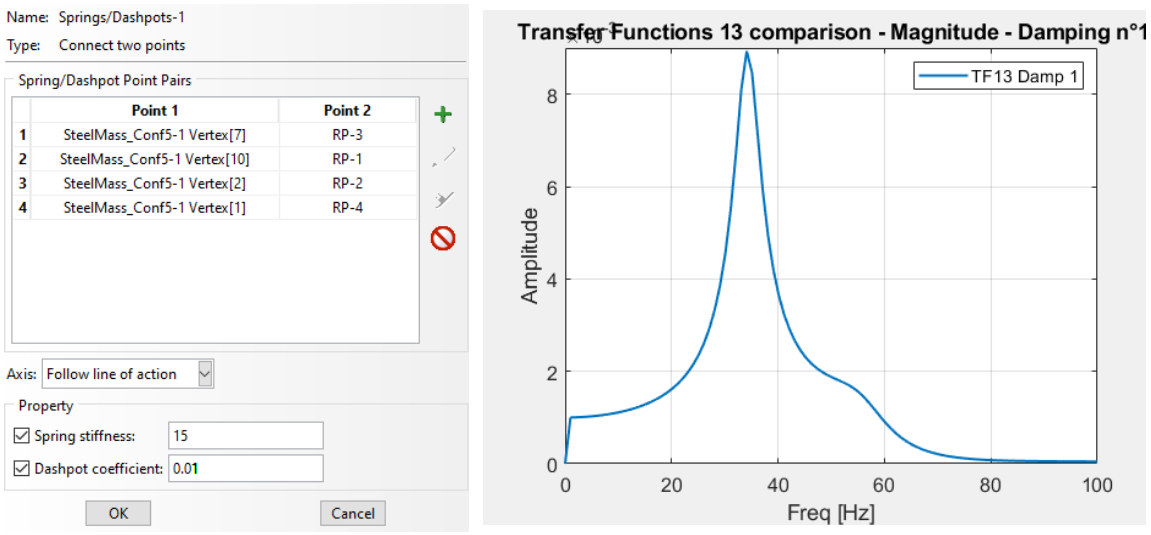

Figure 3.35: Transfer function 13 - Linear spring and dashpot configuration - Magnitude - Higher value of damping

Looking at the first transfer function, it can be seen the first higher peak followed by a second lower peak clearly visible. This behaviour is most similar to the one obtained from experimental tests for the TF13 of configuration 2.

Considering now the second transfer function, that is obtained by doubling the damping coefficient, the second peak is not clearly visible. It can therefore be assumed that by further increasing the damping value, the second peak can be no longer visible obtaining a transfer function with a shape similar to that obtained for the Abaqus TF13 of configuration 2 in which the smaller peak is not visible.

3.4.3 Configuration 3 – Results and Considerations

Configuration 3 is most similar to the previous one, the plots are then presented in the same way since also in this case three accelerometer are used.

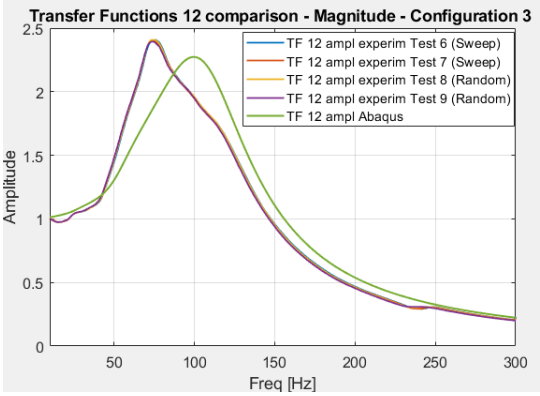

Figure 3.36: Transfer Functions 12 comparison - Magnitude - Configuration 3

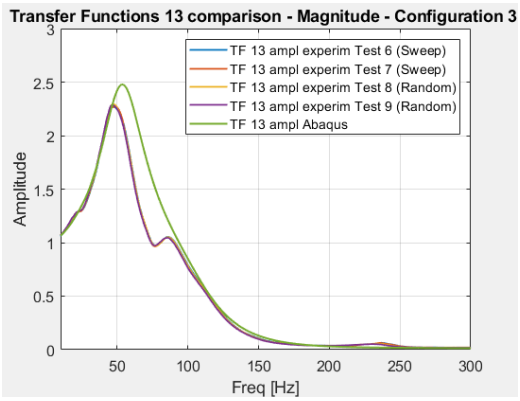

Figure 3.37: Transfer Functions 13 comparison - Magnitude - Configuration 3

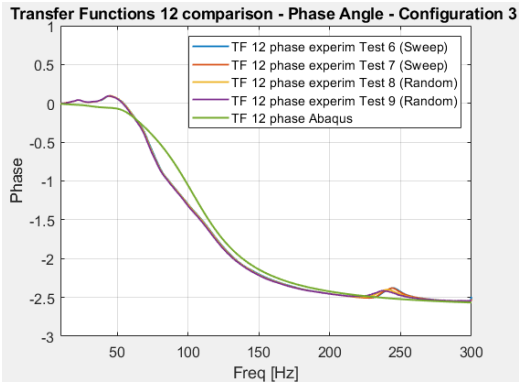

Figure 3.38: Transfer Functions 12 comparison - Phase Angle - Configuration 3

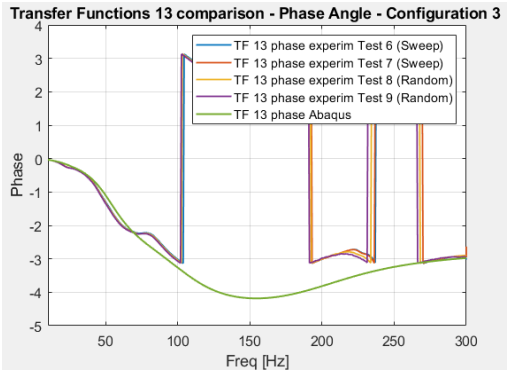

Figure 3.39: Transfer Functions 13 comparison - Phase Angle - Configuration 3

For this configuration it is expected a behaviour more similar to the previous one. In particular, the shape of the obtained transfer functions has to be more similar to the ones of the second configuration. The resonant frequency peaks are influenced by the mass, that is a little bit lower than the previous one, so they should be found at frequencies slightly higher. Comparing the Abaqus data of the two configurations it can be seen that the shape is very similar, especially between the TF 13. Also the peaks are right shifted coherently with the mass decrease.

Considering now the experimental data, it seems that they are not perfectly coherent with the above consideration; for example, comparing the experimental transfer functions, especially looking at the TF13 plots, obtained from experimental data for the second and the third configuration, it can be seen that the resonance peaks of configuration 2 are at a frequency a little bit higher than the ones of the configuration 3, the opposite of what is expected.

Taking into account the previous observations it seems that some differences between the real configuration and the modelled one are present. It has to be considered that the realized geometry

cannot be perfectly symmetrical as the modelled one and also that the Sorbothane pad in the real configuration can present some errors that come from cutting phase or from the attachment phase. Regarding the cut performed through manual cutter, it can be noticed that it can be not enough accurate, to reproduce the dimensions considered in the model. Considering the attachment phase, also in this case it is impossible to assure that the position of the pads in the real configuration is exactly equal to the ones on the model, some uncertainties due to the measurement can be present.

3.4.4 Configuration 4 – Results and Considerations

Plots related to the fourth configuration are now presented.

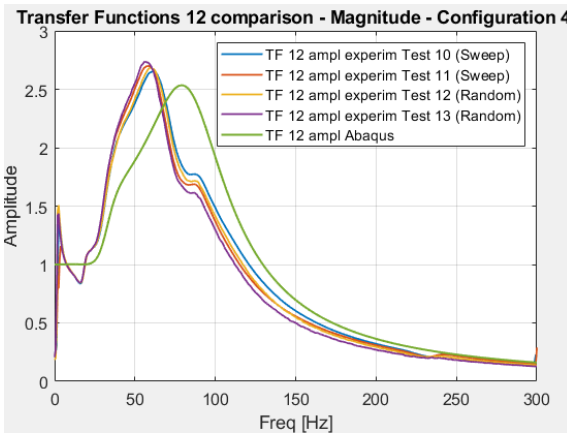

Figure 3.40: Transfer Functions 12 comparison - Magnitude - Configuration 4

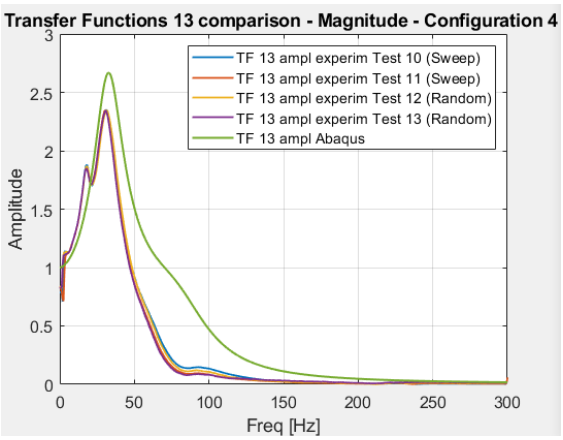

Figure 3.41: Transfer Functions 13 comparison - Magnitude - Configuration 4

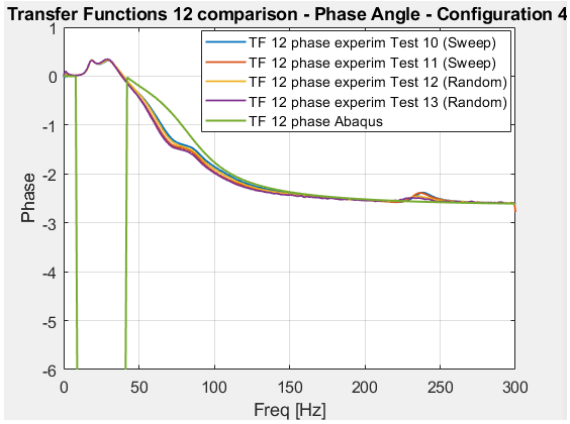

Figure 3.42: Transfer Functions 12 comparison - Phase Angle - Configuration 4

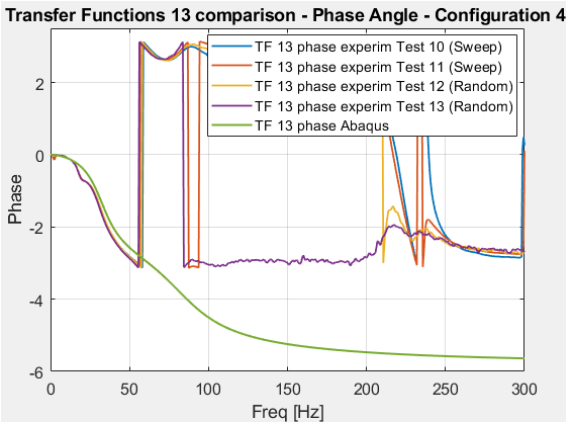

Figure 3.43: Transfer Functions 13 comparison - Phase Angle - Configuration 4

For this configuration the shifting between the experimental and the model peak is less evident. It can be due to the fact that the steel part of this configuration is bigger than the previous one and so the Sorbothane pad is assumed to work better. A double peak in the experimental curve is present also in this configuration.

3.4.5 Configuration 5 – Results and Considerations

This configuration is the last and the biggest one that is tested in order to understand the Sorbothane behaviour. The idea is to test also a configuration heavier than the previous ones. This because the decision to take the height of the pad constant, since it was no possible to guarantee a precise cut with the manual cutter used, does not allow a great compression with the light configurations used so far. The plots resulting from the tests and the modelling of this configuration are presented below.

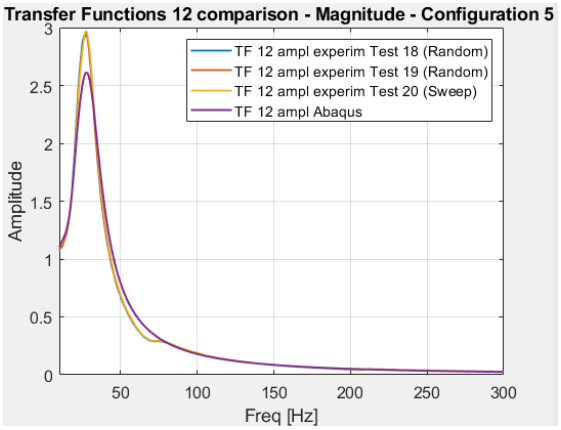

Figure 3.44: Transfer Functions 12 comparison - Magnitude - Configuration 5

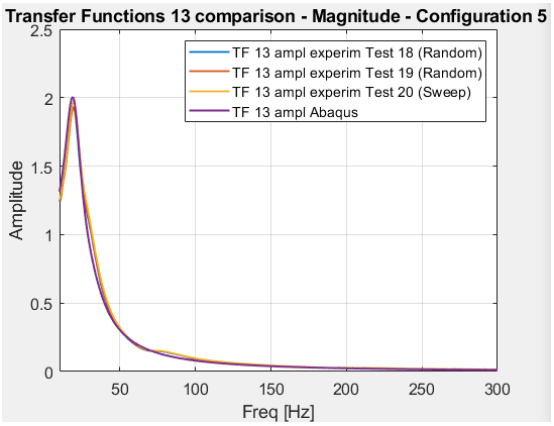

Figure 3.45: Transfer Functions 13 comparison - Magnitude - Configuration 5

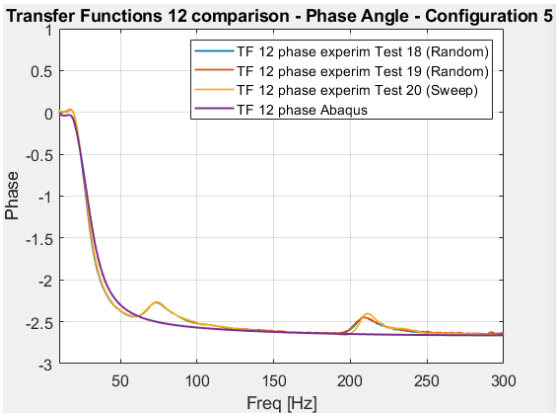

Figure 3.46: Transfer Functions 12 comparison - Phase Angle - Configuration 5

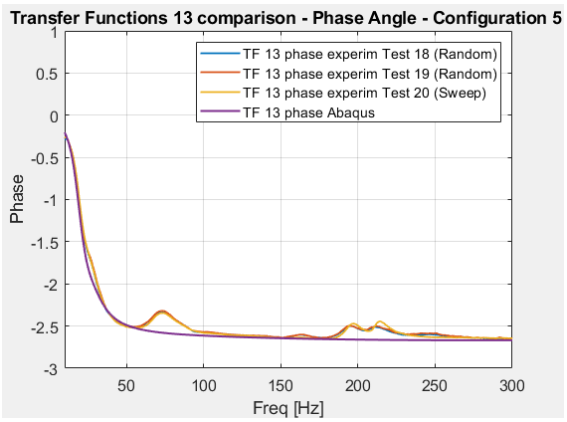

Figure 3.47: Transfer Functions 13 comparison - Phase Angle - Configuration 5

Looking at the above plots it can be noticed that the Abaqus model transfer function and the experimental transfer functions show a very similar behaviour. The amplitudes peak is about the same frequency value and the phases are all coherent. In the TF12 seems that amplitude value of the model peak is lower than the experimental one but overall result for this configuration can be considered satisfactory.

3.4.6 Overall consideration

The above considerations made for the various tested and modelled configurations, combined with the fact that complex Sorbothane behaviour is influenced also by some variability between the production batches and function of the production year, as demonstrate in the previous chapters, makes difficult to reproduce exactly its behaviour during the finite element modelling procedure.

The validation procedure described above with the obtained results show that the characterization of Sorbothane seems to be sufficiently accurate for our purpose. It can be noticed that some uncertainties can derive from the Sorbothane pads cutting phase and some other from the dynamics data of Sorbothane 52 produced in 2016, used to perform the viscoelastic fitting procedure. This one is the most similar with respect to the Sorbothane 50 at our disposal but is not exactly the same.

The Sorbothane characterization parameters validated in this chapter are used to define the material properties of the pads placed under a real wood Crate.

4. Dynamic response of the piece of art to be protected

4.1 Overview

Having to develop a procedure in order to design systems for protecting works of art from vibrations and impacts during the transportation phase within the Tech4MUBAS project, it is important to consider the behaviour of the typical works of art that must be transported.

In addition to that, in this thesis, it is important to know the dimensions and the dynamical characteristics of the object to be transported. The dimensions are important in order to choose a crate, to be tested, able to contain the object. The dynamical properties are needed to understand the levels of vibrations that have to be filtered using Sorbothane pads under the crate in order to protect the transported manufact. For these reasons, it is necessary to have a "type" object to consider.

The case of study, considered in this thesis, is the one related to the protection of earthenware made vases during the transportation. To define the properties of the considered objects, 3D Research made some 3D scans of ancient earthenware vases.

An earthenware vase, with characteristics very similar to those most frequently found in the museum, is then chosen to be reproduced by an expert ceramist. The dimensions of the vase to be protected, considered for the following studies, are reported in the following figure.

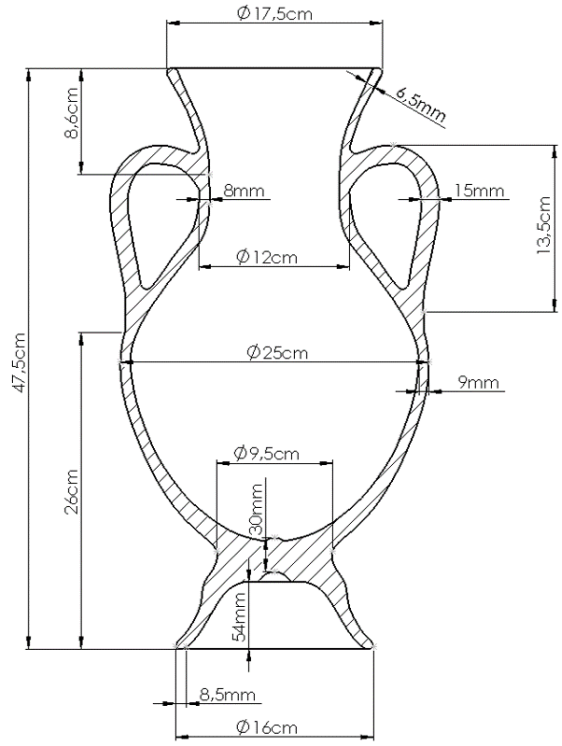

Figure 4.1: Dimensions of the considered earthenware vase

Since the considered vase is made by earthenware, quite rigid material, it is expected that the resonant frequencies are higher, in the order of a thousand Hz. Having the reproduction of the vase available, it is decided to test it experimentally in order to determine the first natural frequencies in which we are mainly interested in this this thesis and in order get all the information needed, for the main project, to model the complete system. This complete system is obtained placing the vase surrounded by a protective material into an internal crate (in case of double crate configuration) protected by vibration absorbers then placed into an outer crate also supported by vibration absorbers, the experimental validation of the FE model realized by 3D Research for the reproduced vase is needed. This validation is important in order to evaluate its dynamic response and to estimate the values of important mechanical properties such as Young Modulus of the material from which it is made.

Starting from the knowledge of the expected deformations associated to the various vibration modes, determined by the FE analysis performed by 3D research, the idea is to perform a dynamical analysis on the reproduction of the vase.

Detailed description of the procedure adopted for the experimental evaluation of the dynamical properties of the vase are detailed described in the next section.

4.2 Description of the experimental tests performed

In order to evaluate the vibration modes of the vase, three different approaches have been considered. In all cases the vase is suspended through a string on the ceiling, in order to obtain a good approximation of the free system vibration condition, coherently with FEM simulation.

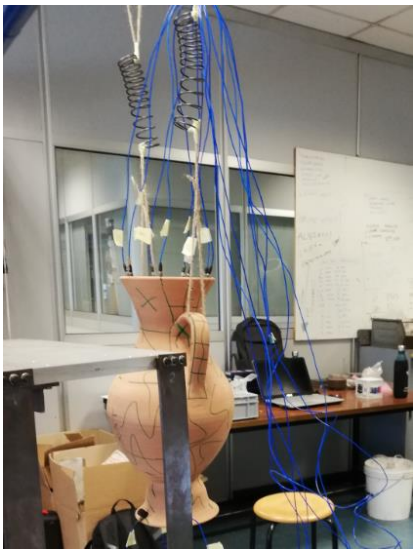

Figure 4.2: Vase pending from the ceiling

The difference between performed tests campaign is on the adopted excitation source. At the begging a Vibe-Tribe speaker is considered: in the first test campaign it is used the Vibe-Tribe placed on a resonant structure, as shown in the following figure, to produce the sound that trough air excites the vase. In order to have higher excitation energy, in the second test campaign the speaker is placed inside the vase, directly transmitting the vibration.

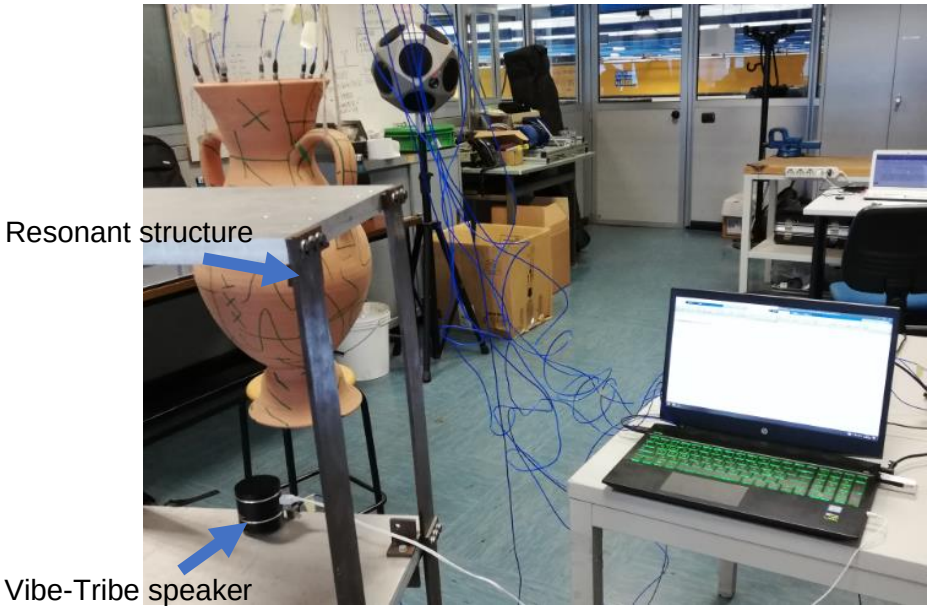

Figure 4.3: Setup for experimental test Campaign 1

To further increase the input power, the third test campaign is performed using the TiraVib shaker as excitation source, on which a steel plate put in contact with the vase is mounted. To avoid relative movement between plate and vase, plastic ties to constrain a little the vase are used. For better understanding, the setup can be seen in the following figure.

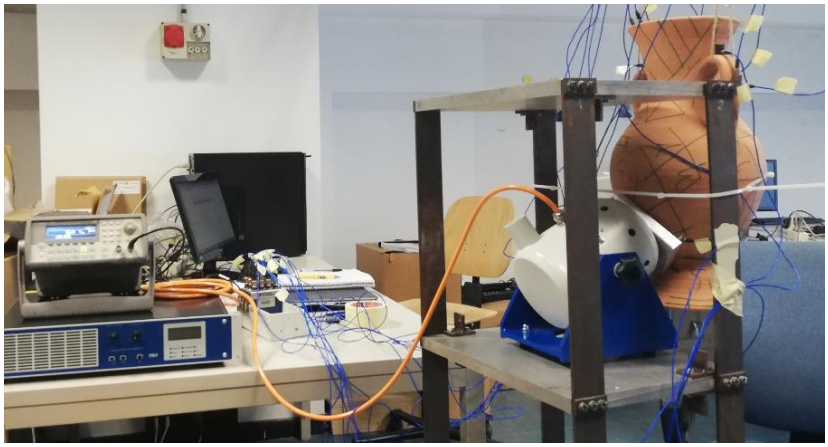

Figure 4.4: Setup for experimental test Campaign 3

To measure the vibration, 12 accelerometers are attached on the vase in two different configurations. Each configuration is studied in order to analyse a specific section of the object. The adopted accelerometers are listed in table reported below. The two configurations are shown in the following two figures.

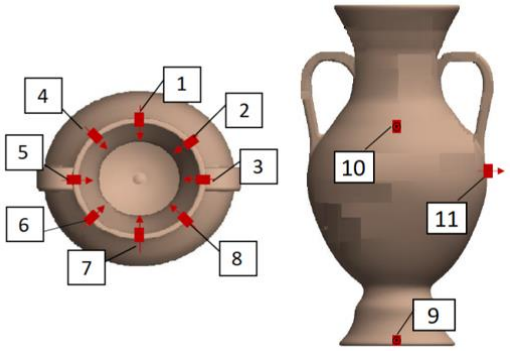

Figure 4.5: Configuration 1

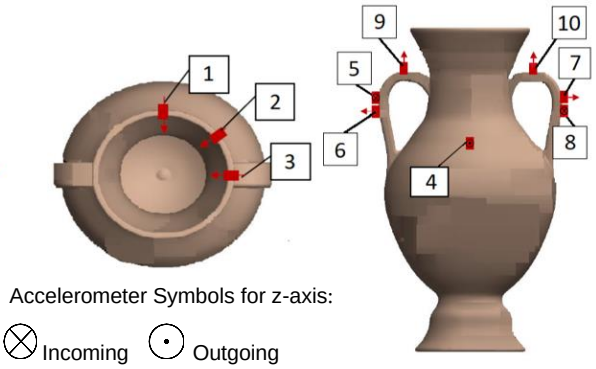

Figure 4.6: Configuration 2

Accelerometer	Model	Sensitivity
1	PCB 333B30	100 mV/g
2	PCB 333B30	100 mV/g
3	PCB 333B30	100 mV/g
4	PCB 333B30	100 mV/g
5	PCB 333B30	100 mV/g
6	PCB 333B30	100 mV/g
7	PCB 333B30	100 mV/g
8	PCB 333B30	100 mV/g
9	Kistler 8628B5	1000 mV/g
10	Kistler 8628B5	1000 mV/g
11	PCB 333B30	100 mV/g
12	PCB 333B30	100 mV/g

Table 4.1: Accelerometers employed for measurements

The produced input is measured by means of accelerometer n°12 in the first configuration and by accelerometers n°11 and n°12 in the second one. The reference point considered during the three test campaigns is not the same: in the first tests, reference accelerometers is placed on the resonant structure, near the Vibe-Tribe; for tests conducted with Vibe-Tribe inside the vase, only the accelerometer n°12 is placed directly on Vibe-Tribe top surface; finally, for tests with shaker, the plate between vase and shaker is considered as reference for input acceleration measures.

Tests are performed by using random noise and a Sweep Sine as input, produced by using a Matlab script in case of Vibe-Tribe tests, and by a function generator in case of shaker tests.

4.3 Analysis of the obtained results

Data obtained from the three campaigns of tests have been analysed in Matlab. Unfortunately, it is observed that results of tests with Vibe-Tribe as excitation source gave poor results, not so easy to be interpreted; this can be mainly due to the fact that a sufficient quantity of energy cannot exerts with this excitation source. For this reason, it is decided to pay attention only on the tests performed using the shaker as excitation source.

The collected data have been analysed separately for the two configurations through Matlab. Analysis of the transfer functions, plotted for all the accelerometers with respect to the reference one in a range between 500Hz to 3000Hz in terms of magnitude and phase, are performed. The upper limit is chosen since represent the higher limit for accelerometers used. The obtained transfer function plots are shown in the following figures.

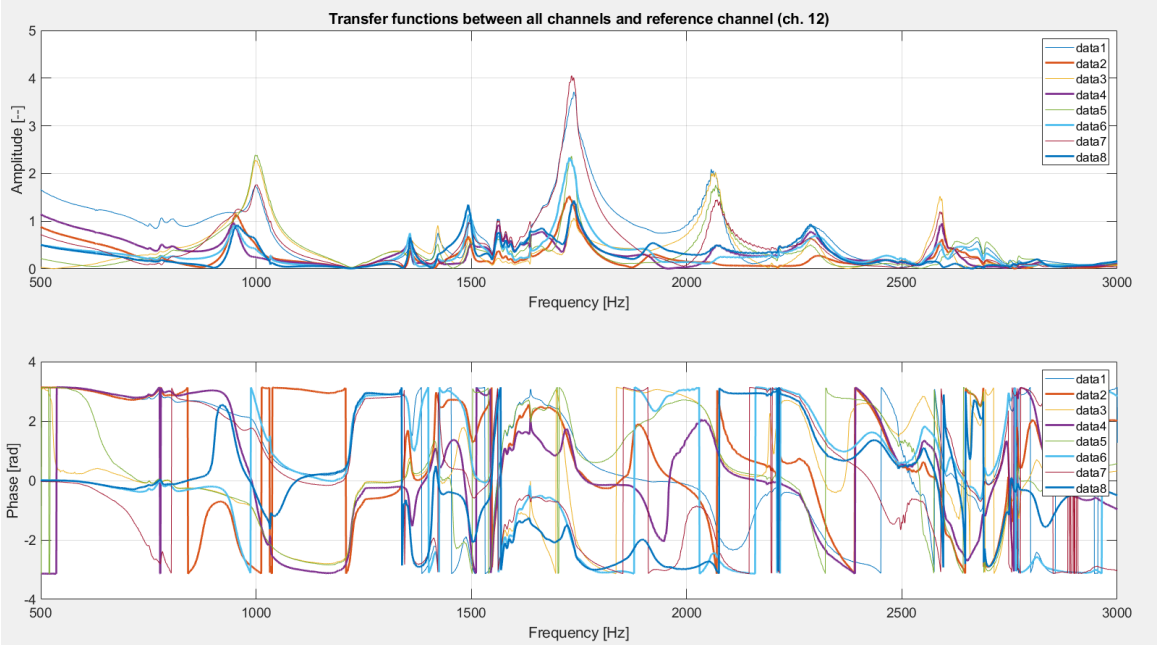

Figure 4.7: TF Configuration 1 - Sweep- Neck accelerometers (1 to 8) with respect to 12

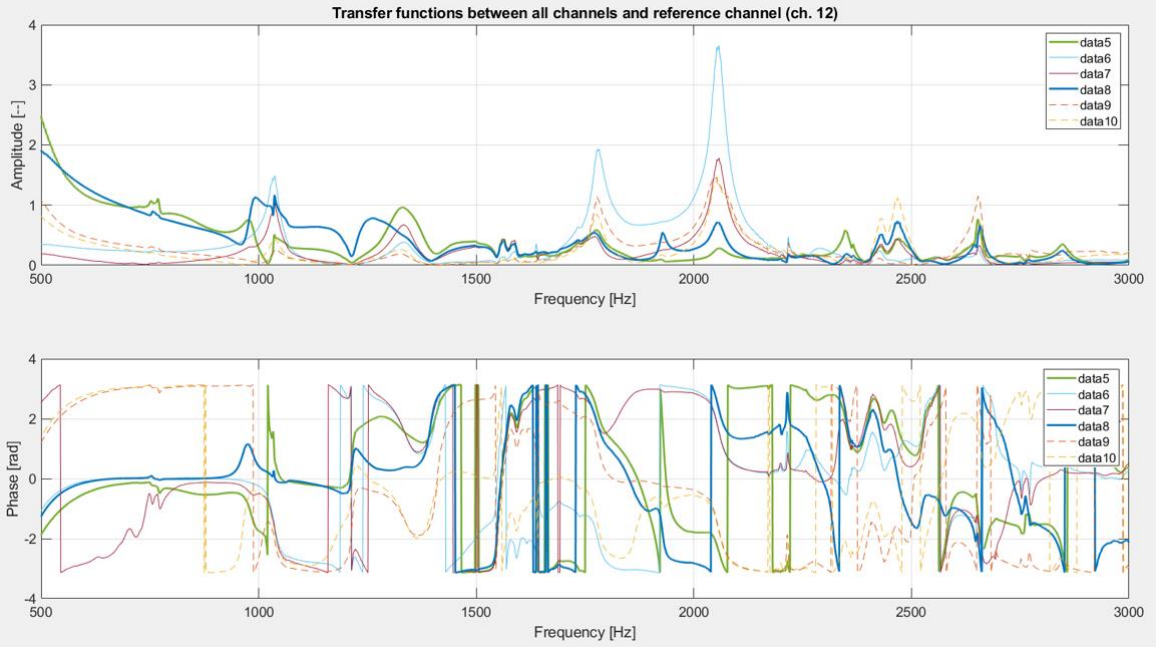

Figure 4.8: TF Configuration 2 - Sweep - Accelerometers (1 to 10) with respect to 12

Natural frequencies of vase are searched by considering peaks visible on transfer functions, analysing their consistency with the expected first six shapes of the vibration modes obtained through FEM analysis and reported in the following figures.

Figure 4.9: Mode 1

Figure 4.10: Mode 2

Figure 4.11: Mode 3

Figure 4.12: Mode 4

Figure 4.13: Mode 5

Figure 4.14: Mode 6

For the first mode, considering the Figure 4.9, the most of deformation seems to be in correspondence of the vase neck. According to that, configuration 1 is considered. In this case it is searched for a frequency values in which transfer function between reference channel and accelerometers 2, 4, 6, 8 (curves 'data 2', 'data 4', 'data 6' and 'data 8' of the following plot) generate a peak value higher than the others. In that point it is expected also a phase shift. In addition to that, having observed the deformation associated to that vibration mode, the accelerometers couple 2-6 has to move in-phase and even the 4-8 couple has to show the same behaviour. The two accelerometer pairs have to move 180° out of phase among them. The frequency value for which could be observed a similar behaviour was equal to 950 Hz.

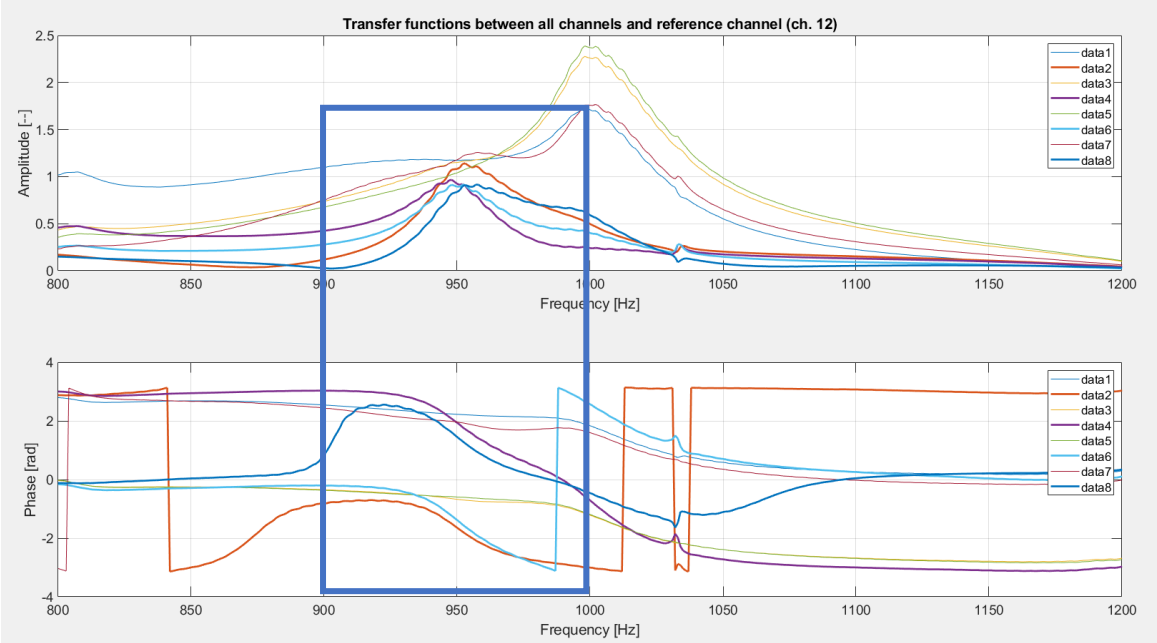

Figure 4.15: Mode 1 Identification on experimental Transfer Function Configuration 1

Considering the second mode (Figure 4.10), it can be observed that most deformed points are again on the vase neck so, also in that case, configuration 1 is analysed. For this mode, it is expected that the transfer function shows a clear peak for accelerometers couples 3-5 (‘data 3’ and ‘data 5’ on the plot) and 1-7 (‘data 1’ and ‘data 7’). A phase shift has to occur. The curve representing the accelerometer 3 has to move in-phase with the ones related to accelerometer 5, the same regarding the curves associated to accelerometers 1 and 7. The two couples have to move 180° out of phase among them. Such a behaviour was observed at a frequency equal to 1000 Hz.

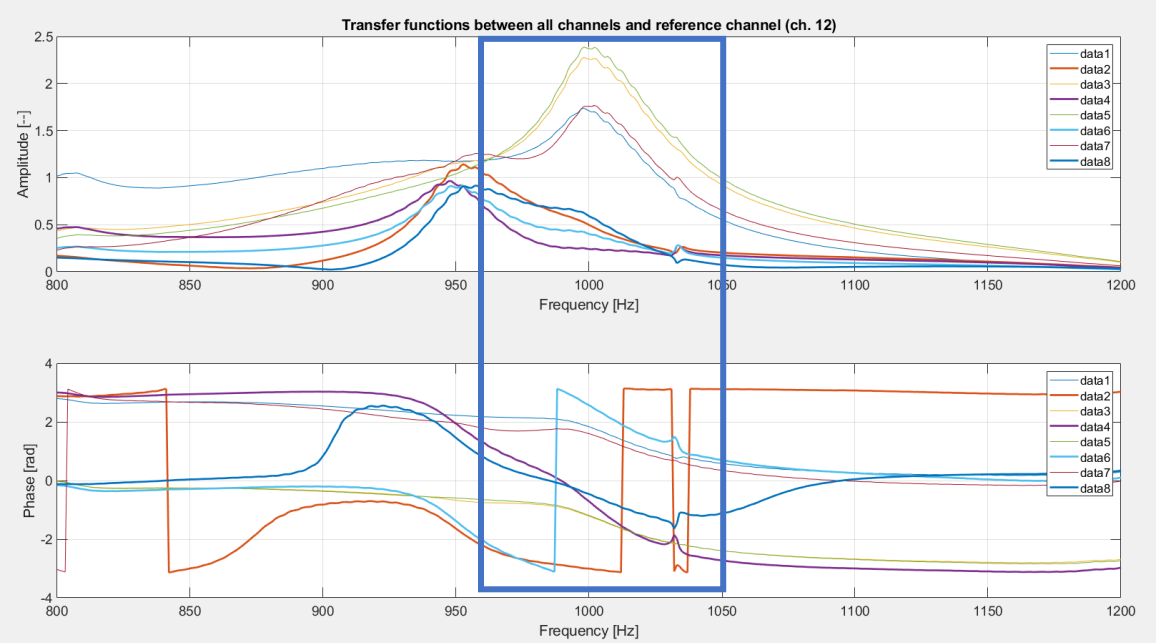

Figure 4.16: Mode 2 Identification on experimental Transfer Function Configuration 1

For the fifth mode (Figure 4.13), most deformed points seem to be in correspondence of the accelerometers 1 and 7. Anyway, the deformation extends also in the areas of accelerometers 2, 4, 6 and 8. Hence, considering configuration 1, it is looked for a peak involving all channels, but showing with higher amplitude for accelerometers 1 and 7. It is expected that a phase shift occurs in this point. In correspondence of the searched frequency, point 1 has to move in reverse phase condition with respect to point 7. The same behaviour has to be for couples 2-6 and 4-8. With more uncertainties than for the previous identified frequencies, it is found a peak consistent with previous observations at a frequency equal to 1735 Hz.

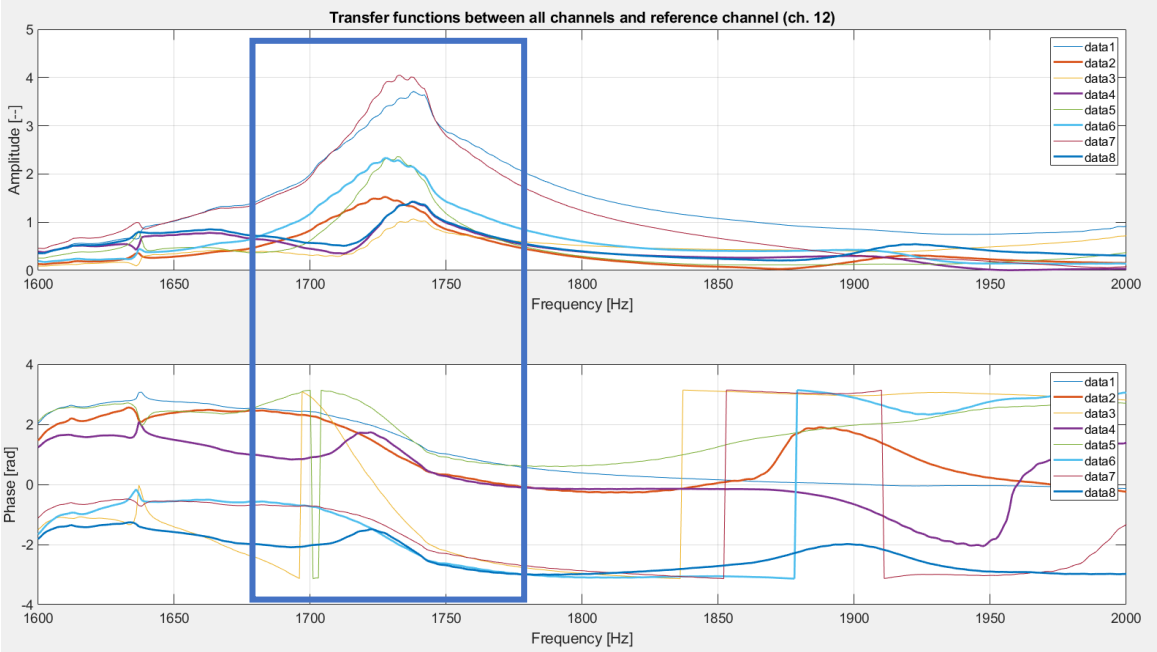

Figure 4.17: Mode 5 Identification on experimental Transfer Function Configuration 1

Looking at the deformed shape of the FEM analysis for the sixth mode (Figure 4.14) it can be seen that the higher deformation results at the handles of the vase: for this reason, this mode is searched analysing configuration 2. It is looked for a frequency value for which clear peak in the transfer function is visible for accelerometers 6 and 7 (radially directed towards the centre of vase); in addition, lower peaks given by accelerometers 9 and 10 should also be present. Phase shift has to be present. It is expected that point 6 moves in-phase with 7 and point 9 in-phase with point 10. The two couple of points have to move 180° out of phase among them. This kind of behaviour can be found at a frequency at about 2070 Hz

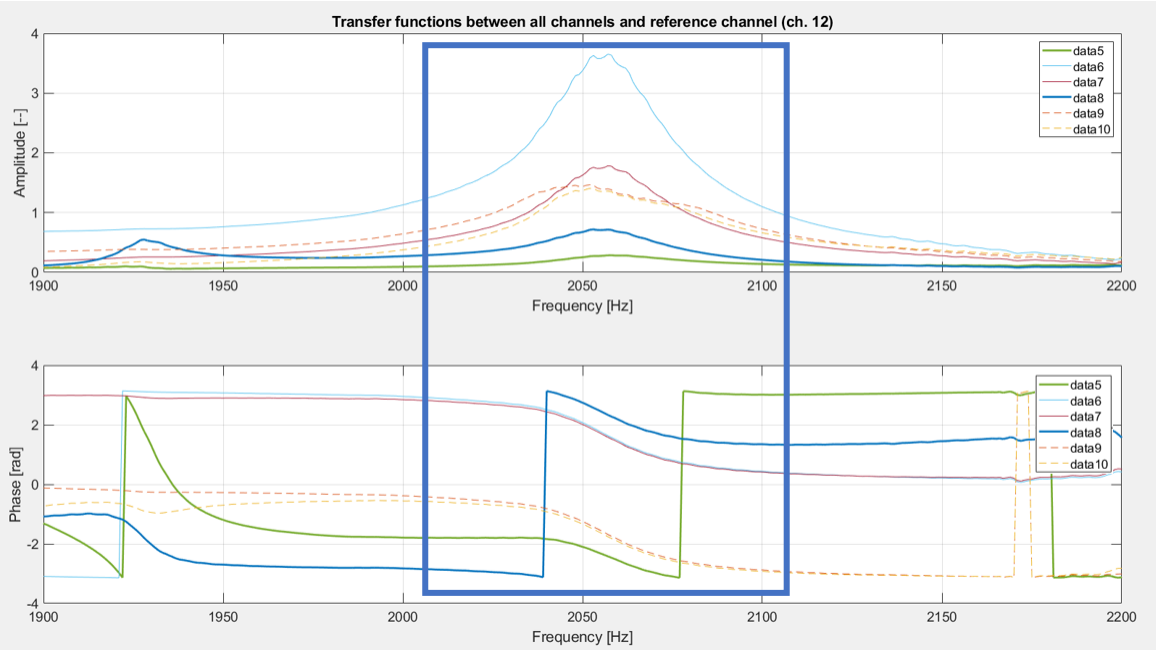

Figure 4.18: Mode 6 Identification on experimental Transfer Function Configuration 2

About third and fourth modes (Figure 4.11 and 4.12), it is expected to find them in a frequency range approximately between 1000 Hz and 1735 Hz, that is between the frequency of the second mode and the one of the fifth mode. Below the transfer function plots, zoomed in this range of frequencies, are shown. Even if some peaks are visible, it is not possible to find a correspondence between the characteristics of these peaks and the expected one from FEM analysis. Most probably, following our approach, we are unable to sufficiently excite these two modes.

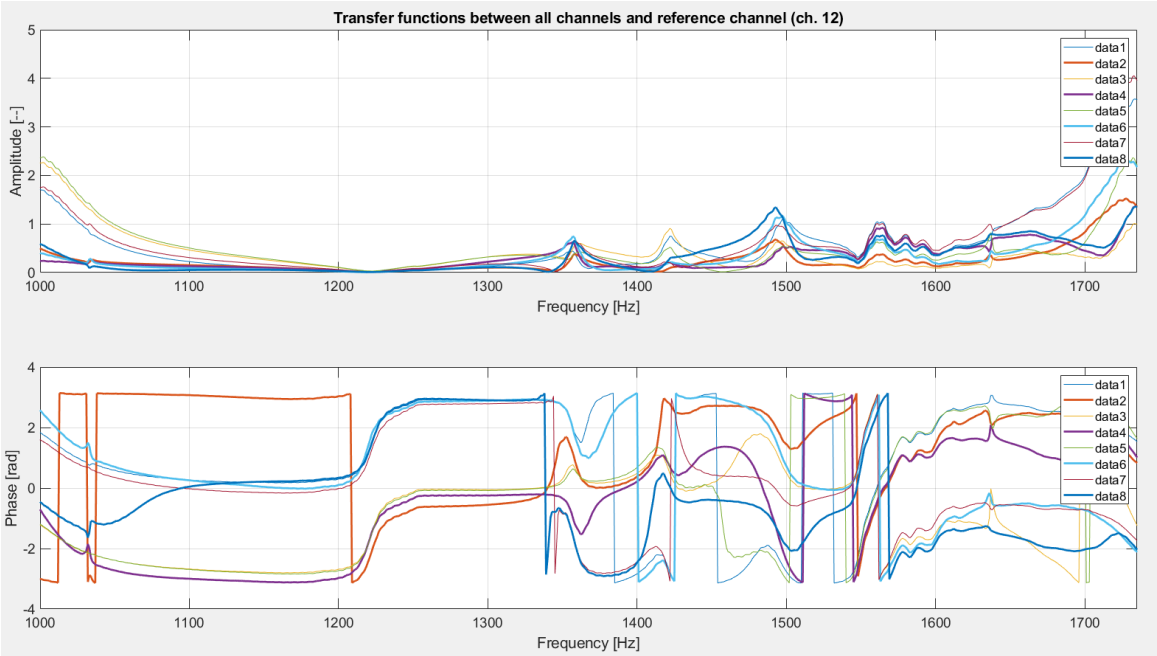

Figure 4.19: Mode 3 - Mode 4 - Transfer function plot - Configuration 1

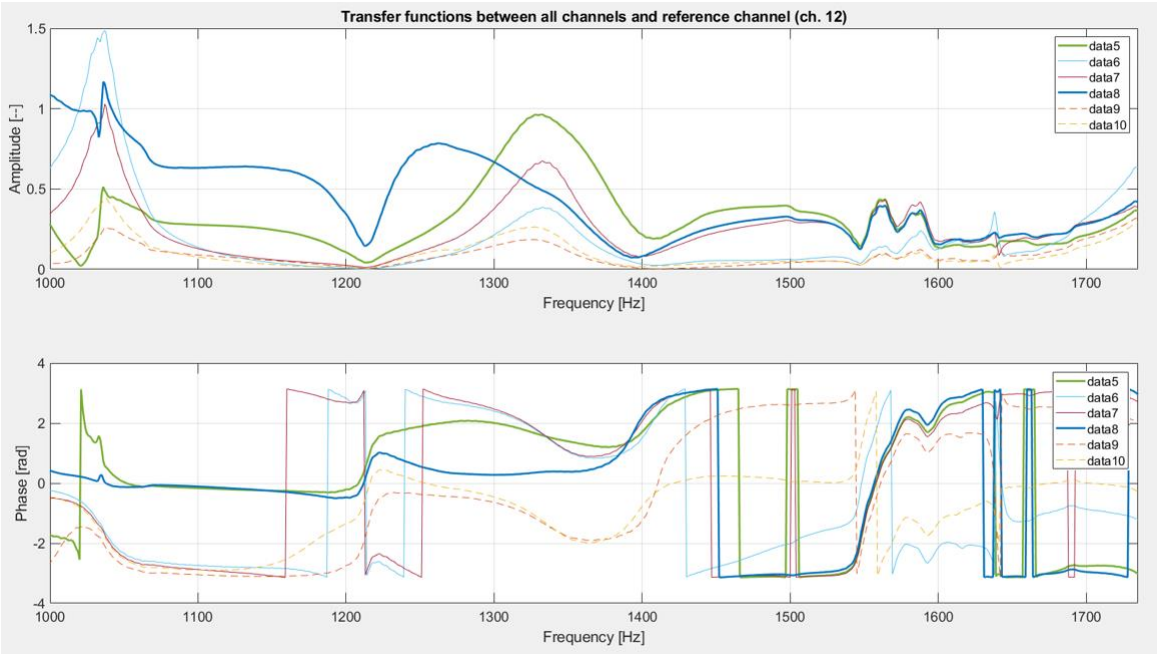

Figure 4.20: Mode 3 - Mode 4 - Transfer function plot - Configuration 2

At the end of this experimental testing procedures it can be seen that the natural frequencies for an earthenware made vase are higher, as can be expected for a rigid material like the one considered. Following table is reported in order to summarize the identified natural frequencies.

Mode N°	Corresponding Frequency [Hz]
1	950
2	1000
3	Unknown
4	Unknown
5	1735
6	2070

Table 4.2: Identified natural frequencies

The determined values of vibrating modes are consistent with what it is expected since the first mode is found at a frequency equal to 950 Hz.

The dimensions of the vase considered in these analyses are than used in order to define the size of the crate to be tested in order to validate the procedure presented in chapter 3 on a configuration most similar for the ones in we are interested in.

5. FEM and experimental validation of a Crate supported by Sorbothane pads

5.1 Overview

The Sorbothane material parameters validated in chapter 3 on small configurations are now used to model the pads designed to support a bigger component represented by a wood crate. The idea is to understand if the material properties previous determined are coherent also for this configuration, more complex than the previous considered. In order to do that also in this case a FE model is realized, and experimental tests are performed. Unfortunately, given the impossibility to having a crate specifically made for the transport of works of art such as the one experimentally analysed in the previous chapter, in the short term, the following analyses and simulations are performed on a wood crate typically used for the transport of heavy products such as metal parts, described in the following section. It has to be noticed that despite drawbacks previously mentioned, the considered crate is very similar in size and weight to the ones used to transport artworks as the earthenware vase previously analysed.

5.1.1 Description of the tested crate

The considered wood crate is made using wooden planks joined by spikes to wooden crosspieces to increase the solidity in order to support the weight of the elements positioned inside. For the field of use of this type of crate not much importance is given to the details, so irregularities in the used wood and in the assembly can be present, causing small mass imbalance, that in the crate used to transport of works of art must be avoided.

To obtain more stability and more rigidity an MDF (Medium Density Fibreboard) plate is realized to be attached under the longitudinal crossbars of the crate. This plate has a thickness at about 20 mm and dimensions little bit higher than the ones of the crate.

To determine the wood density necessary to carry out the finite element analysis is decided to weigh the crate using a crane scale and to obtain the volume value from the 3D model realized for this crate by using Inventor 2017 software. In this way we can obtain directly the density. Due to the geometry complexity, the difficulties related to modelling the real wood behaviour and since the interest in the following described analysis regards the determination of the vertical resonance, the idea is to consider the crate as a rigid body in the finite element analysis. The experimental tests help us to understand if this hypothesis can be considered valid or not.

Considering the crate as rigid body it is possible to measure the total mass of the crate with the attached MDF plate to obtain a single value of density to assign at the Abaqus model. In the following figure is showed the weigh phase.

Figure 5.1: Weighting of the wooden crate

The weight of the crate is equal to 33.6 kg and the total volume equal to 0.056 m^3, so the density obtained and directly expressed in Abaqus CAE consistent units results $5.97e^{-10}$ ton/mm^2.

At this point four Sorbothane pads are pre-dimensioned considering a static value of Young modulus and the weight of the crate that has to be supported in order to obtain a static deformation at about 10% of the total thickness. The obtained pads have each one a square shape and dimensions equals to 50 x 50 x 12.7 mm. They are positioned under the FDM panel in correspondence of the extremities of the above crate crossbars.

5.1.2 General description of the model and experimental test performed

Remembering the goals of the considered project, an interesting test to perform regards the evaluation of the vibration transmitted from the source, that in the reality are produced during the transport. To do that our configuration can be fixed on a suitable support mounted on the vibrating table to simulate this vibration transmission. The problem is that there is not a suitable support to correctly place the crate and so another kind of test has to be performed.

It is decided to realize a configuration in order to measure the vertical resonance of our system. To do that a shaker is placed inside, in the middle of the crate to force the system using external harmonic force produced by the oscillating mass of the shaker.

By the ratio between the vertical acceleration and the force it is possible to determine the searched vertical resonance of the system.

The results of both Abaqus model and experimental tests have to be represented in this form in order to be compared.

The system so obtained can be simplified as a 1 degree of freedom system reported in the figure below.

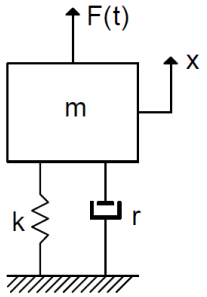

Figure 5.2: 1 d.o.f. Damped System with applied external harmonic force

In our configuration the mass m is represented as the sum of the crate mass and the shaker mass that are assumed to be rigids. The stiffness k and the damping r are represented by the Sorbothane pads placed above the crate. The external harmonic force is given by the mass of the moving element of the shaker, multiplied by the acceleration measured during the experimental test.

The motion equation to describe the above system is,

$$m\ddot{x} + r\dot{x} + kx = F(t) = F_0 \cos \Omega t \tag{5.1}$$

The solution of the previous equation, $x(t)$ can be written as,

$$x(t) = x_G(t) + x_P(t) \tag{5.2}$$

Where $x_G(t)$ represents the general integral of the associated homogeneous equation describing the initial transient, and $x_P(t)$ the particular integral due to the known term $F(t)$, describing the steady-state response.

The convenient approach to calculate the steady-state response $x_P(t)$ of a system with harmonic excitation is to use a complex vector representation of the excitation and of the response [19]. Thanks to this method the actual force $F_0 \cos \Omega t$ can be considered as a projection on the real axis of a vector (complex number) $F(t) = F_0 e^{i\Omega t}$ rotating in the gauss plane at angular speed Ω as reported in the following representation.

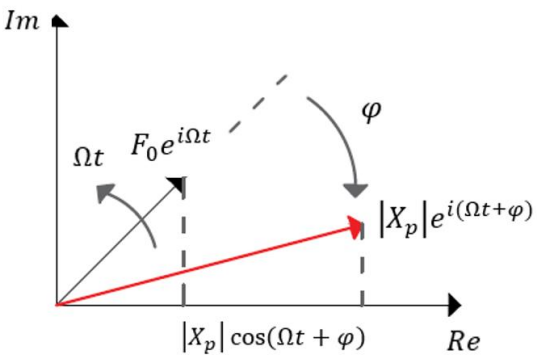

Figure 5.3: Vectors of the Harmonic excitation and steady-state response in Gauss Plane

Equation of motion in complex notation can be written as,

$$m\ddot{x} + r\dot{x} + kx = F_0e^{i\Omega t} \tag{5.3}$$

and in complex field the solution under steady-state condition is,

$$x_p = X_pe^{i\Omega t} = |X_p|e^{i(\Omega t+\varphi)} \tag{5.4}$$

By substituting the particular solution and its time derivative with respect to time in the equation of motion of the system, we obtain,

$$(-m\Omega^2 + ir\Omega + k)X_pe^{i\Omega t} = F_0e^{i\Omega t} \tag{5.5}$$

As can be seen, with this approach it is possible to eliminate the dependence on time.

The expression of the complex solution is then,

$$X_p = \frac{F_0}{(k - m\Omega^2) + ir\Omega} \tag{5.6}$$

And since in this case acceleration is needed, second derivative with respect to time is considered, obtaining,

$$\ddot{X}_p = \frac{-\Omega^2F_0}{(k - m\Omega^2) + ir\Omega} \tag{5.7}$$

Dividing both terms by F_0 and multiplying the numerator and the denominator of the right part by $\frac{1}{m}$ the obtained expression is,

$$\frac{\ddot{X}_p}{F_0} = \frac{-\frac{1}{m}}{(\frac{k}{m\Omega^2} - 1) + i\frac{r}{m\Omega}} \tag{5.8}$$

The modulus of the steady-state response is obtained after some common passages as composition of both real and imaginary parts of the response,

$$\left|\frac{\ddot{X}_p}{F_0}\right| = \sqrt{Re\left(\frac{\ddot{X}_p}{F_0}(\Omega)\right)^2 + Im\left(\frac{\ddot{X}_p}{F_0}(\Omega)\right)^2} = \frac{\frac{1}{m}}{\sqrt{\left(\frac{1}{a^2}-1\right)^2 + \left(\frac{2h}{a}\right)^2}} \tag{5.9}$$

The following plot represent the shape obtained for the above function

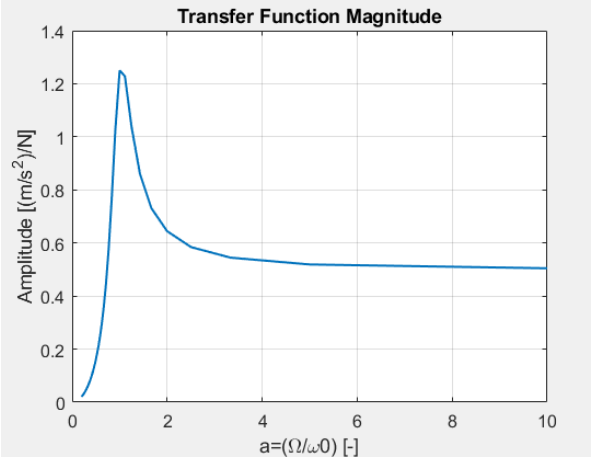

Figure 5.4: Shape of the Transfer Function eq. (5.9)

5.2 Finite element model of the crate configuration with Abaqus CAE

To perform the finite element analysis on this configuration most of the observation done for the smaller configuration considered in the previous chapter are still valid with some modifications needed to be adapted to the actual system. The three main steps required to the software in order to perform the analysis, consisting in pre-processing, solution and post-processing are following considered using the module division of the Abaqus CAE environment.

In **Part** module the various pieces composing the system are created. In this case the needed parts are four. The first one is the crate for which the geometry is created in Inventor 2017 and then imported in Abaqus CAE as a single part.

In the following figure it can be seen the crate reproduced in Inventor 2017.

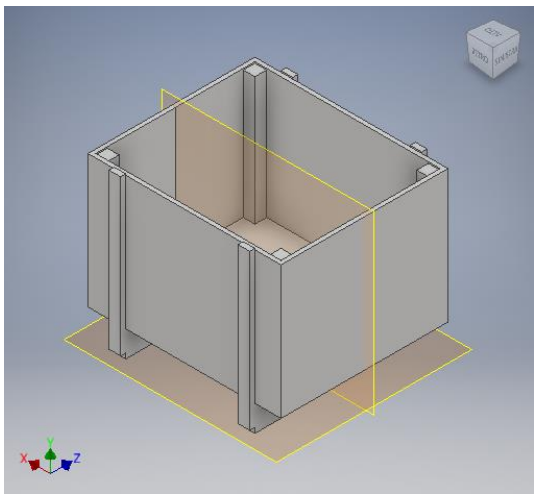

Figure 5.5: 3D reproduction of the crate realized in Inventor 2017

The second part is represented by the MDF plate placed under the case to stabilize the structure, and also this one is designed in Inventor 2017 and then imported in Abaqus CAE.

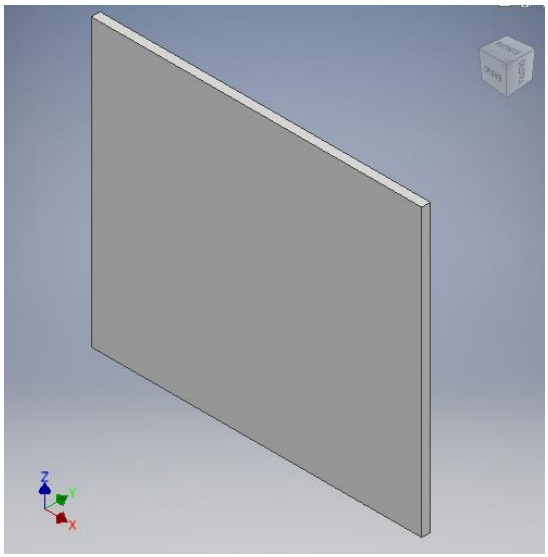

Figure 5.6: 3D reproduction of the MDF plate realized in Inventor 2017

The third one is a rectangular mass that reproduce the shaker and the eventually added masses placed into the crate during the experimental testing procedures. That part is of the type 3D discrete rigid. The following figure represent the simple shape of this part, directly realized in Abaqus CAE.

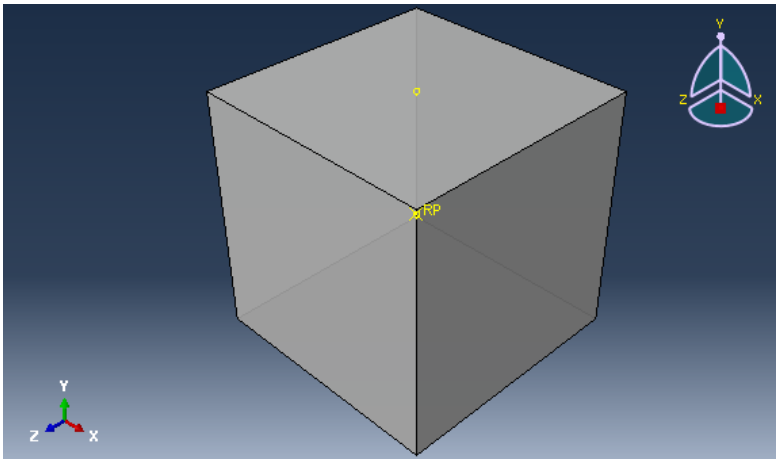

Figure 5.7: Solid mass reproducing Shaker and added masses into the Crate

The last part is represented by the Sorbothane 50 pad, realized directly in Abaqus CAE, of dimensions 50 x 50 x h 12.7 mm. This can be seen in the following image.

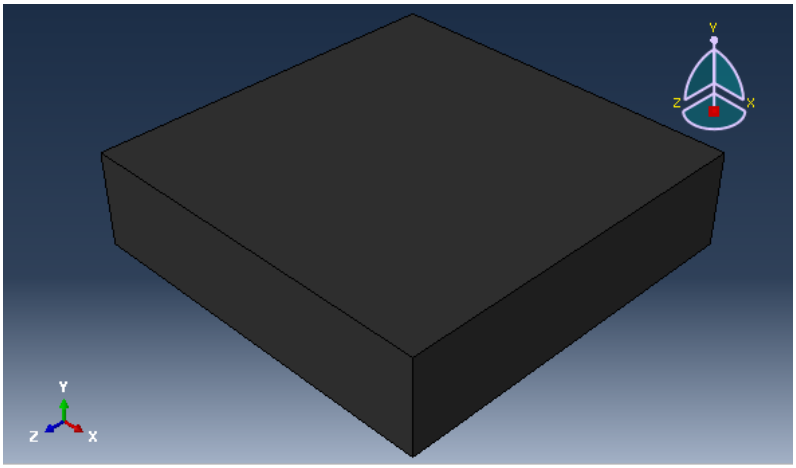

Figure 5.8: Sorbothane pad part

Once the parts are realized passing into Property module it is possible to assign a material to each of the previous created parts.

As it has been said in the introduction of this chapter, the case is weighed considering also the MDF panel obtaining a global value of density, so a unique material is used for both the two, named Wood.

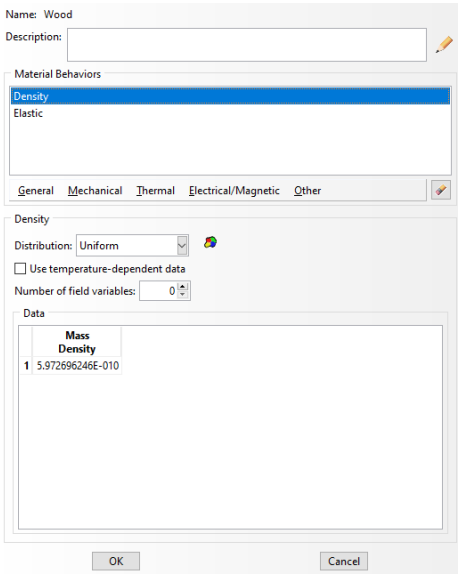

Figure 5.9: Wood material Properties – Density

The material to be assigned to the pads is the Sorbothane 50 also used for the configurations reported in chapter 3 and so can be directly imported from the material libraries into the current model.

Considering now the solid mass, it is possible to use a special feature to assign an Inertia value in the centre of gravity, of the part to simulate its weight. This is important because it is possible, by modifying one parameter named mass, to obtain different configurations to reproduce the experimental ones. In the following figure is reported the inertia used for the second experimental configuration obtained by the sum of the shaker mass and of an additional mass.

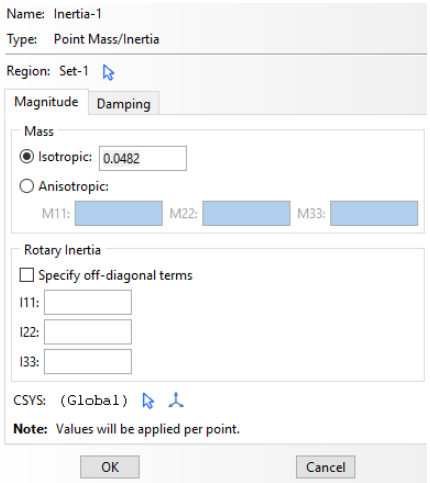

Figure 5.10: Inertia setting menu for solid mass to simulate the shaker weight and other additional weight

Once the material properties are assigned to the correspondent parts it is possible to continue the model definition passing into the **Assembly** module. In this module the part instances are created and constrained obtaining the final desired configuration.

The number of part instance requested is equal to one, except for Sorbothane pad that are four and placed as described above. At the end of this procedure the final shape of the configuration, reported at the following figure is obtained.

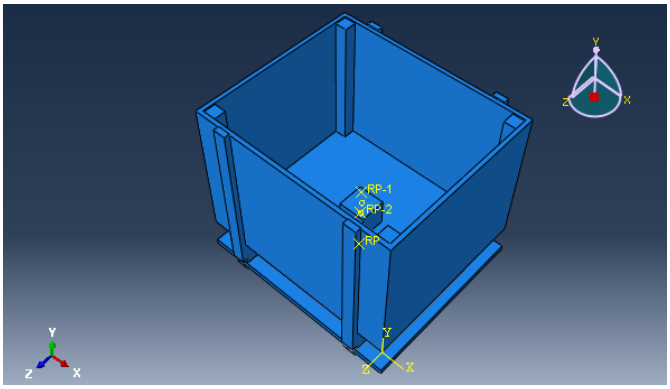

Figure 5.11: Configuration final Assembly

As can be seen by looking at the figure above, the solid mass is placed in correspondence of the centre of the crate.

The realized instances are chosen to be dependent, so they represent only a pointer to the original part with whom they share both geometry and mesh. For this reason, in the **Mesh** module, it is necessary to assign the meshes only at the original parts. The crate is meshed using tetrahedral element for the complexity of the geometry. The mesh dimension chosen is very coarse, this because the aim is to consider the crate as rigid body. The MDF plate instead, being a simple geometry, is meshed using hexahedral elements. Also for this part, coarse mesh is chosen since the idea is to set also that part to behave as rigid body.

The solid mass placed into the case is directly generated as 3D discrete rigid part, so it doesn't need to be meshed.

The Sorbothane pad part is meshed using hexahedral elements of quadratic geometrical order specifying during the element type definition the use of hybrid formulation since the material is considered to be incompressible.

The mesh dimension for this part is chosen equal to 5 mm, finer enough to correctly show its behaviour during the analysis phase. The meshed configuration is shown in the figure below.

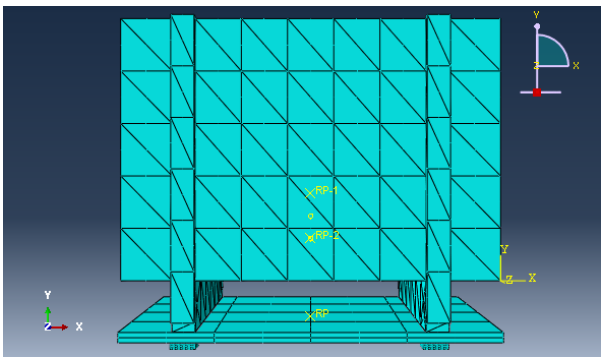

Figure 5.12: Meshed configuration

By using the **Interaction** module it is possible to set constraint on the analysis degrees of freedom. In this model a tie constraint is used to attach the bottom surface of the MDF plate with the top surface of the Sorbothane pads to avoid relative motion between them. Other two tie constraints are used in this configuration. The first one to fuse the bottom part of the solid mass and the internal base of the crate, and the second one in order to fix the crate and the crossbars of the crate with the MDF panel. In this way the nodes of the tied surfaces have the same motion.

As anticipated, the idea is to consider the MDF plate and also the crate as rigids. In this module it is possible to do that by using a constraint called rigid body. This constraint is created by simply selecting the part that has to become rigid and a reference point created in the centre of gravity of the part. In the following figure is shown the result of application of this constraint onto the crate part. The part is put in evidence and the reference point selected, named RP-1, is red.

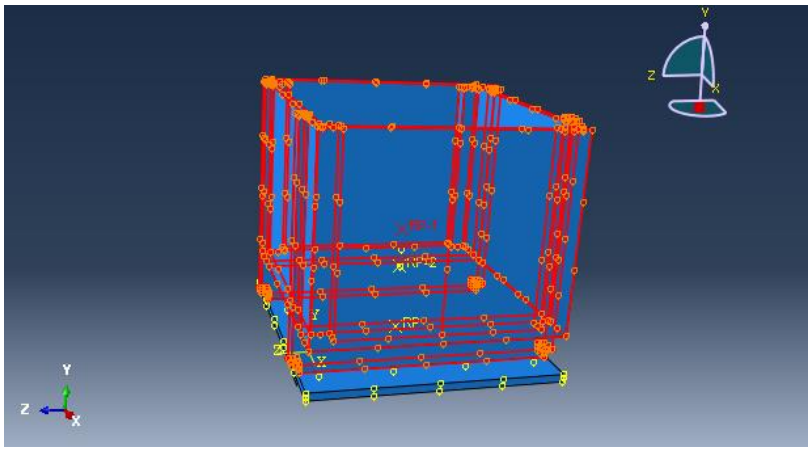

Figure 5.13: Rigid body constraint definition for the crate

At the end of this step, the pre-processing phase is finished, and the characteristics of the model are defined.

The next phase considers that the analysis to be performed on this model has to deal with the determination of the steady-state response of a system subjected to an external force, so in the **Step** module a sequence of steps to reproduce this has to be defined. A preliminary static analysis can be useful to understand the compression effect produced by the sum of the masses of crate, MDF and shaker with eventually an additional mass, on the Sorbothane pads.

After the static step a steady-state Dynamic Analysis is performed, as for the simple configurations, to directly obtain the response of the system in terms of physical degrees of freedom of the model. The frequency range of interest in this analysis ranges between 10 Hz and 100 Hz with a number of points to be considered equals to 90, equally spaced along the frequency axis (Bias value equal to one).

It is now necessary to specify loads and boundary conditions of the model, needed for the analysis step. By entering in the **Load** module it is possible to specify the gravity acting on the system, in the same way used for the simplest configurations, and additionally to create a force, to simulate the external harmonic force, in the steady-state dynamic direct step. This force is defined with a value of 10 N and it is applied in the centre of gravity of the solid element inside the crate, directed in the vertical direction.

In the following figures it can be seen the menu in which the force is defined and the point of application of that force.

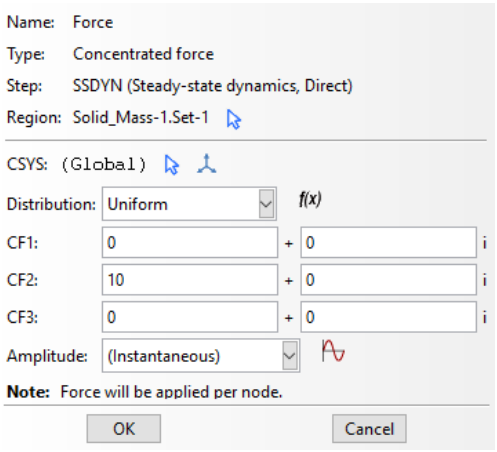

Figure 5.14: Parameter definition of the harmonic external force to be applied to the model

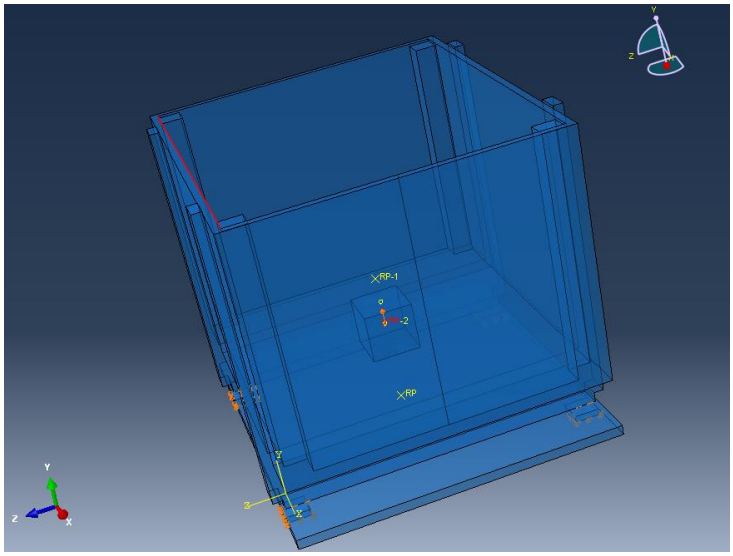

Figure 5.15: Harmonic external force - Application point and direction

The concentrated force can be defined considering both the real (in-phase) part and the imaginary (out-of-phase) part. It is decided to consider only the real part for this analysis, so the imaginary part is set to zero.

The boundary condition for this configuration is specified in terms of Displacement/Rotation to prevent the translation of the Sorbothane bottom pads in all the directions.

This boundary condition is maintained for all the analysis steps. Figure below shows the boundary condition application.

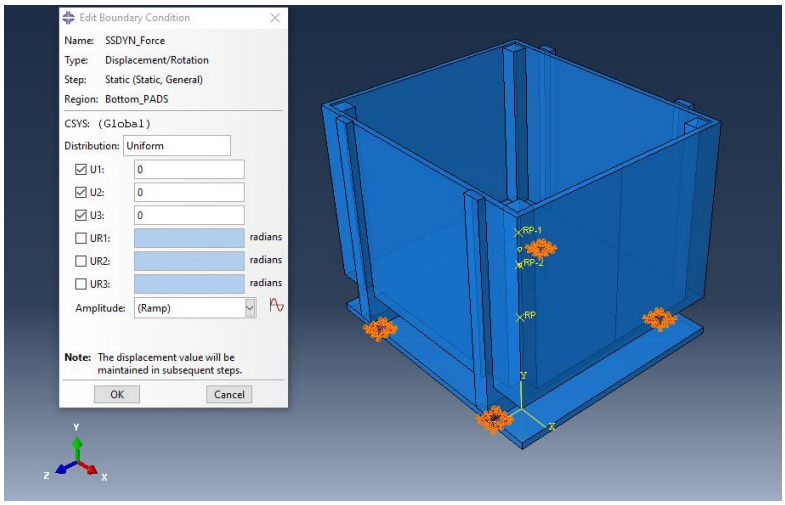

Figure 5.16: Boundary condition application to Sorbothane pads

The model is created and ready to be submitted to analysis.

In the **Job** module the job to be submitted to perform the analysis is create, also in this case the simulation is carried out using an Intel(R) Core (TM) i7-8750H CPU @2.20GHz processor. In this case two different jobs are submitted, the difference between the jobs is represented by the inertia mass set to the solid element. In the first job, in addition to the shaker mass, a mass of an aluminium plate is considered, so the resultant mass is 28.64 Kg. Instead, in the second job, the additional mass is given by a steel plate and the total mass is 48.2 Kg.

When the finite element simulation is finished, passing into the **Visualization** module, it is possible to see a graphical representation of the results. For example, it is possible to visualize the vertical displacement obtained in the static step, that represents the compression of the Sorbothane pad due to the above mass. The following figures show the vertical displacement of the two realized configurations.

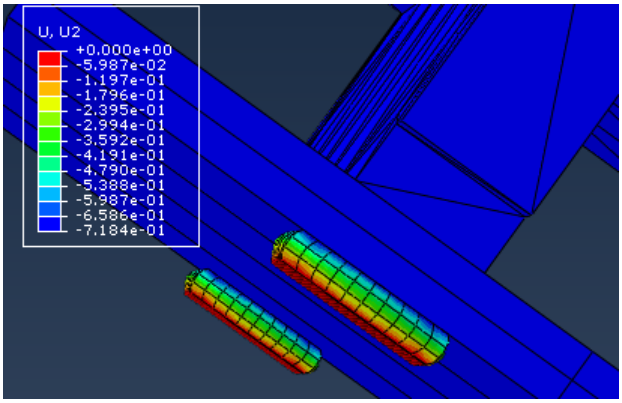

Figure 5.17: Vertical displacement - Visualization module - Static Step – Configuration 1

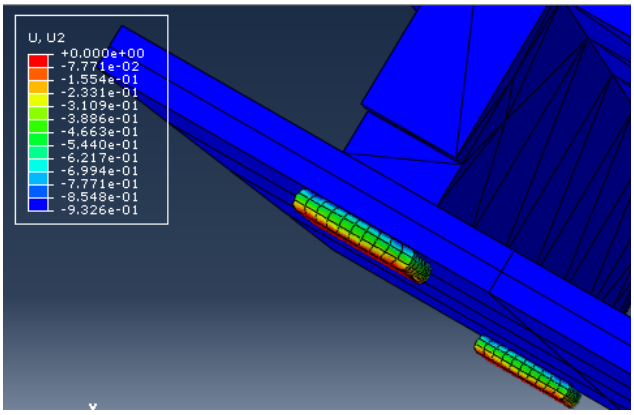

Figure 5.18: Vertical displacement - Visualization module - Static Step – Configuration 2

Considering the first configuration in figure 5.16, the vertical displacement is about 0.72 mm and total thickness of the pad that is 12.7 mm, the resulting compression of the Sorbothane pads is about 5.7%. While looking at the second configuration in figure 5.17, the vertical displacement is about 0.93 mm and considering the same total thickness of the pad, the compression of the Sorbothane pads in this case is about 7.3%.

In the above figures it can be also seen that except Sorbothane pads, the other parts are blue, this since these are defined to be rigid and so no deformations are showed.

Considering the steady-state dynamic direct analysis, the result in which we are interested in is represented by the response of the system due to the harmonic applied force. In Abaqus CAE it is possible to plot the value of the acceleration function of frequency, considering only the vertical component (indicated as A2 in Abaqus CAE), represented in the following figures.

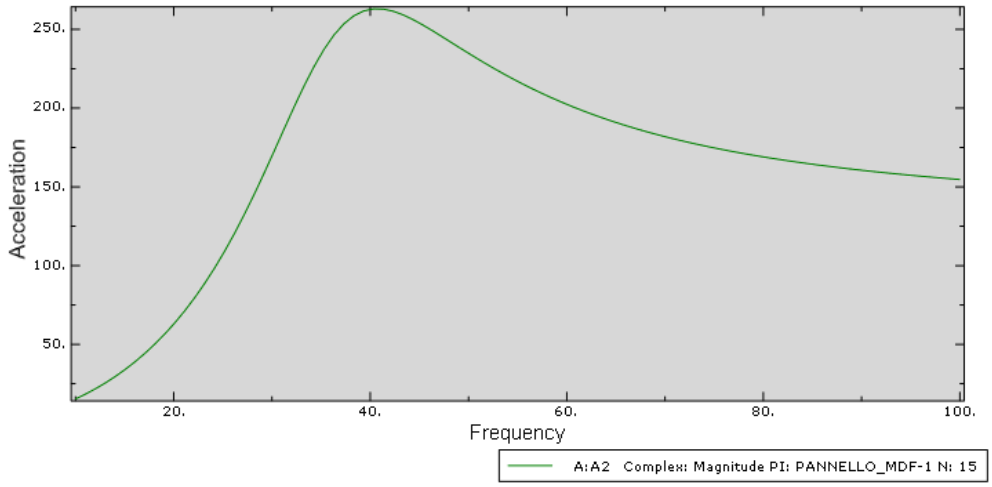

Figure 5.19: Vertical acceleration function of frequency - Steady-state dynamic analysis result – Magnitude

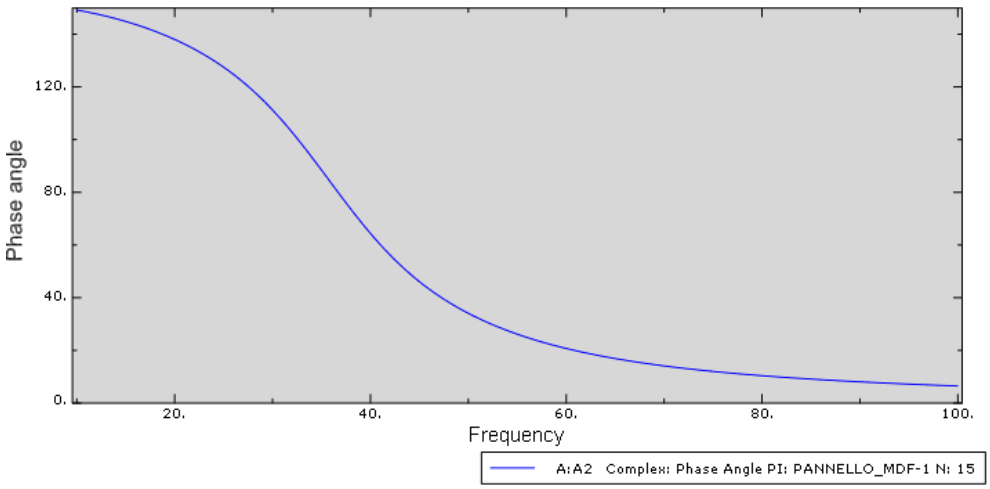

Figure 5.20:Vertical acceleration function of frequency - Steady-state dynamic analysis result - Phase Angle

This curve is extracted by considering a nodal point placed on the MDF plate, but since all the parts above the Sorbothane pads are modelled as rigid, it is possible to choose another point obtaining the same result. The previous Abaqus CAE output needs to be deeply analysed and scaled to obtain a comparable result with the experimental ones, following the expression described by the equation (5.9). The procedure adopted is explained later in this chapter.

5.3 Experimental testing procedure description

5.3.1 Testing procedure and needed equipment

As anticipated, the aim of the following tests is to search for the system resonance.

The input is produced by a function generator connected to the shaker amplifier. The vibrations are measured by means of accelerometers placed in various point of the crate and of the MDF plate fixed below. The input is measured through a reference accelerometer placed on the moving element of the shaker. The accelerometer data are transferred to a PC by means of acquisition device for the following analyses.

In the following table is presented a description of the equipment employed to perform the tests.

Type of instrument	Model	Additional notes
Accelerometer	PCB 393B12	Sensitivity 10000 mV/g
Accelerometer	PCB 393B12	Sensitivity 10000 mV/g
Accelerometer	PCB 393B12	Sensitivity 10000 mV/g
Accelerometer	PCB 393B12	Sensitivity 10000 mV/g
Accelerometer	PCB 393B12	Sensitivity 10000 mV/g
Accelerometer	PCB 393B12	Sensitivity 10000 mV/g
Accelerometer	PCB 333B30	Sensitivity 100mV/g
Function Generator	KEYSIGHT 33500 B	
Shaker	LDS V406	Usable freq. range 5 Hz-9 kHz Moving element mass 0.2 Kg
Power Amplifier	LDS PA 100 E	
Acquisition Device	NI 9234	4 channels, IEPE
Acquisition Device	NI 9234	4 channels, IEPE

Table 5.1: Instrumentations employed for measures

Accelerometer positioning and correspondence with the acquisition channel can be clearer by looking at the following figures.

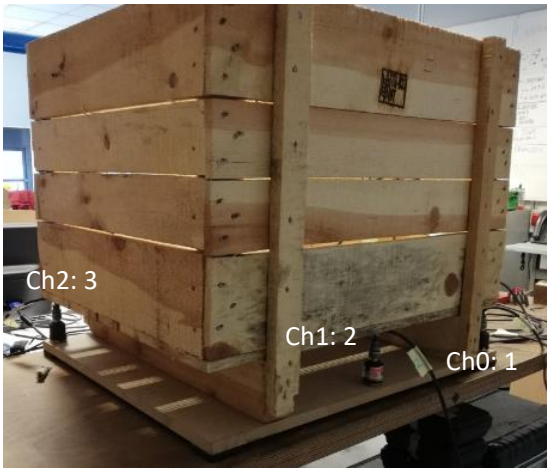

Figure 5.21: Accelerometers placed on the MDF plate - Ch0 -Ch1 - Ch2 – PCB393B12

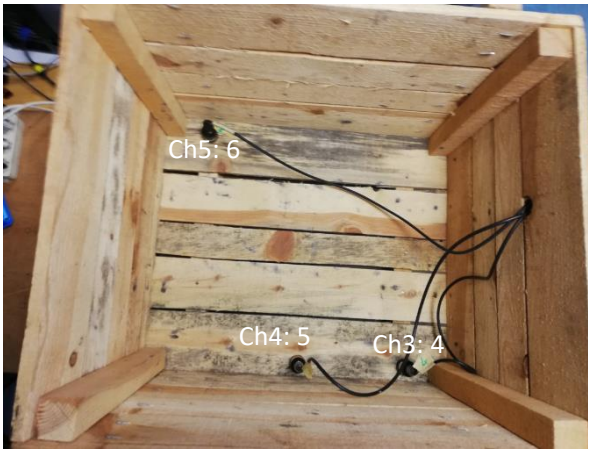

Figure 5.22: Accelerometer placed inside the crate - Ch 4 - Ch5 - Ch6 - PCB393B12

Figure 5.23: Accelerometer placed on the moving mass of the shaker - Reference - Ch6- PCB333B30

As can be seen by looking at the above figures, the accelerometer used to read the generated input is the one connected to the channel 6 of the acquisition device. It is different respect to the others to avoid saturation problem. The knowledge of the exact position of the accelerometers is needed for the analysis of the acquired data.

Since the behaviour of the wood crate is unknown, it is not easy to predict if it can have some lower resonance that can be confused with the frequency corresponding to the vertical vibration modes of the whole crate. In other words, it is interesting to understand if the hypothesis of rigid crate used to define the finite element can be coherent with the reality.

In the first configuration the shaker is positioned over an aluminium plate. This plate is used to transfer the vibration at the two crossbars of the crate directly, reducing the transmission to the

internal crate base and so increasing the rigidity of the system. The used plate is actually shorter than the distance between the two crossbars making possible the excitation of the lower resonances of the crate. The following image represents the real case ready to test this first configuration.

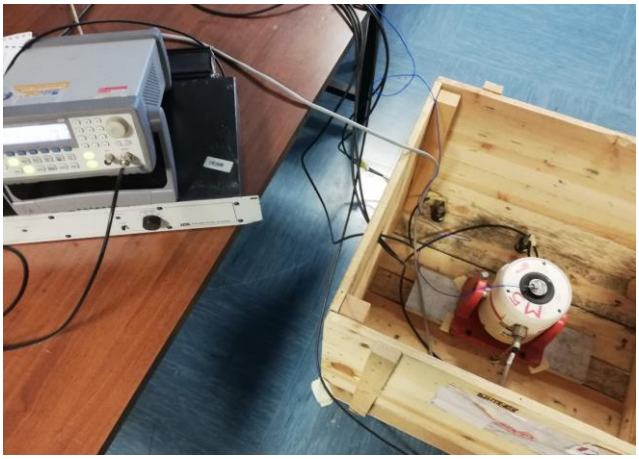

Figure 5.24: Configuration 1 - Shaker positioned over aluminium plate

The input signal, generated using a function generation, is a sweep from 10 Hz to 170 Hz with an acquisition time equal to 8 minutes and amplifier gain of 2.5 V.

To understand better the behaviour of the system a second configuration is realized. In this configuration the shaker is placed over a steel plate. The plate is longer than the distance between the two crate crossbars. The weight of this bar is about five times the ones used in the first configuration, so it is expected a better force transmission at the crossbars with a consequent decrease in the probability of excite the lower resonances of the crate. The following figure represents the second configuration ready to be tested.

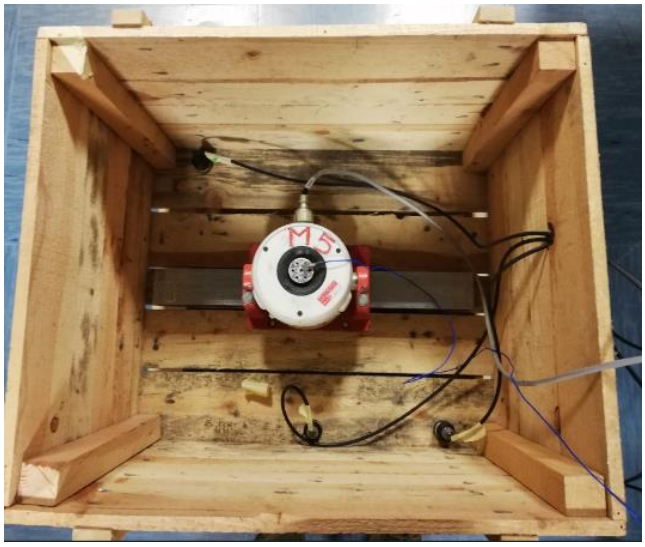

Figure 5.25: Configuration 1 - Shaker positioned over steel plate

In this case the input of the system is represented by a frequency sweep from 10 Hz to 100 Hz performed in 4 minutes.

The sampling frequency for both configurations is equal to 2560 Hz.

Once the testing procedure is finished, the acquired data are imported into a Matlab script to perform some preliminary analysis and considerations on the obtained results for both configurations.

5.4 Validation procedure and results

Before the comparison between the experimental and the model results, some consideration to understand how the systems and its components behave when subjected to an external excitation are made.

Considering the first configuration, the results presented in the following two figures are the transfer functions, in terms of magnitude and phase, obtained as the ratio between output accelerations measured by the accelerometers placed both in the crate (n°4, n°5, n°6) and on the MDF (n°1, n°2, n°3) and the input acceleration measured by the accelerometer placed over the moving element of the shaker (n°7).

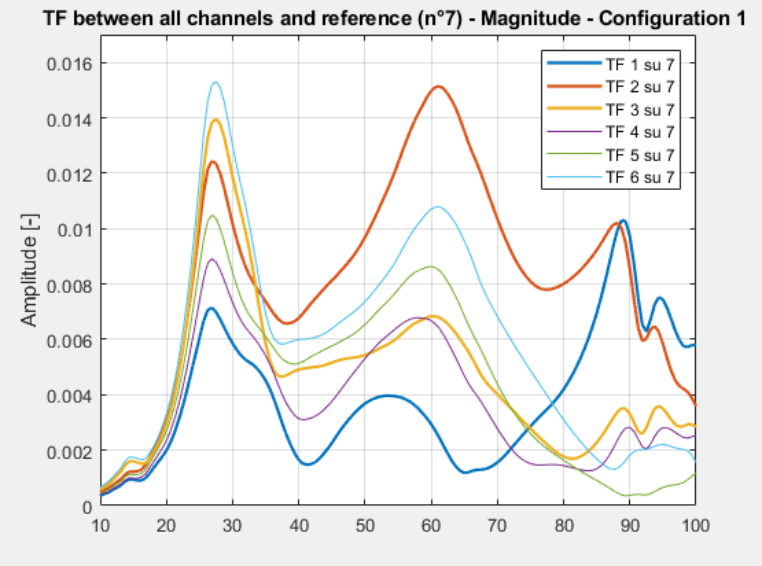

Figure 5.26: Transfer functions between all channels and the reference one - Magnitude - Configuration 1

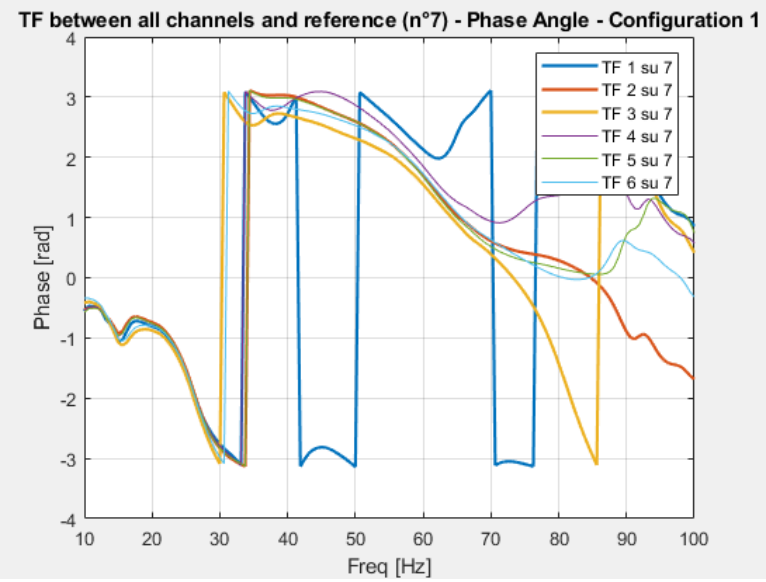

Figure 5.27: Transfer functions between all channels and the reference one - Phase Angle - Configuration 1

Looking at the above plotted transfer functions two peaks are visible. The first one is at a frequency equal to 27.5 Hz. At that frequency the phase plot shows a phase change for all the channels, so it can be assumed that it represents a resonance peak. Also the same consideration can be done for the larger peak at a frequency about 60 Hz except for the accelerometer n°1 that shows the peak at a frequency little bit lower; this behaviour is difficult to be interpreted but it seems to be that in that point there is a second resonance.

Since from Abaqus model, the resonance peak for this first configuration is found about 45 Hz, and considering that the experimental results comes from the configuration in which the shaker is placed over an aluminium plate shorter than the distance between the two crossbars, it is reasonable to assume that the flexional modes related to the wooden planks base of the crate are also excited. These modes can have relative lower frequencies and so can be attributed to one of the two higher peaks found. The other peak can also be attribute to another mode of the crate or can also be the vertical resonance that is searched. This second case implies that the behaviour of the material during the simulation is not correctly assessed.

Analysing deeply the plots and considering the range of frequencies around 45 Hz, it can be seen an interesting unfinished phase change at a frequency about 33 Hz with a correspondent little peak in the magnitude plot, but it is difficult to assess that represent the vertical resonance of the whole system covered by the two other higher amplitude resonances.

To better understanding the behaviour of the system it is necessary a preliminary analysis of the second configuration. This configuration is realized so that the steel plate on which the shaker is placed is long enough to enable the force transmission directly at the crossbars, so it is reasonable to assume that this case approximate better the Abaqus model in which the crate and the MDF plate are considered rigids. The following plots, as for the configuration 1, represent the magnitude and

phase of the transfer functions obtained between all the accelerometers placed on the system and the reference one on the shaker moving mass.

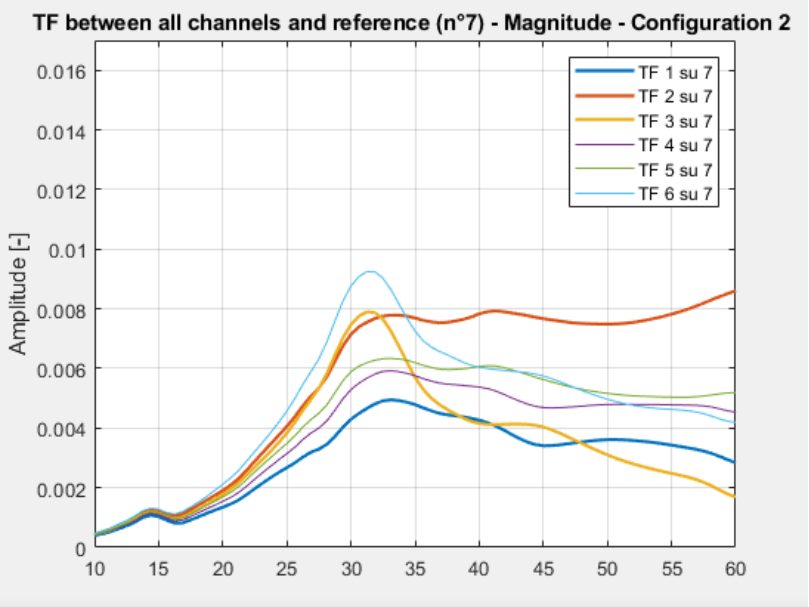

Figure 5.28: Transfer functions between all channels and the reference one - Magnitude - Configuration 2

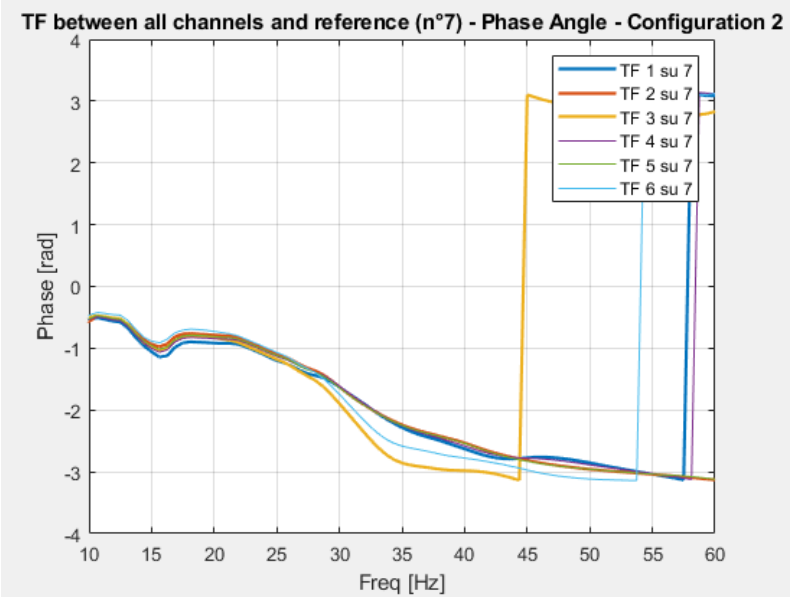

Figure 5.29: Transfer functions between all channels and the reference one - Phase Angle - Configuration 2

Considering the plots of the configuration 2 the first thing that can be observed is that the two higher peaks at 27.5Hz and at 60 Hz are no more presents.

It can be seen a lower peak at a frequency equal to 33 Hz with a correspondent phase change clearly visible in the phase angle plot. This peak is near to the one found in the Abaqus CAE model at a frequency equal to 40 Hz.

It's clear that forcing the system with the shaker on the steel plate the system the response changes completely and it is now possible to assume that the crate and the MDF plate cannot considered rigid.

Looking deeply in the detail the two plots and considering one couple of accelerometers at time, for example starting with the couple 3-6 representing respectively the accelerometer on the MDF plate and on the crate in the same corner of the system, it can be seen that they show a pronounced resonance compared to the couple of accelerometers 1-4 placed in the same positions of the opposite corner. This may be due to the fact that the real system motion is not perfectly vertical oriented or also that the weight of the system is not perfectly balanced causing the part of the system in which accelerometer 3 is placed to vibrate more than the portion of the system on which is placed the accelerometer 1. This can be assumed since in the Abaqus CAE rigid model that is also symmetric each point shows the same output value.

An important thing that can be assumed, at the end of this preliminary analysis, is that a wood crate can have some resonances at lower frequencies. That fact has to be considered to make sure that the crates to transport artwork are designed to have resonances at frequencies that cannot be excited during the transport to protect the contained work of art. The accuracy in the realization is very important since errors performed during the assembly phase can be cause local resonances, during the transport, dangerous for the unique masterpieces contained.

It has to be clear that correct packaging operations are the basis for the success of a transport.

For the validation procedure following presented, only the second configuration is considered, since in the first one the vertical resonance is not visible.

The comparison between the Abaqus CAE model results and the experimental tests results is done in terms of transfer functions expressed by the equation (5.9) illustrated at the beginning of this chapter. This transfer function expresses the ratio between the response acceleration in steady-state condition and the known forcing frequency given as input to the considered system.

The preliminary considerations formulated in the previous section are still valid but now it is necessary to analyse more in the detail the types of output obtained by the model and by the experimental testing procedure.

The output obtained from the finite element analysis performed in Abaqus is a sort of output spectrum. The frequencies are correct but the amplitude value as to be modified since represent the acceleration response to a harmonic force defined to have amplitude equal to 10 N phase equal to 0 rad. It is also to be noticed that for consistent Abaqus units this value of acceleration is expressed into mm/s^2 and it has to be converted into m/s^2.

The first thing to do is the division of the acceleration output by the forcing frequency of 10 N, and then the obtained quantity has to be divided by 1000 to obtain the accelerations in m/s^2. Defining the Abaqus output obtained by the simulation as a_{model} and the force as F_{model}, the transfer function modulus is obtained as,

$$H_{model} = \frac{a_{model}}{F_{model}\ 1000} \tag{5.10}$$

That now have the same form of $\frac{\ddot{X}_p}{F_0}$ desired.

Also for the values obtained by the experimental testing data it is necessary to make some adjustment to obtain the desired form of transfer function. The transfer functions obtained by Matlab script, used for the preliminary analysis, are obtained as ratio between the accelerations measured as output by accelerometers placed on the system in different positions and the reference or input value measured on by an accelerometer placed on the moving element of the shaker. For each output accelerometer the modulus of the transfer function can be simply written as,

$$T = \frac{a_{output}}{a_{input}} \tag{5.11}$$

The excitation force given as input, defined as F_{input}, can be simply obtained as,

$$F_{input} = m\ a_{input} \tag{5.12}$$

where the mass m is the mass of the moving element of the shaker, from datasheet equal to 0.2 kg, and the acceleration a_{input} is the acceleration experimentally measured by the reference accelerometers placed on the shaker.

Considering the above relation the transfer function modulus express as a ratio between output acceleration and force can be written as,

$$H_{exp} = \frac{a_{output}}{a_{input}} * 5\frac{1}{kg} \tag{5.13}$$

The transfer functions thus calculated can be plotted, in magnitude and phase, for both model and experimental test of configuration 2 in order to be compared.

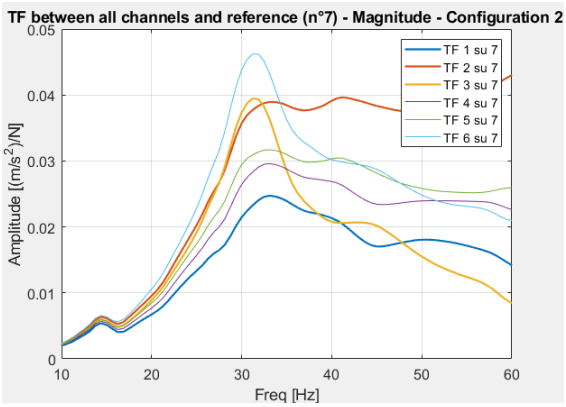

Figure 5.30: Transfer functions between all channels and the reference one - Magnitude - Configuration 2

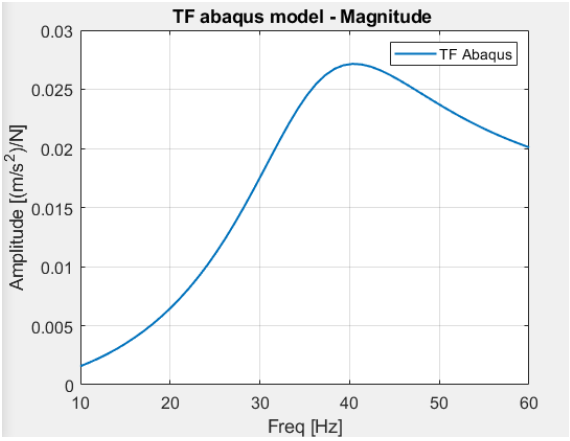

Figure 5.31: Transfer Functions Abaqus CAE model - Magnitude -Configuration 2

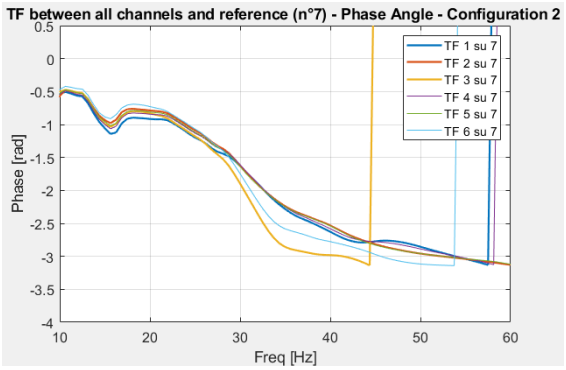

Figure 5.32: Transfer functions between all channels and the reference one - Phase Angle - Configuration 2

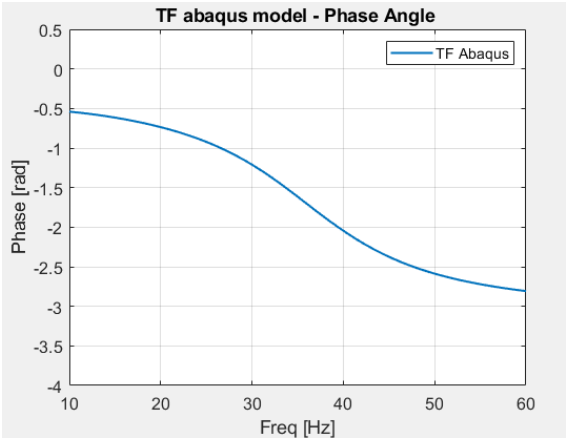

Figure 5.33: Transfer Functions Abaqus CAE model – Phase Angle -Configuration 2

It can be seen that the maximum amplitude reached by all the peaks is very low. The amplitude of the vertical resonance obtained by the Abaqus model stay in the middle of the resonances obtained from the experimental testing procedure with a peak at about 40 Hz. That peak is right shifted with respect to the peaks obtained from experimental transfer function that are about 31 Hz. This difference can be considered acceptable remembering the difficulty to model Sorbothane material and the complexity of its behaviour. In addition it has to be considered that in the model the crate and the MDF plate are considered as rigids but in reality, as it has been showed, they are not at all. The considerations made in the section related to preliminary analysis for the configuration 2 are valid also here so they are not repeated.

Thanks to the above considerations the validation procedure of the model can be considered satisfactory also in case of a system more complex than the previous treated in chapter 3. It seems to be that the Sorbothane characterization procedure is performed in a right way for the field of interest considered in this thesis.

Conclusions

During this thesis work, issues related to the characterization of a polymeric material called Sorbothane were addressed. Starting with the knowledge of the hyperelastic and viscoelastic properties of this family of materials it was possible to set up a procedure in order to determine a suitable set of parameters to simulate the Sorbothane behaviour in a finite element environment such as Abaqus CAE.

The determined parameters are then used to realize simple configurations in Abaqus CAE, and the results compared, in terms of transfer function, with the ones obtained through experimental tests performed in laboratory thus allowing to validate the model parameters.

Since the results obtained by the comparison are considered satisfactory, the case of study related to the protection of an earthenware vase is considered. Through experimental testing procedure the first and the second modes of vibrates are determined coherently with the deformation shape obtained by 3D Research as output of a FE analysis. The frequency values corresponding to this two modes are important to understand the filtering operation that has to be performed on the real crate to avoid vibrations transmission near to the resonances of the vase.

The validate parameters for Sorbothane are than reported in a configuration composed by a wood crate supported by Sorbothane pads. The crate used to realize this configuration is different by the crates used to transport works of art, in terms of design and assembly accuracy, but coherent in terms of dimensions and weight to the ones that can be used to transport an earthenware vase as the considered one. This operation is performed to understand the goodness of the procedure also for a configuration that comes closest to the purpose of the project. Also for this configuration, the comparison between FE model and experimental tests allowed to get good results.

Considering the obtained results, the proposed procedure can be repeated for any study configuration obtaining good approximations of the real Sorbothane behaviour as long as the viscoelastic parameters determination is performed considering a preload level similar to the one expected in a specific application and also that the initial parameters, used as input for the determination of the hyperelastic and viscoelastic properties, are consistent with the ones used to realize the real configuration. This latter observation, although it seems quite obvious, is not so for the Sorbothane for which, as demonstrated, the variability of the characteristics according to the year of production and the production batch is very high.

The following operation can be the use of this procedure in order to obtain the response for a configuration composed by a real crate containing the packaged vase considered and supported by Sorbothane pads, using as source input the vibrations measured during a transport. Comparing the obtained response with the ones obtained for a configuration realized without Sorbothane pads, it is possible to evaluate the performances of this material for vibration absorption, in order to obtain greater protection for the transported work of art. The same operation can be than repeated using

a double crate configuration, in which the packaged vase is placed into an internal crate supported by Sorbothane pad and then placed into an outer crate also supported by Sorbothane pads.

Various configurations can be realized by considering a different number of Sorbothane pads, shapes and dimensions in order to find the best solution for vibrations absorption.

Bibliography

[1] *EN: 16648:2015 (E) - Conservation of cultural Heritage - Transport Methods,* 2015.

[2] M. p. i. b. e. l. a. culturali, *D.Lgs. n.112/98 art.150 comma 6,* Italy, 1998.

[3] M. -. M. p. i. B. e. l. A. Culturali, *Guida per l'organizzazione di mostre d'arte,* Italy, 2000.

[4] U. e. al., "Equipment transporter and storage module". Culver City, California Patent 3,754,803, 28 08 1973.

[5] D. P. e. F. J. Paule, "Container-Chest for transporting fragile and or valuable objects". Saint-Hilaire-de-Brethmas (FR) Patent EP 0 988 239 B1, 03 April 2002.

[6] G. W. Harte, "Protective containment of valued articles". Denville, NJ (US) Patent US 7,686,169 B1, 30 March 2010.

[7] H. F. B. L. Brinson, Polymer Engineering Scence and Viscoelasticity - An introduction - Second Edition, New York: Springer, 2015.

[8] P. Flory, Introduction to Branched Molecules, New York: Annals of New York Accademy of Science, 1953.

[9] K. S. P. G. L. G. Robert L. Taylor, "Thermomechanical of Viscoelastic solids," vol. 2, 1970.

[10] N. W. Tschoegl, The phenomenological theory of linear viscoelastic behavior : an introduction, Berlino: Springer, 1989.

[11] R. A. Schapery, "A Simple Collocation Method for Fitting Viscoelastic Models to Experimental data," 1962.

[12] N. T. I. Emri, "Rheologia Acta, Generating line spectra from experimental responses. Part I: Relaxation modulus and creep compliance," vol. 32, no. 311, 1993.

[13] L. B. R. Bradshaw, "A Sign Control Method for Fitting and Interconverting Material Functions for Linearly Viscoelastic Solids," vol. 1, 1997.

[14] T. L. C. E. B. Becker, "A multidata method of approximate Laplace transform inversion," 1970.

[15] S. inc, "www.sorbothane.com," Sorbothane, 2019. [Online].

[16] M. S. J. K. G. S. J. S. M. A. Kraus, "Parameter identification methods for visco- and hyperelastic material models," 2017.

[17] D. S. S. Corp, Abaqus/CAE User's Manual.

[18] LS-DYNA, "https://www.dynasupport.com/howtos/general/consistent-units," LS-DYNA , 2020. [Online]. Available: https://www.dynasupport.com/howtos/general/consistent-units. [Accessed September 2019].

[19] F. C. G.Diana, Advanced Dynamics of Mechanical Systems, Springer, 2015.